ISSN: 0128-7680

Pertanika Journal of

SCIENCE & TECHNOLOGY

VOLUME 9 NO.1 (SUPPLEMENT)
JANUARY 2001

A scientific journal published by Universiti Putra Malaysia Press

Pertanika Journal of Science & Technology

About the Journal

Pertanika, the poineer journal of UPM, began publication in 1978. Since then, it has established itself as one of the leading multidisciplinary journals in the tropics. In 1992, a decision was made to streamline Pertanika into three journals to meet the need for specialised journals in areas of study aligned with the strengths of the univeristy. These ara **(i) Pertanika Journal of Tropical Agricultural Science, (ii) Pertanika Journal of Science and Technology (iii) Pertanika Journal of Social Science and Humanities**.

Aims and Scope

Pertanika Journal of Science and Technology welcomes full papers and short communications in English or Bahasa Melayu in the fields of chemisty, physics, mathematics and statistics, engineering, environmental control and management, ecology and computer science. It is published twice a year in January and July.

Articles must be reports of research not previously or simultaneously published in other scientific or technical journals.

Communications are notes of a significant finding intended for rapid publication. It should not exceed five double-spaced typerwritten pages and must be accompanied by a letter from the author justifying its publication as a communication.

Reviews are critical appraisals of literature in areas that are of interest to a broad spectrum of scientists and researchers. Review papers will be published upon invitation.

Submission of Manuscript

Three complete clear copies of the manuscript are to be submitted to

The Chief Editor
Pertanika Journal of Science and Technology
Universiti Putra Malaysia
43400 UPM Serdang, Selangor Darul Ehsan
MALAYSIA
Tel: (603) 89468855 Fax (603) 89416172

Proofs and Offprints

Page proofs, illustration proofs, the copy-edited manuscript and an offprint order form will be sent to the author. Proofs must be checked very carefully within the specified time as they will not be proofread by the Press editors.

Authors will receive 20 offprints of each article. Additional copies can be ordered from the Secretary of the Editorial Board by filling out the offprint order form.

Published by Universiti Putra Malaysia Press
ISSN No.: 0128-7680

Pertanika Journal of Science & Technology

Volume 9 No. 1, 2001 (Supplement)

Contents

ISSN: 0128-7680
Pertanika J. Sci. & Technol. Supplement 9(1): 1 - 9 (2001)

Kinetic Studies on the Adsorption of Sungai Sireh Raw Water's Natural Organic Matters

Ahmad Jusoh[1], Megat Johari Megat Mohd Noor[2] & See Boon Piow[2]
[1]Universiti Putra Malaysia Terengganu
[2]Department of Civil Engineering, Universiti Putra Malaysia
43400 UPM, Serdang, Selangor

ABSTRACT

The presence of dissolved organics in potable water supply is aesthetically undesirable. Apart from imparting colour, taste and odour to treated water, it is also potentially hazardous to health. Two types of coconut shell derived activated carbon, KI-6070 and KI-8085, provided by *Kekwa Indah Sdn Bhd*, were studied for the removal of dissolved organic compounds from Sungai Sireh Water Treatment Plant raw water, notorious of its high organic content. The respective external surface area of the KI-6070 and KI-8085 are approximately 277 m^2/g and 547 m^2/g.

The rate constant (K_L) for the KI-8085 was higher than that of the KI-6070, ranging between 30 and 70 %, for adsorbent dosages between 1.0 and 3.0 g. This was expected since the total surface area (specific and external surface areas) of the KI-8085 was higher than that of the KI-6070. The rate constant for the mass transfer was a function of the adsorbent dosage where both adsorbents indicated a proportional increase in the rate constant with increasing adsorbent dosage. The increasing dosage raised the intraparticle diffusion rate constant (K_{id}) for both the KI-6070 and KI-8085, with the KI-8085 having a higher intraparticle diffusion rate.

Keywords: Kinetic, adsorption, natural organic matter, granular activated carbon

INTRODUCTION

Conventional treatment processes are not sufficiently efficient in removing dissolved organic carbon (DOC) in water. Water containing high organic matter requires greater dosage of chlorination at the disinfection stage and consequently increases the formation trihalomethanes (THMs) in the treated water. This indirectly increases the cost of processing water. Higher THMs concentration in the water also poses a health hazard to consumers.

Recently, activated carbon has been identified as the most suitable and economical way to the removal of selected organic compounds. A thorough understanding of the adsorption and diffusion qualities of these humic substances is required, as macro-molecular organic matter is ubiquitous in the aqueous environment (Summers and Roberts 1988).

The rate of adsorption can be categorised to several steps as follows:

- Transport of solute from bulk solution phase to the boundary layer or surface film surrounding the adsorbent particle.
- Transport of solute across the boundary layer to the exterior surface of the adsorbent particle.
- Diffusion of solute within these pores, from the exterior of the particle to the interior surfaces of the particle.
- The physical or chemical binding of adsorbate to the internal surface of the adsorbent.

In water treatment, the steps of bulk transport and chemical or physical bonding are generally rapid, a either film diffusion or pore diffusion or both control the overall rate of adsorption.

NOM Removal Kinetics

The resolved mass transfer equation is as follows:

$$\frac{dC_t}{dt} = K_L a[C_e - C_t] \quad (1)$$

The equation can be resolved under the following boundary conditions:

$$C = C_o \text{ for } t = 0 \text{ and } C = C_e \text{ for } t \rightarrow \infty$$

And the solution of this equation is similar to the Lagergren's mass transfer equation as shown in the equation below (Namasivayam and Yamuna 1995 ; Low *et al.* 1996):

$$\log(q - q_t) = \log q - \frac{K_L a}{2.303} t \quad (2)$$

In order to calculate virtual initial concentration Co', the Lagergren's mass transfer equations can be modified by introducing an 9 to the logarithmic equation as shown in equation (3) and (4).

$$\text{In}\frac{C_e - C_t}{C_e - C_o} = \alpha - K_L at \quad (3)$$

$$\frac{C_e - C_t}{C_e - C_o}\frac{1}{e^{\alpha}} = \frac{C_e - C_t}{C_e - C_o} \quad (4)$$

Intraparticle Diffusion

The rate for intraparticle diffusion (Kid) is given by Weber and Morris (Namasivayam and Yamuna 1995) as

$$q = K_{id}\, t^{0.5} \quad (5)$$

The kinetics adsorption study by Namasivayam and Yamuna (1995) show that the linear portions of the curves do not pass through the origin indicating that intraparticle diffusion is not the only rate limiting control in the adsorption of dye on biogas residual slurry.

Empirical Model

In order to estimate the rate removal of adsorbate from effluent by an adsorbent, the following empirical mathematical model has been developed between contact time for the adsorption of adsorbate (Prakash *et al.* 1987):

$$\log(t+1) = K(C_i - C_t)^A \quad (6)$$

$$\log(C_i - C_t)\frac{1}{A}\log[\log(t+1)] - \frac{1}{A}\log K \quad (7)$$

MATERIALS AND METHODS

Preparation of GAC

The GAC used in this study is manufactured by KEKWA INDAH SDN BHD in Nilai. Two types of activated carbons made from coconut shell were used in this study (KI-6070 and KI-8085) and the characteristics of both activated carbons supplied by the manufacturer are given in Table 1.

TABLE 1
Characteristics of the activated carbon

Grade	Iodine No. mg/g	CTC (%)	Bulk Density G/cm^3	Ash (%)
KI-6070	1200 – 1300	60 – 70	0.47 – 0.51	3.0 – 4.0
KI-8085	1300 – 1400	70 – 80	0.40 – 0.44	3.0 – 4.0

The information given in Table 1 does not show the specific surface area, characteristics of the pore size distribution and type of pore volume (micropore, mesopore and macropore) available in the activated carbons though being important in the adsorption process (Lambert and Graham 1995; Kameya *et al.* 1997). Hence, an additional test (Brunauer, Emmett and Teller (BET) method) is required to characterize the physical properties of the adsorbents used in study.

The GAC used in this experiment was thoroughly washed with hydrochloric acid 1.0 M and rinsed before boiling with distilled water. This is to remove the unknown impurities, which will affect the adsorption of the activated carbon (Summers and Roberts 1988; Srivastana and Tyagi 1995). The GAC was soaked in distilled water for 24 hours and heated in an oven at 105°C for 2 days (Peel and Benedek 1980; Cooney and Xi 1994). Finally the porosity and specific gravity of the GAC were determined. The GAC was stored in dessicator until required.

Batch Experiment

All tests were carried out at room temperature and distilled water was used for cleaning off the apparatus control samples were simultaneously carried out to ensure sorption was done by activated carbon and not by the wall of the container.

The GACs (KI-6070 and KI-8085) used in the study were supplied by KEKWA in 20x50 mesh size (0.3-0.84 mm U.S Standard). Wetted GAC was ground with mortar and pestle to pass a 300 mm sieve mesh. This was done since smaller particle will achieve an equilibrium stage faster as compared to large particle size and therefore, it can reduce the experimental time required (David *et al.* 1983; Snoeyink 1991). Normally for batch studies, the adsorbent material was powdered and sieved to 200-250 mesh particle size (Srivastana and Tyagi 1995). The resulting powdered carbons were dried at 103°C for 24 hours and stored until for further use.

Time Course Study

Sample of activated carbon (KI-6070 and KI-8085) in the particle size of less than 300 mm were mixed with filtered (0.45 mm filter paper) raw water at 150 rpm where the NOM concentration was predetermined at a volume of 400ml for 3 days. The pH was adjusted to pH 5.0 using mild hydrochloric acid (pH 4) for the batch experiment. Each

solution (4 ml) in the batch reactor was removed after the predetermined contact time; the reaction mixture was then filtered with 0.45 mm filter paper again and the filtrate was analyzed for COD and DOC. Both activated carbons reached an equilibrium stage at about 6 hours.

Kinetic Study

The various quantities of adsorbents (KI-6070 and KI- 8085) ranging from 1.0 to 3.0 g was added to a 400 ml of predetermined NOM concentration of water samples. The mixture was mixed at 150 rpm. The sample of carbon was introduced to the reaction flask at time zero and then 4 ml of the solution was withdrawn at various intervals of time. This solution was filtered with 0.45 mm of filter paper to remove particulates and the solution was analyzed for DOC.

Aqueous Solutions

The raw water was taken from the intake point of the Sungai Sireh Water Treatment Plant. This plant receives a highly coloured (450 TCU) raw water, typical of swampy and peaty waters, containing material normally attributed by the humic and formic acid . The concentration of natural organic matter in the raw water was measured directly in terms of DOC using TOC analyzer.

RESULTS AND DISCUSSION

Characteristics of Activated Carbon

The physical characteristics of activated carbon are very important in determining the capacity and feasibility of the activated carbon to adsorb certain substances in terms of physical aspects. The surface and pore characteristics of the activated carbon samples (KI-6070 and KI-8085) as measured by BET method are given in Table 2. It was found that the specific surface area of KI-8085 is about 20% higher than that of KI-6070. Hence, we can conclude that the extra 20% surface area of KI-8085 was mainly attributed to the external surface area of the activated carbon itself.

It is also observed that both types of activated carbon have approximately the same mean pore radius of about 14Å. This pore radius is in the micropores region of less than 20Å (Cheremisinoff 1993).

After the experiment, it was found that KI-8085 has a higher adsorption capacity compared to KI-6070, this is mainly caused by "molecular sieves" mechanism which is influenced by the changes in the size and shape of the macromolecule (Brasquet *et al.* 1997; Newcombe *et al.* 1997b). Size exclusion of this molecular sieves effect is obvious, when the capacity of the adsorbent increases with increasing external surface area

TABLE 2
Structural characteristics of the adsorbents

Parameter	KI-6070	KI-8085
BET surface area (m^2/g)	1053	1266
Langmuir surface area (m^2/g)	1402	1705
External surface area (m^2/g)	277	547
Micropore volume (cm^3/g)	0.362	0.334
Mean pore radius (Å)	14.6	14.4

(mesopore size) of the adsorbent (Brasquet *et al.* 1997). As the pores size increases, it will allow more dissolved organic matters and also bigger molecular size of solutes to gain access to the micropores area where most of the adsorption processes are taking place (Cheremisinoff 1993; Brasquet *et al.* 1997; Newcombe *et al.* 1997a).

Time Course Study

The sorption of NOM as a function of contact time for various dosages of adsorbents, KI-6070 and KI-8085, ranging from 1.0 g to 3.0 g is shown in Figs. 1 and 2. The fractional sorption of organic matters by both the activated carbons increases as the dosage of adsorbent increased. Fast sorption occurred during the first 80 minutes and the equilibrium was achieved after 150 minutes for all dosages studied as indicated in both figures.

NOM Removal Kinetics

The time course studies showed sorption to be a rapid phenomenon as illustrated in Figs. 1 and 2. The resolved mass transfer equations (1) and (2) were used to estimate the rate constant of the adsorption (Table 3). These results demonstrated that the ordinate interception was not negligible and that double mechanism would have occurred; first an instantaneous sorption, inducing a rapid decrease in initial concentration (C_o) to a virtual initial concentration C_o', followed by a sorption occurring at a rate given by the slope of the linear plots (Guibal *et al.* 1995). Hence Lagergren's mass is not valid to illustrate, this condition and the equation can be modified by introducing an α component to the logarithmic equation (3) which yields the equation (4), to allow C_o to be estimated as shown in Table 3.

The value of α can be determined from the interception of the linear plot of equation (3). The result of the kinetics data and mass transfer coefficient as a function of the dosage are shown in Table 3.

The rate constant (K_L) for KI-8085 were higher than that of KI-6070, ranging from 30 to 70 %, due to the specific surface area and external surface area of KI-8085 being higher than that of KI-6070. This is because KI-8085 provides more surface area and bigger pore sizes which facilitates the adsorption of NOM with larger molecular size

TABLE 3
Determination of rate constant of NOM Removal Kinetics

Adsor -bent	Dose g	C_e,mg/l	C_o',mg/ l	α	K_L,min^{-1}	R2
KI-	1.0	20.601	30.924	-0.041	1.70×10^{-2}	0.992
6070	1.5	17.857	32.005	0.047	1.80×10^{-2}	0.998
	2.0	16.102	32.106	0.048	1.76×10^{-2}	0.997
	2.5	12.860	33.686	0.125	2.11×10^{-2}	0.995
	3.0	12.386	28.105	-0.188	2.03×10^{-2}	0.994
KI-	1.0	16.394	26.415	-0.045	2.48×10^{-2}	0.995
8085	1.5	13.438	26.285	-0.045	2.34×10^{-2}	0.965
	2.0	10.213	30.063	0.175	3.09×10^{-2}	0.988
	2.5	7.525	30.646	0.178	2.79×10^{-2}	0.997
	3.0	5.106	27.449	0.026	2.20×10^{-2}	0.994

Note: Initial concentrations of sample were 31.3576 and 26.87 mg/l for KI-6070 and KI-8085 respectively

(Cornel *et al.* 1985; Brasquet *et al.* 1997). External surface area (mesopore) was found to be more important for the mass transfer coefficient of the adsorption process. A study by Newcombe *et al.* (1997b) also showed that mesopores volume in activated carbon had a greater effect on the adsorption of NOM.

The rate constant of the mass transfer is also a function of adsorbent dosage. Both adsorbents (KI-6070 and KI-8085) how that the rate constant of the adsorbents increased proportionally with an increase in adsorbent dosage. As the dosage of activated carbon increases, it provides greater surface area for adsorption to take place, as compared to lower dosage of adsorbents.

The virtual initial concentration C_o', in both equation (3) and (4) is the concentration of the solution, where the adsorption process follows the first order kinetic reaction. The estimation of virtual concentration for both adsorbents (KI-6070 and KI-8085) was slightly higher than initial concentrations for most cases studied (Table 3). The instantaneous removal of the adsorbate was not significant in the study, because the concentrations of the NOM used in the study were able to give a constant rate of the adsorption process.

Intraparticle Diffusion

The adsorption of the NOM took place in two phases (Figs. 1 and 2). The first phase of solute uptake, the 'immediate solute uptake,' which was achieved within a few minutes was followed by the subsequent uptake of solute; the latter phase continued for a longer period of time. The contact-time experimental results can be used to study the rate limiting step in the adsorption process. Since the particles were vigorously agitated during the adsorption period, it is reasonable to assume that the rate is not limited by mass transfer from the bulk liquid to the particle external surface. Therefore, the rate limiting step may be film or intraparticle diffusion.

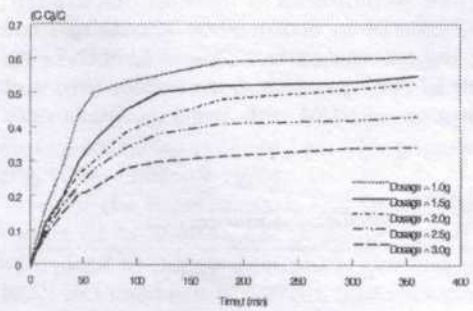

Fig. 1: Time course study of the actived carbon KI-6070 or removing of NOM. Conditions: 400ml of 31.356mg/l of NOM with different amounts of activated carbon

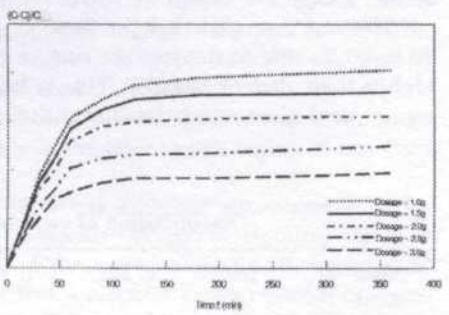

Fig. 2: Time course study of the activated carbon KI-8085 for removing of NOM. Conditions: 400ml of 31.356mg/l of NOM with different amounts of activated carbon

From the rate constant for intraparticle diffusion of equation (5), the plots of q versus $t^{0.5}$ are shown in Figs. 3 and 4. All plots have the same general features. The initial curved portion is attributed to the bulk diffusion effect, the linear portion to the intraparticle diffusion effect and the plateau to the equilibrium. The linear portions of the curves do not pass through the origin indicating that intraparticle diffusion is not the only rate controlling step for the adsorption of NOM onto adsorbents used in the study. Kid values obtained from the slope linear portions of the curves at each different

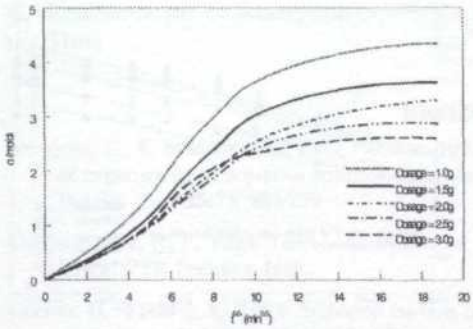

Fig. 3: Plots of NOM adsorbed versus t 0.5 for different adsorbent (KI-6070) dosages

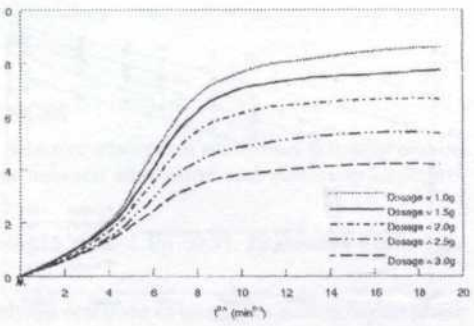

Fig. 4:Plots of NOM adsorbed versus t 0.5 for different adsorbent (KI-8085) dosages

dosage of adsorbents are shown in Table 4. The results generally show that increasing adsorbent dosage increased the intraparticle diffusion rate constant for both KI-6070 and KI-8085. KI-8085 gave a higher intraparticle diffusion rate compared to KI-6070 at each different dosage of adsorbents.

TABLE 4
Kinetic constant of adsorption for KI-6070 and KI-8085

Dose, g	KI-6070		KI-8085	
	K_{id}	R^2	K_{id}	R^2
1.0	0.2322	0.8789	0.3805	0.9283
1.5	0.2766	0.9854	0.5182	0.9195
2.0	0.2829	0.9916	0.6689	0.9318
2.5	0.3397	0.9919	0.7960	0.9478
3.0	0.3858	0.9786	0.8568	0.9458

Higher K_{id} indicates an enhancement in the rate adsorption. The adsorption capacity for KI-8085 was higher than that of KI-6070 for the same dosage of activated carbon.

Empirical Model

To estimate the rate of removal of NOM from water by different dosages of activated carbon, the empirical model of equations (6) and (7) were used. The values of K and A were reported depending on influent concentration, C_i the density and particle size of the adsorbent. The values of K and A were determined from the plots of log $(C_i - C_t)$ versus log (log(t + 1)) (Figs. 5 and 6). The straight lines thus obtained indicate the applicability of the model to the present study.

The relationships between dosage and the adsorbate removal rates for both activated carbons, KI-6070 and KI-8085, are presented in Table 5. It is clear that the removal of NOM in water can be computed at various time or a given dosage of adsorbent.

CONCLUSIONS

Activated carbons namely KI-6070 and KI-8085 were used in the study to adsorb NOM. Generally, KI-8085 performed better compared to KI-6070. This is mainly due to its

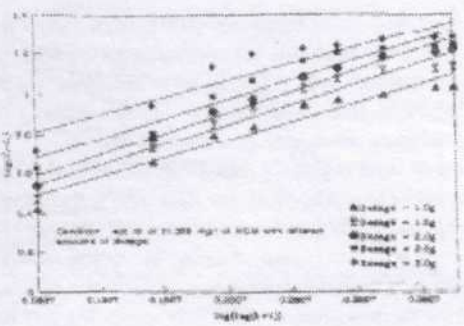

Fig. 5

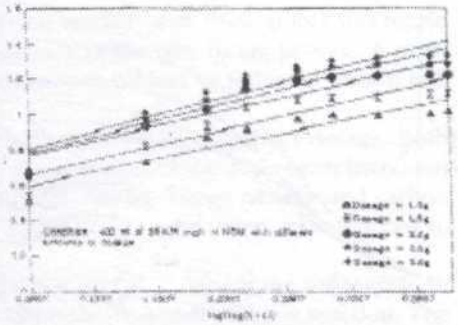

Fig. 6

TABLE 5
The empirical model for KI-6070 and KI-8085

Adsorbent	Dose, g	Empirical Model	R^2
KI-6070	1.0	Log(t+1)=0.6495(Ci-Ct)0.5462	0.9413
	1.5	Log(t+1)=0.6472(Ci-Ct)0.4961	0.9424
	2.0	Log(t+1)=0.6303(Ci-Ct)0.4770	0.9671
	2.5	Log(t+1)=0.5405(Ci-Ct)0.5129	0.9268
	3.0	Log(t+1)=0.3888(Ci-Ct)0.6027	0.8602
KI-8085 1.0	1.5	Log(t+1)=04748(Ci-Ct)0.6725	0.8677
	2.0	Log(t+1)=0.4898(Ci-Ct)0.5949	0.8610
	2.5	Log(t+1)=0.4116(Ci-Ct)0.6063	0.8565
	3.0	Log(t+1)=0.4489(Ci-Ct)0.5477	0.8645
		Log(t+1)=0.4485(Ci-Ct)0.5304	0.8783

higher specific surface area and a greater percentage of mesopores, which allows greater accessibility of macroorganic to the internal pores.

The rate constant (KL) for KI-8085 were higher than that of KI-6070, ranging from 30 to 70 %, due to the specific surface area and external surface area of KI-8085 being higher than that of KI-6070. External surface (mesopores) was found to be more important for the mass transfer coefficient of the adsorption process. The rate of the mass transfer is also a function of adsorbent dosage. Both adsorbents (KI-6070 and KI-8085) showed that the rate constant of the increased proportionally with increasing adsorbent dosage.

NOTATION

a Specific surface area
A,K Empirical Constant
C_e Equilibrium Concentration
C_i Influent Concentration
C_o,C_t Concentration at time zero and at time t
q Unit, mass of adsorbate/mass of adsorbent
q_t Amount of adsorbate adsorbed at time t
K_{id} A constant that depicts rate factor

K_L Rate constant of adsorption
t Time

REFERENCES

BRASQUET, C., E. SUBRENAT and P. Le CLOIREC. 1997. Selective adsorption on fibrous activated carbon of organics from aqueous solution: correlation between adsorption and molecular structure. *Wet Sci. Tech* **35(7)**: 251-259.

CHEREMISINOFF, N. P. 1993. *Carbon Adsorption for Pollution Control.* Pp 50-57. Engleweed Cliffs, New Jersey: PTR Prentice Hall.

COONEY, D. O and Z. XI. 1994. Activated carbon catalyzed reactions of phenolics during liquid-phase adsorption. *J. AICHE* **40(2)**: 361-364.

CORNEL, P. K., R. S. SUMMERS and P. V. ROBETS. 1985. Diffusion of humic acid in dilute aqueous solution. *J. Colloid Interface Sci.* **110**: 149-164.

DAVID, W. H., J. C. CRITTENDEN, M. ASCE and W. E. THACKER. 1983). User-oriented batch reactor solutions to the homogeneous surface diffusion model. *J. Environ. Eng.* **109**: 83-101.

GUIBAL, E., R. LORENZELLI, T. VINCENT and P.L. CLOIREC. 1995. Application of silica gel to metal ion sorption: static and dynamic removal of uranyl ions. *Environ. Technol.* **16**: 101-114.

KAMEYA, T., T. HADA and K. URANO. 1997. Changes of adsorption capacity and pore distribution of biological actived carbon on advanced water treatment. *Wet. Sci. Tech.* **35**: 155-162.

LAMBERT, S. D and N. J. D. GRAHAM. 1995. Removal of non-specific dissolved organic matter from upland potable water supplies-I. Adsorption. *Wat. Res.* **29**: 2421-2426.

LOW, K.S., C. K. LEE and A. M. WONG. 1996. Carbonized spent blenching earth as a sorbent for some organic dyes. *J. Environ. Sci. Health* **31(3)**: 673-685.

NAMASIVAYAM, C and R. T. YAMUNA. 1995. Adsorption of direct red 12B by biogas residual slurry: equilibrium and rate processes. *Environmental Pollution* **89**: 1-7.

NEWCOMBE, G., M. DRIKAS., S. ASSEMI and R. BECLATT. 1997a. Influence of characterised natural organic adsorption: 1. Characterisation of concentrated reservoir water. *Wat. Res.* **31(5)** : 965-972.

NEWCOMBE, G., D. MARY and H. ROB. 1997b. Influence of characterised natural organic material on activated carbon adsorption: II. Effect on pore volume distribution and adsorption of 2-methylisoborneol. *Wat. Sci.* **31(5)**: 1065-1073.

PEEL, R. G and A. BENEDEK. 1980. Attainment of equilibrium in activated carbon isotherm studies. *Environ. Sci. Technol.* **3**: 66-71.

PRAKASH,O., I. MEHROTRA and P. KUMAR. 1987. Removal of cadmium from water by water hyacinth. *J. Environ. Eng.* **113(2)**: 352-365.

SNOEYINK, V.L. 1991. Adsorption of Organic Compounds. In *Water Quality and Treatment.* A Handbook of Community Water Supply, p. 782. ed. W.P. Frederick. McGraw Hill. New York.

SRIVASTANA, S.K and R. TYAGI. 1995. Competitive adsorption of substituted phenols by activated carbons developed from the fertilizer waste slurry. *Wet. Sci.* **29(2)** : 483-488

SUMMERS, R. S. and P.V. ROBERTS. 1988. Activated carbon adsorption of humic substances. I. Heterodisperse mixture and desorption. *J. Colloid Interface Sci.* **122(2)** : 367-381.

ISSN: 0128-7680
Pertanika J. Sci. & Technol. Supplement 9(1): 11 - 21 (2001)

Application of Iterative Technique (IT) Using SPT N-Values and Correlations for Analysis of Tip and Shaft Capacity for an Axially Loaded Pile in Sand

Rosely Ab.Malik[1] & Jasmin Ambrose[2]
[1]Department of Civil Engineering, Universiti Putra Malaysia
[2]Universiti Putra Malaysia, 43400 UPM, Serdang, Selangor

ABSTRACT

This is a theoretical method on how to analyze the axial capacity (tip and shaft) of a single pile using iterative technique on SPT-N values and SPT-N correlation. This technique allows the engineer who conducts the analyses to control the input and output information of the analyses in a systematic and organized fashion. This method is also very helpful especially for the development of pile capacity prediction using reliability method. Research on the subject is being carried out at Universiti Putra Malaysia (UPM).

Keywords: SPT N-values, iterative technique (IT), axial pile capacity

INTRODUCTION

The Standard Penetration Test (SPT), developed around 1927 (Bowles 1996), is still one of the most popular and economical means to obtain subsurface information of soil. It has been used in correlation to determine unit weight, (γ), relative density, (D_r), angle of internal friction, (ϕ), and the undrained compressive strength,(q_u) . It has also been used for estimating the stress- strainmodulus,(E), and the bearing capacity of foundations.

Iterative Technique (IT) is an approach that is being used based on the logical assumption that the correlation used to relate N-Values and the sand properties (ϕ , D_r, γ_n) is valid. A very brief description of this technique will be presented here, covering the iteration process, some analysis of results and the suggested correlations. This IT is presented in a stepwise manner to achieve better understanding of this method.

STEP 1. N-Values are firstly corrected for the water table and to account for fine or silty sand below water (Heydinger 1984; Coyle & Costello 1981), as given in Eqn. 1. Water table correction on N-Values is just an example of one correction factor that can be applied on N-Values for discrepancies occurring due to, for instance, difference in equipment's manufacturers, uncertainties in geotechnical parameters and the drive hammer configuration.

$$N' = \frac{1}{2}(N - 15) + 15 \quad (1)$$

STEP 2. Using a similar method suggested by Wolff (1989) and Ab.Malik (1992), the effective friction angle of sand, (ϕ), can be correlated with the corrected N-Values, (N"), using the relationship as presented by Peck *et al.* (1974), which can be approximated as:

$$\phi = 26.7 + 0.36N" - 0.0014(N")^2 \quad (2)$$

However, because (N") is not available due to lack of overburden stress data, σ_v, where N " is N-Value corrected for overburden stress. Because the unit weight, γ_n, is not usually available, therefore, a preliminary assumption of N' = N" is presumed in Eqn. 2. After the first iteration of LOOP 1 (1st LOOP 1), when N" is available, (ϕ) can be

calculated using N". This step requires at least two complete iterations, i.e. second iteration of LOOP 1 (2nd LOOP 1).

STEP 3. Meyerhof (1959) relates the effective angle of shearing resistance (ϕ') and the relative density, (D_r), in equation 3. This equation is rearranged to obtain(D_r) as a function of (ϕ') in Eqn. 4. Where:

$$\phi' = 28 + 0.15\ D_r \tag{3}$$

$$D_r \frac{\phi'-28}{0.15} \tag{4}$$

Even though Eqn. (4), can give a rough approximation of D_r, the expression in Eqn. 3 was not derived for the purpose of evaluating relative density from effective angle of internal friction, ϕ'. In other words, $D_r = f(\phi')$ is not a correct function representation.

STEP 4. Now the relative density can be applied in Eqn. 5 to find the probable unit weight, g_n, of sand.

$$D_r = \frac{(\gamma'_n - \gamma'_{min}) \times (\gamma'_{max})}{(\gamma'_{max} - \gamma'_{min}) \times (\gamma'_n)} \tag{5}$$

Where γ_{max} and γ_{min} are arbitrarily chosen values considering medium and dense sand as a preset limit for normal sand condition. Preset values chosen are γ_{max} = 20 kN/m^3 (D_r=0.65) for dense sand and γ_{min} = 17 kN/m^3 (D_r=0.35) for medium dense sand (relative density for most soil is in between 0.35-0.65). The simplification of this formula is as shown in Eqn. 6:

$$\gamma_n = \frac{340}{20 - 3D_r} \tag{6}$$

Eqns. 4, 5 and 6 are applied to find D_r and γ_n', this will be identified as route A. To obtain effective unit weight, γ_n',γ_w (9.8 kN/m^3) is subtracted from the unit weight in Eqn. 6 (for submerged cases).

$$\gamma_n' = \gamma_n - \gamma_w \tag{7}$$

STEP 3 and *STEP 4* are highly debatable because of the assumptions used to derive D_r and γ_n. One method that could overcome this problem is by using empirical values for ϕ', D_r, and γ_n of granular soils based on the N-Values at about 6m depth for normally consolidated sand derived by Shioi and Fukui (1982) to replace Eqns. (4) and (6). These data were fitted using a spreadsheet program and the formula for fine, medium and course sand is as below :

$D_r = 0.07\phi' - 1.92$	}fine sand
$D_r = 0.05\phi' - 1.54$	}medium sand
$D_r = 0.03\phi' - 1.00$	}coarse sand
$\gamma_n = -0.016\phi'^2 + 1.64\phi' - 20.4$	}fine sand
$\gamma_n = -0.019\phi'^2 + 1.90\phi' - 24.7$	}medium sand
$\gamma_n = -0.046\phi'^2 + 3.75\phi'1 - 54.3$	}coarse sand

The alternative equation introduced above will be identified as route B. A comparison of results obtained using route A and B will be discussed in the results and discussion section later in the paper.

STEP 5. It is known from basic soil mechanics theory that the effective overburden stress, σ_v', can be determined as long as the unit weight and the depth of the soil element can be determined accurately. Therefore, overburden stress, σ_v', can be represented as:

$$\sigma_v' = \sum_{i=0} [\gamma_n' z] \tag{8}$$

STEP 6. The final link for this procedure is completed using a correction factor similarly used by Wolff (1989) and Ab. Malik (1992). Liao and Whitman (1986) introduced this correction factor for effective overburden stress.

$$N'' = N'[95.76/\sigma_v']^{\frac{1}{2}}; (\sigma_v' \text{ is in kPa}) \tag{9}$$

However, the correlation in Eqn. 9 causes a very rapid increase in N-Values especially for lower overburden stress values (shallow depth). Therefore, the authors have suggested another correlation proposed by Heydinger in 1984, (Coyle *et al.* 1981):

$$N'' = N'0.77*[\log(1915.2/\sigma_v')] \tag{10}$$

Eqn. 10 will be used in all the analyses of data as presented in Table 1.

STEP 7. Now a loop has been created where the corrected SPT-N value N" can be used to obtain ϕ', D_r and γ_n' by continuous iteration. This loop as shown below is named LOOP 1. This is done simply for identification purposes. Notice that the whole procedure only uses one data input, N-Value.

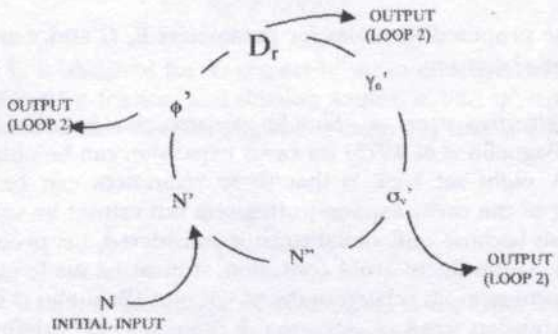

Fig. 1: LOOP 1

Similar IT were used by Fleming *et al.* (1992), to obtain the ultimate tip capacity in sand. Fleming used overburden stress, σ_v', and relative density, D_r, as his initial input. This method will be explained in detail in the next section, but the initial input will be originated from LOOP 1. This means that LOOP 1 and 2 (as discussed in the next section) are linked.

TIP CAPACITY IN SAND

Randolph (1994) and Fleming *et al.* (1992), applied cavity expansion theorem to further develop this method of axial pile capacity analysis. However, Randolph's method of analysis was more refined and found better agreement with numerical solutions compared to Fleming's. Tip capacity in sand was derived using the analogy between spherical cavity expansion and bearing failure by Randolph in 1994 (Gibson 1950). This leads to the relationship between end-bearing pressure, q_b, and limit pressure, p_{lim}, (Eqn. 11).

$$qb = p_{lim} \{ 1 + \tan\phi_{cv}' \tan (45 + \left(\frac{\phi'_{cv}}{2}\right))\} \quad (11)$$

Limit pressure, plim, solutions can be very long and confusing. However, Yu & Houlsby (1991) have published analytical solutions that comply with numerical solutions. Parameters needed to solve the limit pressure equations (Eqns. (11), (28) and (29)) are E, G, ν, c, ϕ', ψ', p_o and m are as explained below:

i. Stress-strain Modulus, E in kPa, Bazaraa, in 1982 (D'Appolonia 1970) is:

Saturated sand,	$E = 250(N + 15)$	(12)
N.C sand,	$E = 500(N + 15)$	(13)
O.C sand,	$E = 40{,}000+1050N$	(14)

ii. Shear modulus, G, in kPa (Randolph 1994) is:

$$G = 40{,}000*\exp(0.7D_r)*(p'/100)^{0.5} \quad (15)$$

iii. Poisson's ratio, n, is a dimensionless factor. From the original expression $G = \frac{E}{2(1+\nu)}$, and using the solution for E and G (Eqns. (12)-(15)) above:

$$\nu = \frac{E}{(2G)-1} \quad (16)$$

Notice that the proposed formulas for parameters E, G and ν are all derived from N-Values using correlations.

iv. Initial mean effective stress p_o. Simple explanation (Briaud 1992) and detailed explanation (Baguelin *et al.* 1978) on cavity expansion can be obtained from various references. (A slight set back is that these references can be used for general understanding of the cavity expansion theorem but cannot be used directly for pile capacity analysis because only radial stress is considered, i.e. pressuremeter analysis, and not axial). However, to avoid confusion, it must be made clear that the initial mean effective stress, p_o' is related to the p' - q' plot (Baguelin *et al.* 1978) and is not similar to overburden stress σ_v. Atkinson & Bransby (1982) defined mean effective stress p' as:

$$p' = \frac{1}{3}(\sigma_v' + 2\sigma_h') \quad (17)$$

v. Factor, identifying cavity type, m, for spherical expansion solutions is equal to 2(m = 2).

vi. Two important parameter are still left unsolved, effective angle of friction and dilation, ϕ' and ψ', respectively. To solve these we will use input from LOOP 1. We will require the input of overburden stress, σ_v', bearing capacity factor, N_q, and relative density, D_r, to find the suitable ϕ'_{cv} (Fleming *et al.* 1992 ; Bolton 1986).

Solution for ϕ' and ψ'

Following the work of Bolton (1986, 1987), rigidity index, I_r, is related to relative density, D_r, and mean effective stress, p', Eqns. (18-19).

$$I_r = D_r\,[5.4 - \ln(p'/100)]\text{-}1 \text{ for } p' < 150\text{kPa} \quad (18)$$

$$I_r = 5D_r - 1 \qquad \text{for } p' \geq 150\text{kPa} \quad (19)$$

Fleming suggested that the mean effective stress at failure p', be approximated using Eqn. (20)

$$p' \approx \sqrt{N_q} * \sigma_v' \quad (20)$$

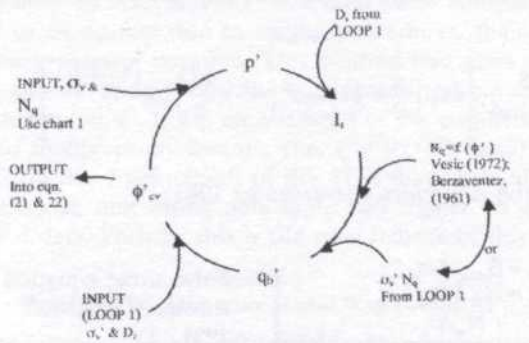

Fig. 2: LOOP 2

Rigidity index, I_r, is obtained for its respective mean effective stress p' and D_r using Eqns. (18)-(19)). Effective friction and dilation angles, ϕ' and ψ', are deduced, which leads to effective friction and dilation angles for cavity expansion solutions as in Eqns. (21) and (22).

$$\phi = \phi'_{cv} + 1.5I_r \quad (21)$$

$$\psi' = 1.875I_r \quad (22)$$

This angle of friction, ϕ and angle of dilation, ψ, is the final input into the limit pressure equation (Eqns. (11), (28) and (29)) required for solving the limit pressure, plim, equation. Simplified formula for input into the plim solution is given by Eqns. (28) and (29). The critical state angle of friction, ϕ_{cv}, relates to conditions where soil shears with zero dilation (i.e. at constant volume).

A logical question that should arise is that, why not apply relative density, D_r, straight into Eqns. (18)-(19) to find the corresponding ϕ and ψ for analysis? This is simply because relative density, D_r, in this analysis must be a function of critical state angle of friction, ϕ_{cv}. How many iterations should be conducted before a good solution is

achieved? (i.e. Fleming *et al.* (1992) used three iterations to find the corrected bearing capacity factor, N_q, for tip capacity analysis). Parameters D_r and ϕ'_{cv} is extracted from LOOP 2 to find ϕ' and ψ' using Eqns. (21)-(22).

SHAFT CAPACITY IN SAND

Peak Shaft Capacity Phenomenon and Its Analyses

The peak shaft capacity occurs near the tip of the pile. This phenomenon has been observed using instrumented piles (Vesic 1970; Lehane *et al.* 1993). The peak shaft resistance ratio to the overburden stress, $\left(\frac{\tau_s}{\sigma'_v} = \beta\right)$ that is maximum at the tip of the pile in sand has to be determined. Where β is similar to the effective stress coefficient originally introduced by Burland (1973), Zeevaert (1960), Eide *et al.* (1961) and Chandler (1968). β_{max} is a function of S_t, δ and N_q.

Where;

S_t = $2*\exp(-7\tan\delta)$

δ = Angle of friction between pile and soil, can be determined as in Potyoundy (1961).

$$Nq = \frac{3}{3-\sin\phi'}\left[\exp\left(\frac{\pi}{2}-\phi'\right)\tan^2\left(45+\frac{\phi'}{2}\right)\mathrm{Irr}^{\left(\frac{1.33\sin\phi'}{1+\sin\phi'}\right)}\right]$$

or use Chart 1 in the Appendix (Berzavantez 1961)

$$\left.\begin{aligned} \tau_{max} &= \beta_{max} * \sigma_v' \\ q_b &= N_q * \sigma_v' \\ \tau_{max} &= \left(\frac{N_q}{50}\right) * \sigma_v' * \tan\delta \end{aligned}\right\}$$ Solve these equation to obtain equation. (23) - (24)

where $1/50 \cong S_t$

$$\frac{\tau_{max}}{q_b} = \frac{\beta_{max}}{N_q} = S_t \tan\delta \qquad (23)$$

so; $\beta_{max} = N_q * S_t \tan\delta$

because, $\beta_{max} = K_{max} * \tan\delta$; (24)

then, $Kmax = Nq * St$ (25)

Shaft Friction Distribution Along Pile

Randolph adopted the work by Toolan *et al.* (1990) to postulate β_{min} which is believed to be linked to the active earth pressure coefficient, K_a. Randolph also adopted a simple distribution of shaft capacity as proposed by Heerema (1980). The shaft capacity distribution is represented by the formula:

$$\frac{\tau_s}{\sigma'_v} = \beta(z) = \beta_{min} + (\beta_{max} - \beta_{min}) * \exp\left[-\mu\left(\frac{L-z}{d}\right)\right] \qquad (26)$$

Where, $\beta_{min} \approx K_a = \frac{1-\sin\phi'}{1+\sin\phi'}$; β_{max} as in equation. (24)

and K_{max} as in Eqn. (25). Therefore;

$$\frac{\tau_s}{\sigma'_v \tan\delta} = K(z) = K_{min} + (K_{max} - K_{min}) * \exp\left[-u\left(\frac{L-z}{d}\right)\right] \quad (27)$$

Where μ is the rate of exponential ($0.025<\mu<0.1$). Exponential decay, m, can be determined by having a large database of instrumented piles, L is the total embedment length of the pile, z = depth below ground level, d = pile diameter and (L-z)/d is the normalized length of pile driven past that particular location.

Advantages and Improvements Needed

The purpose of this whole procedure is to have only one data input (N-Values) to calculate axial capacity of a single pile in sand using previously proposed correlations. This itself makes this method a versatile tool for analysis. However, this method is only suggested as an option for analyses and not to be used solely. Another advantage is that, if data is unreliable or inaccurate due to testing procedures, then these data can be averaged through the process of iteration. This method also gives a new meaning for determining shaft capacity using empirical correlations, where it considers several important soil parameter (i.e. ϕ', I_r, D_r, etc.) instead of the empirical correlation using N-Values directly into shaft capacity formula (i.e. $\tau_s = (N/50)\tan\delta$)

An obstacle faced in the development of this IT is that, since all the formulas and correlation are interlinked, one wrong data input can trigger off a chain reaction of wrongfully interpreted data. Perhaps this is the only setback of this procedure.

TABLE 1
Results of IT using route A and B of (LOOP 1)

Depth / m	SPT-N	N'	ϕ^A	ϕ^B	D_r^A	D_r^B	γ_n^A	γ_n^B	N'^A	N'^B
0.762	37	37	38.1	38.1	67.4	49	18.9	17.17	62	59
			43.6	43.1	104.3	68.7	20.15	21.3	60	59
2.286	44	44	39.8	39.8	78.8	55.8	17.2	21.6	57	54
			42.7	42.1	97.8	64.6	17.3	21.5	57	54
3.81	51	33	37.1	37.1	61	64	18.7	19.6	36	36
			38.1	37.8	68	68	18.9	19.9	36	36
5.33	58	37	38.2	38.2	68	70.7	18.9	20.13	37	36
			38.2	37.9	68	68.7	18.9	19.97	37	36
6.555	64	40	38.9	38.9	73	74.8	19.1	20.4	37	37
			38	38	66.5	69.6	18.9	20.04	37	36

RESULTS

For each depth, Table 1, the first iteration (1st LOOP for each depth) is represented by the first row, and the second iteration by the second row.

DISCUSSION AND CONCLUSION

The result in Table 1 shows that the number of iteration required to achieve satisfactory results is 2 iterations (2nd LOOP 1). These are results of data analysed using IT, for the Northwestern pile prediction symposium and the results comply with the results obtained by Heydinger (1984) in the symposium. Compared with the other 24 predictors, Heydinger obtained a predicted to measured pile capacity ratio of more than 90%. However, the application of LOOP 2 in non-homogenus or residual soil (i.e. Malaysian soil) is still being experimented with.

Suggested Correlation for Further Application

Bazaraa (1967) suggested these correlations:

N' = N; for fine to coarse sand
N' = 0.6N; for very fine or silty sand

D' Appolonia *et al.* (1970) and Gibbs *et al.* (1957):

$N' = 4N/(1+4p')$ for $p' \leq 0.75 kg/cm^2$
$N' = 4N/(3.25+p')$ for $p' \geq 0.75 kg/cm^2$

Thornburn *et al.* (1971) & Meyerhof (1976).

$\tau_s = \overline{N}/50$ tons
$\tau_t = 4N$ tons
} Driven pile in sand

$\tau_s = \overline{N}/60$ tons
$\tau_t = 2.5N$ tons
} Driven pile in silt

Limit Pressure, Plim, Solutions

For spherical cavity expansion in the associated Mohr-Coulomb material (i.e. m=2 and $\beta = \alpha$) is E, ν, c, ϕ, ψ, p_o.

$$R\alpha = \frac{(m+\alpha)(\alpha-1)p_{lim}}{\alpha(1+m)(\alpha-1)p_o} \tag{28}$$

$$\left(\frac{\eta}{\gamma}\right)(1-\delta)^{\frac{(\beta+m)}{\beta}} = \frac{\xi}{n!(n-\gamma)} * \left[R\alpha^{(n-\gamma)} - 1\right] \tag{29}$$

Solving Eqns. (28)-(29) will produce the value of p_{lim}. And this p_{lim} should be replaced in Eqn. (11) to give the tip capacity, q_b. Where symbols are:

$$\alpha = \frac{1+\sin\phi'}{1-\sin\phi'} \qquad M = \frac{E}{1-\nu^2(2-m)}$$

$$\beta = \frac{1+\sin\psi}{1-\sin\psi} \qquad \gamma = \frac{\alpha(\beta+m)}{m(\alpha-1)\beta}$$

$$\eta = \frac{(\beta+m)(1-2v)*[(\alpha-1)p_o]*[1+(2-m)v]}{E(\alpha-1)\beta}$$

$$\xi = \left\{\frac{\left[1-v^2(2-m)\right]*(1+m)\delta}{(1-v)*(\alpha-1)\beta} * \left[\alpha\beta + m(1-2v) + 2v - \frac{mv(\alpha+\beta)}{1-v(2-m)}\right]\right\}$$

Appendix:

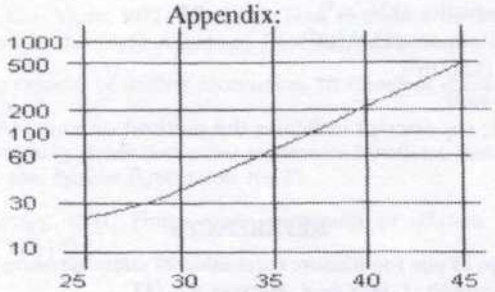

Chart 1. Berzavantez et al. 1961

ACKNOWLEDGEMENT

This paper was made possible under the financial assistance of University Putra Malaysia, and the constant guidance provided by GeoEnTech Sdn Bhd., with collaboration of the Ministry of Science, Technology & Environment. The authors would also like to acknowledge the constructive comments made by the reviewers of the paper prior to publication.

NOTATION

c soil cohesion
D_r relative density
E Young's modulus of soil
G shear modulus of soil
I_r rigidity index
K_a active earth pressure coefficient
K_{max} maximum ratio of radial effective stress at pile surface to in situ vertical effective stress
m factor identifying cavity type
N SPT N-Values
N' SPT blow count after initial correction (for 1st LOOP 1)
N' SPT blow count after correcting for overburden stress (for 2nd LOOP 1)
N_q bearing capacity factor

p_{lim} limit pressure for spherical cavity expansion
p_o initial total stress
q_b tip bearing capacity (kN)
q_u unconfined compressive strength (kN/m^2)
S_t ratio of radial effective stress to end bearing pressure in vicinity of the pile
β_{max} maximum ratio of shaft friction to effective overburden stress
β_{min} minimum ratio of shaft friction to effective overburden stress
ϕ' effective angle of shearing resistance
ϕ'_{cv} critical state friction angle
γ_n' effective unit weight of soil (kN/m^3)
γ_n total unit weight of soil (kN/m^3)
γ_w unit weight of water (kN/m^3)
ν Poisson's ratio of soil
$\sigma'h$ effective horizontal stress
$\sigma'v$ effective overburden stress
τ_{max} unit peak shaft capacity (kN/m^2)
τ_s unit shaft friction capacity(kN/m^2)
τ_t unit tip capacity (kN/m^2)
ψ' dilation angle of soil
$N^{"A}$, $N^{"B}$ as in Table 1; superscript indicates the method or route (A or B) used to derive g_n' and D_r.

REFERENCES

Ab.Malik, R. 1996. Design of pile foundation: correlation of safety measures from deterministic and reliability-based approach. *J. Insti Engi.* Malaysia **57: (1).**

Baguelin, F., J.F. Jezequel and D.H. Shields. 1978. The Pressuremeter and Foundation Engineering. *Trans Tech Publication.* Ed. A.R. Bazaraa, W. Germany, Clausthal-Zellerfeld. (1982). Standard Penetration Test, in Foundation Eng., Vol 1, Soil properties – Foundation Design & Construction, Ponts et Chaussees.

Bolton, M.D. 1986. The strength and dilatancy of sands. *Geotechnique* 36, No. 1, U.K.,: 65-78.

Bolton, M.D. 1987. Discussion on the strength and dilatancy of sands. *Geotechnique* **37(2)**: 219-226.

Coyle,H.M. and R.R. Costello. 1981. New design correlations for piles in sand. *J. Geot. Eng.* (ASCE) July **107(17).**

D'Appolonia, D.J., E.D' Appolonia and R.F. Brisette. 1970. Discussion on settlement of spread footings on sand. *Jour. Soil. Mech. & Found. Div.* ASCE.

Fleming, W.G.K., A.J. Weltman, M.F. Randolph and W.K. Elson. 1992. *Piling Engineering.* 2nd Ed. Glasgow: Blackie Halsted Press.

Gibbs, H.J. and W.G. Holtz. 1957. Research on Determining the Density of Sands by Spoon Penetration Testing. In *Proc. 4th Int. Conf. Soil. Mech. & Foun. Eng.*, Vol. 1. London.

Gibson, R.E. 1950. *J. Inst. Civ. Engrs* **34:** 382-383.

Heerema, E.P. 1980. Predicting pile drivability: heather as an illustration of the friction fatigue theory. *Ground Eng.*, Apr. 13.

Heydinger, A.G. 1984. Predicted and Observed axial Behaviour of Piles; Northwestern Pile Prediction Symposium; ASCE, *Geo.* Pub. No. 23.

Briaud, J.L. 1992. *The Pressuremeter.* Rotterdam, Brookfield: Balkema.

LEHANE, B.M., R.J. JARDINE, A.J. BOND and R. FRANK. 1993. Mechanisms of shaft friction in sand from instrumented pile tests. *J. Geo. Eng.* Div. ASCE 119, No. 1.

LIAO, S.S and R.V. WHITMAN. 1986. Overburden correction factors for sand, *J. Geo. Eng.*, ASCE, Vol.112, No. GT3, Mar.

MEYERHOF, G.G. 1976. Bearing capacity and settlement of pile foundations. *J. of Geo. Eng. Div. ASCE* **102**: GT3.

MEYERHOF, G.G. 1959. Compaction of sands and the bearing capacity of piles. *JSMFD.* ASCE.

PECK., R.B., W.E. HANSON and T.H. THORNBURN. 1974. *Foundation Engineering.* 2nd Ed. New York: John Wiley and Sons.

POTYOUNDY, H.G. 1981. Skin friction between various soils and construction materials. *Goetechnique* **2**: 339-353.

SHIOI, Y., & J. FUKUI. 1982. Application of N-Value to Design of Foundation in Japan. 2nd ESOPT. Vol. 1.

THORNBURN, S. and R.S. MAC VICAR. 1971. Pile Load Tests to Failure in the Clyde Alluvium, Proc. Load Test to Failure in the Clyde Alluvium, *Proc. Conf., Behaviour of Piles,* London.

VESIC, A.S. 1975. Bearing capacity of shallow foundation. In *Handbook of Foundation Engineering.* Van Nostrand, New York.

WOLFF, T.H. 1989. Pile capacity prediction using parameter functions, Results of a pile Prediction Symposium, ASCE *Geo.* Special Publication No.23.

YU, H.S and G.T. HOULSBY. 1991. Finite cavity expansion in dilatant soils: loading analysis. *Geotechnique* **41(2)**: 173-183.

ISSN: 0128-7680
Pertanika J. Sci. & Technol. Supplement 9(1): 23 - 30 (2001)

Experimental Evaluation of Hydraulic Performance of Outlet Structures with Baffle Blocks under Supercritical Flows

Aziz F. Eloubaidy, J.A. Maatoq & Abdul Halim Ghazali
Department of Civil Engineering
Faculty of Engineering,
Universiti Putra Malaysia
43400 UPM, Serdang, Selangor

ABSTRACT

The design of outlet transition in field irrigation system requires the flow attaining a uniform velocity at the end of such structures. In addition, supercritical flow condition requires maximising the dissipation of hydraulic energy possessed by the flowing water to hold its erosion capacity to a minimum. Floor baffle blocks incorporated in the outlet transition are useful for the above objectives. This laboratory investigation attempts to evaluate the effects of the relative sizes and arrangements of different types of baffle blocks on hydraulic performances of outlet transition of different configurations operating at supercritical flow conditions.

Dimensional analysis techniques were used to develop dimensionless ratios describing the geometry and the flow within an outlet transition containing certain types of appurtenance structures. The solution was evaluated in the laboratory with respect to measurable elements of the flow to achieve standardisation and general evaluation of the effectiveness of the different types of baffle blocks. The results are presented in the form of dimensionless plots, which show the variation of the ratios developed earlier, with the controlled variation of Froude numbers.

Expanding channel outlet transitions of straight-wall type of angle 10 o , 20 o and 30 o with two expansion ratios of 4 and 6 were tested with and without floor baffles. The outlets with baffles are generally found to be effective in creating optimum flow conditions than the plain outlets. The use of baffles also resulted in higher dissipation of energy within the outlets, with baffles having curved upstream edge (in plan) dissipated up to 42.7% more energy than the plain outlets.

Keywords: Outlet structures, baffle blocks, hydraulic energy dissipation, velocity distribution

INTRODUCTION

In field irrigation system, outlet structures are normally placed as a transition between the end of a conveyance conduit and the entrance to the earthen delivery canal. The free surface flow in the outlet structures can either be supercritical or subcritical. The high velocity super critical flow possesses a high percentage of kinetic energy and hence high capacity for erosion. In addition, the flow conditions are complicated by the likelihood of flow separation along one or both expansion walls normally associated with the outlet structures. The occurrence of either of these separations may lead to disastrous results in the unlined channel downstream in the form of scour, either to the banks or to the channel bed.

In view of the above facts, for the outlet structures with supercritical flow condition, it is imperative as much energy as possible should be dissipated from the flow prior to its entering the delivery canal. Another design consideration of an outlet structure is the attainment of uniform velocity distribution along the end section of the structure. As shown by Abdul-Nabi (1989), Miraigaoker and Swaroop (1967), Smith and James (1966) and Abdul-Hameed (1990), one way of achieving the aforementioned goals is by

installing baffle blocks on the outlet structure. Thus, the objective of this study is to evaluate the hydraulic performance of an outlet transition structure with an expanding channel with different configurations of baffle blocks under supercritical flow conditions.

DIMENSIONAL ANALYSIS

Evaluation of the effects of baffle blocks and other variables in simple outlet transitions is performed by dimensional analysis.

The head loss, hL, between sections 1 and 2 can be represented by

$$h_L = f_1 (Y_1, Y_2, V_1, D, B, \theta, W, w, h, r, \mu, \rho, \gamma) \quad (1)$$

where

Y_1 & Y_2 depths at sections 1 and 2 respectively,
V_1 the velocity at section 1, and
ρ, μ & γ the density, dynamic viscosity and weight respectively, of the fluid.

By the Pi-theorem and with the selection of Y_1, V_1 and r as the repeating variables the problem reduces to

$$\frac{h_L}{Y_1} = f_2\left(\frac{Y_2}{Y}, \frac{D}{Y_1}, \frac{B}{Y_1}, \frac{W}{Y_1}, \frac{w}{Y_1}, \frac{S}{Y_1}, \frac{h}{Y_1}, \frac{r}{Y_1}, \frac{V_1}{(\gamma/\rho Y_1)^{0.5}}, \frac{\rho V_1 Y_1}{\mu}, \theta\right) \quad (2)$$

where $\frac{V_1}{(\gamma/\rho Y_1)^{0.5}}$ is the Froude number F_1 and $\frac{\rho V_1 Y_1}{\mu}$ is the Reynolds number Re_1.

Variable factors may be combined to yield the following:

$$\frac{h_L}{Y_1} = f_3\left(F_1, Re_1, \frac{B}{D}, \frac{W}{D}, \frac{w}{D}, \frac{h}{D}, \frac{S}{W}, \frac{r}{h}, \frac{Y_2}{Y_1}, \theta\right) \quad (3)$$

Forces due to fluid viscosity are considered insignificant as compared to those of inertia, and hence Re_1 could be eliminated. Also for free hydraulic jump, the following relationship holds (Chow 1959),

$$\frac{Y_2}{Y_1} = f_4(F_1) \quad (4)$$

By combining Eqn. (4) with the well-known expression relating hL with the head loss coefficient, C_L such that

$$h_L = C_L \frac{V_1^2}{2g} \quad (5)$$

the following formulation is obtained:

$$C_L = f_5\left(F_1, \frac{B}{D}, \frac{h}{D}, \frac{w}{h}, \frac{r}{h}, \frac{S}{W}, \theta\right) \quad (6)$$

The significance of some of the above parameters may be stated as follows:

B/D (expansion ratio): It indicates the width of the channel after the outlet transition.
h/D (height ratio): It is a design parameter which provides the practical and the most feasible height of baffle blocks to be used under a given diameter of the incoming pipe.
S/W (spacing ratio): This ratio indicates the relative spacing of baffle blocks, which would influence the velocity distribution at the downstream end.
r/h (curvature ratio): It indicates the degree of curvature of the curved baffle blocks used in the study.

EQUIPMENT AND METHODS

The equipment consists of a discharge flume and devices to measure the discharge, depth and velocity of flow. The flume is made up of a truss-supported channel, which is 20 m long, 0.9 m wide and 0.6 m in depth. Water is supplied to the channel over a calibrated V-notch weir from an inlet tank that receives the water from a large sump through a centrifugal pump. The rate of flow of water is controlled by a gate valve and a by-pass valve located in the supply pipe. The depth over the weir is measured with a hook gauge fixed at a distance 1 m upstream of the weir. The depth measurement in the flume is made using a point gauge with a vernier scale, which is movable horizontally and vertically to any point.

A pitot tube fitted to the bottom of a gauge is used to measure the velocity of flow at any point. The velocity head is represented by the differential reading of a U-shape manometer connected to the pitot tube. The velocity can be calculated from the following formula

$$V_p = C_p\sqrt{2gh_p} \quad (7)$$

where Vp - velocity of flow
Cp - coefficient equal to 0.96 as suggested by Al-Tahir (1987)
hp - differential reading on the manometer

A plastic pipe of diameter, D, equals to 15 cm represents a closed conduit through which the water flows before exiting into the transition outlet structure. Three configurations of outlet structures are constructed and tested, with divergence angles, θ, of 10°, 20° and 30°. Baffle blocks on the outlet structure used are the floor baffles blocks, which are divided into two groups. Group A is divided into four subgroups of regular straight baffle blocks, each with different height and width ratios. Group B, with curved floor blocks, is divided into three subgroups; the first two with different radii of curvature, and the third with a straight edge (as shown in Fig. a). The dimensions of each model in each group are given in Table 1.

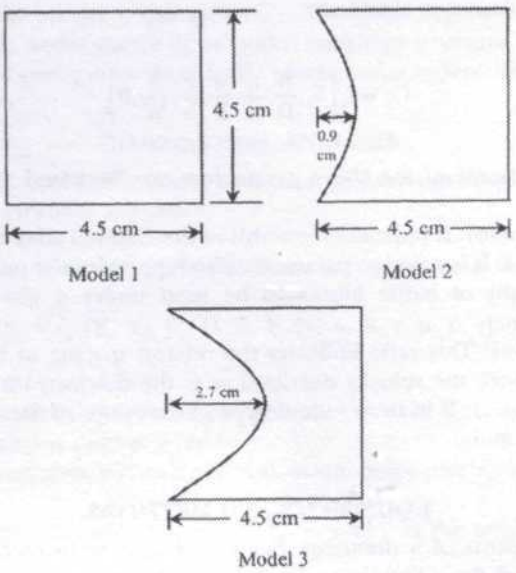

Fig 1. Baffle blocks of Group B in plan

TABLE 1
Dimensions of baffle block models

	No.	Height	Width	Thickness	Radius of curvature
GROUP A	1	2.25	2.25	2.25	-
	2	3.0	3.0	3.0	-
	3	4.5	4.5	4.5	-
	4	2.25	4.5	2.25	-
GROUP B	1	4.5	4.5	4.5	-
	2	4.5	4.5	4.5	0.9
	3	4.5	4.5	4.5	2.7

All dimensions in cm.

A series of tests were conducted for various specific purposes. These can be summarised as follows:

Series 1: Performed on model A2 with $\theta = 10°$ and B/D = 4, to show the effect of spacing ratio on lateral velocity distribution.

Series 2: Performed on model A2 with $\theta = 10°$ and B/D = 4, to show the effect of spacing ratio on head loss coefficient.

Series 3: Performed on models A1, A2, A3 and A4 with $\theta = 10°$ and B/D = 4, to show the effect of straight-edged baffle blocks on head loss coefficient.

Series 4: Performed on model B1, B2, and B3 with θ =10° and B/D = 4, to show the effect of block curvatures on head loss coefficient.

Series 5: Performed on model B3 with θ = 10°, 20° and 30° and B/D = 4, to show the effect of divergence angle on head loss coefficient.

Series 6: Performed on model B3 with θ = 30° and B/D = 6, to show the effect of expansion ratio on head loss coefficient.

RESULTS AND DISCUSSION

The effectiveness of using floor baffle blocks in the outlet transition structures is hereby examined in terms of their relative size, spacing, curvature and location in transition outlets of different divergence and expansion values. The problem is too complex to be evaluated in terms general enough for use in the design of such structures.

Keeping in mind that the main objectives in evaluating the hydraulic performance of outlet transition with certain baffle blocks is to create optimum condition of flow having a low erosion capacity, and also, with a needed amount of energy loss, it would be reasonable to adopt both the degree uniformity in velocity distribution at the end section of the structure and the head loss coefficient, C_L, as the indicators of the hydraulic performance. The higher values of C_L would represent a greater efficiency in energy dissipation when the outlet is operating under supercritical flow condition.

The results of this study are presented in the form of dimensionless plots, which show the variations of variables developed through the dimensional analysis. These plots show the variations of C_L with the upstream Froude number, F_1, and the controlled variations of other variables.

The head loss coefficient, not being a constant, is a function of F_1, and other terms representing the flow and geometry of the outlet transition. On the other hand, the velocity distributions at the downstream sections are prepared and presented in plots. With these plots one could deduce the best type, size and arrangement of baffle blocks.

In the Series 1 tests, the floor baffles were fixed at one location, and in one row, for all experiments conducted. The spacing ratio, S/W, tested were 0.1, 0.2 and 0.3. The resulting effects of the ratios on the velocity distribution across the downstream end of the outlet are illustrated in Fig. 2, with due comparison to the plain transition. As seen from these results, a spacing ratio of 0.2 is the most effective in diffusing the flow more uniformly at the end of the outlet structure. At this ratio, the width of the outlet at the location of the baffle blocks is divided by the baffles into approximately equispaces leading to the uniformity of flow issuing from these spaces.

The results of the Series 2 tests, which shows the variation of C_L with F_1 for different spacing ratios are shown in Fig. 3. It can be seen that an outlet with a spacing ratio of 0.2 provides better performance than the other ratios. Also, the effect of spacing ratio on the performance tends to decrease as the Froude number increases. Analysis of the results on the additional percentage of energy dissipation produced with baffle blocks at different spacing ratios, as compared to energy dissipation within plain outlet, shows that the largest additional dissipation of 32.5% was achieved with the spacing ratio of 0.2, under the following condition:

Upstream Froude number, F_1 = 2.2
Height ratio, h/D = 0.2
and Width ratio, w/h = 1.0

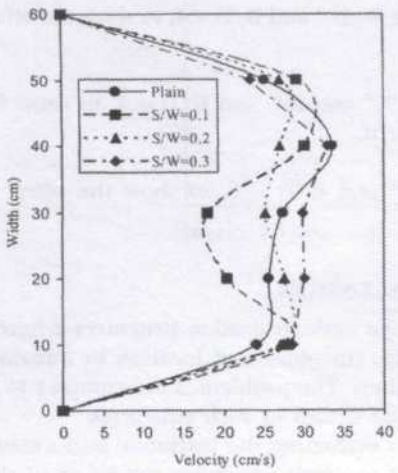

Fig.2. Effect of spacing ratio on velocity distribution

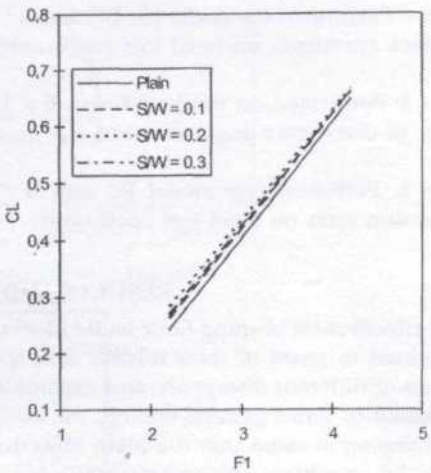

Fig.3. Effect of spacing ratio on head loss coefficient

Series 3 tests were performed with the optimum spacing ratio of 0.2. The effect of the height of the blocks on the head loss coefficient is given in Fig. 4. It clearly shows that as the height of the block increases, the head loss coefficient also increases. This could be due to the increase in the area resisting the flow with a corresponding increase in the loss of energy due to rolling and turbulence. In terms of additional dissipation, the largest value obtained was 35%, which occurred when the height ratio was 0.3 and the Froude number was 2.2.

The results obtained from the Series 4 tests are shown in Fig. 5. These indicate that, for all flow values, the curved baffles are generally more effective as energy dissipators compared to the straight-edged baffles. The figure also illustrates that greater dissipation of energy is obtained with the curvature ratio, r/h, of 0.6. The visual observation on the

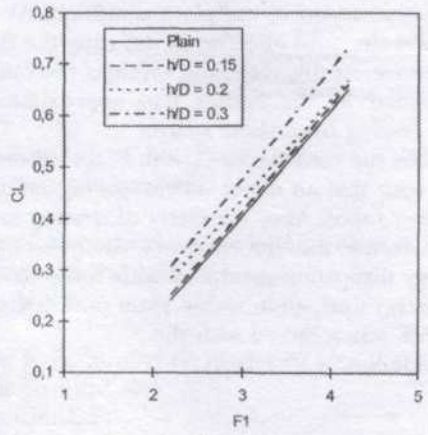

Fig. 4. Effect of height ratio on head loss coefficient

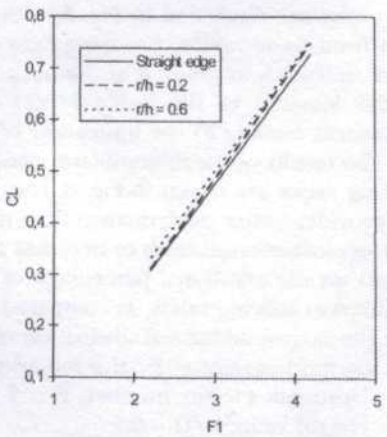

Fig.5: Effect of curvature ratio on head loss coefficient

flow pattern in the outlet structure verifies the finding of a previous work (Abdul-Nabi 1989), that better stability of hydraulic jump was observed with curved baffles. The largest additional dissipation with curved baffles was 42.74%, while the corresponding value with straight baffles was 35%; both obtained under the same conditions.

The results of the experiments in Series 5 are shown in Fig. 6. These illustrations indicate clearly that energy loss within the outlet transition decreases as the divergence angle increases. This finding could be attributed to the fact that with more divergence the width of flow at section 1 becomes larger, and as a result, for a given discharge, the velocity becomes smaller. This reduction in velocity leads to less amount of eddies and turbulence in the flow between sections 1 and 2 with a corresponding decrease in head loss.

Tests in Series 6 were carried out to evaluate the effect of expansion ratio, B/D, on the hydraulic performance of an outlet structure. The results of these tests are shown in Fig. 7, which reveals that as the expansion ratio increases, the dissipation of energy tends to increase. Such expected increase is due mainly to the increase in the length of the transition, and hence the boundary area resisting the flow.

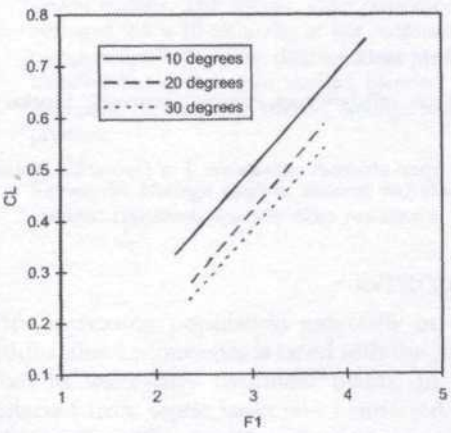

Fig. 6. Effect of divergence angle on head loss coefficient

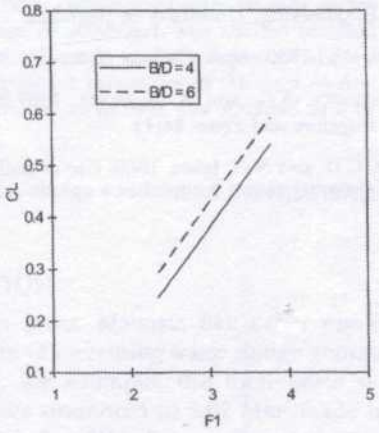

Fig. 7. Effect of expansion ratio on head loss coefficient

CONCLUSION

The use of floor baffles in the outlet transition structure has been shown to result in a more uniform velocity distribution at the downstream end of the structure. Baffles are also effective in the dissipation of more energy contained in the supercritical flow within the structure. There is a set of conditions which involve the size, shape and location of the baffles which gives rise to the optimum flow condition to satisfy the requirements for uniform velocity and large energy dissipation in the structure.

NOTATION

B - Width of downstream channel after transition
D - Diameter of incoming pipe
F_1 - Froude number at section 1

h - Height of baffle blocks
Re_1 - Reynolds number at section 1
r - Radius of curvature of baffles
S - Spacing between baffles
W - Width of transition at upstream face of baffles
w - Width of baffles
Y_1 - Depth at section 1 (upstream depth)
Y_2 - Depth at section 2 (downstream depth)
q - Angle of divergence of transition wall

REFERENCES

ABDUL-HAMEED, M.R. 1990. Hydraulic performance of stilling basin with curved appurtenances, M.S. Thesis, College of Engineering, University of Baghdad.

ABDUL-NABI, J.H. 1989. Dissipation of hydraulic energy by curved baffles, M.S. Thesis, College of Engineering, University of Baghdad.

AL-TAHIR, L.A.J. 1987. Characteristics of irrigation regulators with flat beds, M.S. Thesis, College of Engineering, University of Baghdad.

CHOW, V.T. 1959. *Open Channel Hydraulics.* New York: McGraw Hill.

MIRAIGAOKER, A.G. and A. SWAROOP. 1967.Studies on efficiency of energy dissipating blocks. *J. Irrigation and Power* **24(1)**

SMITH, C.D. and N.G. JAMES. 1966. Use of baffles in open channel expansion. *J. of Hydraulics Division* ASCE 92(HY2): 1-17.

ISSN: 0128-7680
Pertanika J. Sci. & Technol. Supplement 9(1): 31 - 37 (2001)

Natural Polyelectrolyte in Waste Sludge Treatment

Suleyman Aremu Muyibi, Megat Johari Megat Mohd Noor, Ding Tai Ong & Khor Woon Kai
Department of Civil Engineering,
Faculty of Engineering, Universiti Putra Malaysia,
43400 UPM, Serdang, Selangor

ABSTRACT

The study involved laboratory based investigations to determine the efficacy of a Natural Polyelectrolyte, *Moringa oleifera* seeds as a waste sludge conditioner. Waste sludge samples are activated sludge from Taman Tun Dr. Ismail Wastewater Treatment Plant, Kuala Lumpur, Malaysia. *Moringa oleifera* seed was applied as dry powder(shelled blended), solution(shelled blended) and solution(shelled blended oil extracted) . Results of the studies showed that *Moringa oleifera* improved the filterability of waste sludge up to 62 % in the optimum dosage range of 3000 to 6000mg/l. Sludge volume reduction of up to 65% was also achievable using gravity filtration compared to the control (no *Moringa oleifera* added). The specific cake resistance of sludge conditioned with *Moringa oleifera* averaged 2.5 x 10 12 m/kg at the optimum dosage of 4000mg/l. The shelled blended category applied in dry powder form performed the same as the solution of shelled blended but better than shelled blended oil extracted categories of *Moringa oleifera*. Vegetable oil from the shelled *Moringa oleifera* seed of up to 30% was obtained as a by product.

Keywords: *Moringa oleifera*, natural polyelectrolyte, sludge conditioner, gravity settling, vacuum filtration, specific cake resistance

INTRODUCTION

With increasing population especially in urban areas, Malaysia like other emerging industrialised economies is faced with the problem of increasing waste sludge generation from its wastewater treatment plants. In 1994, for example, the total waste sludge collected from septic tanks and connected services amounted to 3.02 Mm^3 made up of 1.13 Mm^3 (37%) from septic tanks and 1.89Mm^3 (63%) from connected services, increasing to 3.4 Mm^3 in 1998. There is, however, a reduction in sludge production of 32 % from septic tanks, with increase in those from connected services to 68 % during the four-year period. The overall increase in sludge production is about 15% in four years (Indah Water 1997). In 20 years, the projected increase in sludge production will be about 75 % using 1998 as base year. The current method of sludge disposal is made up of oxidation pond/aerated lagoons (50 %), drying beds (30 %), others (oxidation ditch, bio-filter, SBR etc. 20%. All these technologies especially oxidation ponds, and drying beds require the use of large areas of land which is a dwindling resource with increasing industrialisation and urbanisation.

The conditioning of waste sludge involves pre-treatment in order to facilitate water removal during subsequent hickening and or dewatering operations. During conditioning, small and amorphous particles are transformed into larger and stronger aggregates. This process increases the rate of water drainage and solid separation. In most dewatering operations, the ability of sludge to form and maintain a porous structure that enhances its compressibility is the desired goal (Clarke *et al.* 1997).

Sludge conditioners may be physical conditioners e.g. fly ash, diatomaceous earth etc or chemical conditioners viz. inorganic compounds (ferric chloride, lime etc) and

synthetic polymers. Synthetic polymers that can be used to alleviate this problem are expensive and have to be imported with scarce foreign currency. A natural polymer that is affordable and environmentally friendly (highly biodegradable), *Moringa oleifera* seed has a potential to be used as a sludge conditioner for thickening and dewatering.

Moringa oleifera belongs to the family *Moringaceae* and is cultivated for a variety of purposes across the whole tropical belt (Jahn 1989). Many researchers have reported on its various uses as coagulant, Muyibi & Okuofu (1995), Ndabigengesere *et al.* (1995) and Muyibi (1998). The purpose of the present study, the first of its kind, was to evaluate the potential of *Moringa oleifera* seed as a natural polymer for use as sludge conditioner prior to dewatering and/ or thickening.

The study that is laboratory based involved using two methods of preparation of *Moringa oleifera* used in the investigation. The forms of *Moringa oleifera* used are, shelled blended, shelled dry powder, and shelled oil extracted. Waste sludge samples used for the studies were obtained from Taman Tun Dr. Ismail Wastewater Activated Sludge Treatment Plant, Kuala Lumpur, Malaysia.

METHODOLOGY

Equipment

A six place jar test apparatus, Jar-Tester CZ150 was used for mixing the *Moringa oleifera* seed with the waste sludge to enhance uniform and thorough distribution/mixing. National model MJ-C85N Juicer-blender with dry mill was used for the preparation of *Moringa oleifera* into powder and solution for use. Sohxlet apparatus was used to extract oil from *Moringa oleifera* seeds. Vacuum pump connected to a Buchner funnel attached to graduated thick walled flask was used for the determination of specific cake resistance. For gravity settling studies, 250ml graduated measuring cylinders were used.

Materials

Waste sludge samples used for the studies were collected from Taman Tun Dr. Ismail Wastewater Treatment Plant, Kuala Lumpur. The dry *Moringa oleifera* seeds used for the studies were obtained from Kano, Nigeria.

Procedure for Preparation of Moringa oleifera Seeds

The seed wings and coat were removed from selected dry good quality *Moringa oleifera* seeds and the nuts ground to a fine powder using the National MJ-85CN. The ground powder was divided into three portions. One portion had the oil extracted using the Sohxlet apparatus.

Stock solution of the seed powder with and without oil extracted were prepared by dissolving 5 grams of each type in 500 ml tap water and mixing it thoroughly at high speed in the National blender to extract the active ingredients. Any insoluble powder was filtered out using a muslin cloth and the concentrated stock solution of 10,000 mg/ l prepared. The third portion, the dry powder, was also set aside for use.

EXPERIMENTAL PROCEDURE

Determination of Sludge Volume Reduction with Increasing Moringa oleifera Dosage

200 ml of sludge samples were put into six, 500ml beakers and placed in the Jar Tester. The six paddles were inserted in the beakers and the speed set at 100 rpm. From the previously prepared stock solution of *Moringa oleifera* (shelled blended and shelled oil

extracted dosages with varying concentration of 1000 mg/1 to 6750 mg/1 were added simultaneously to all six beakers and mixed thoroughly for 1 minute. The six samples were immediately transferred into 250 ml measuring cylinders and the initial sludge heights recorded. A control sludge sample with no *Moringa oleifera* applied was also put in a measuring cylinder and the initial sludge height recorded. The sludge height after 30 minutes settling was recorded. The experiment was also carried out using varying doses of the dry *Moringa oleifera* (shelled) seed powder in the range of 500 mg (2500 mg/l) to 1400 mg(7000 mg/l). The results of the trial test gave the effective dosage in the range 3750 to 5000 mg/l.

Determination of Specific Cake Resistance

The specific cake resistance is used to evaluate the effect of different dosages of chemical conditioners and combination of sludge and conditioning agents on the specific resistance and quality of the cake. A plot of specific resistance versus dose can be used to determine the optimal operating condition.

Theory

Flow through the sludge cake and filter medium may be considered as flow through porous media. Darcy's law may be used to model the process.

$$Q = \frac{dV}{dt} = \frac{kA\Delta h}{\Delta L} \tag{1}$$

where Q = flow rate of filtrate
V = Volume of water
A = Area of flow
k = conductivity
h = head
L = distance
t = time

The resistance parameter depends on Reynolds number, porosity of the media, distribution of grains, and other characteristics of the media. Using the Hagen-Poiseuille law for pipe flow,

$$K = \frac{kg}{v} \tag{2}$$

where K = intrinsic permeability
v = kinematic viscosity
g = gravity

$$\frac{dV}{dt} = \frac{KA\Delta P}{\mu\Delta L} \tag{3}$$

where ΔP = positive pressure differential
ΔL = depth of the medium
μ = dynamic viscosity of the filtrate

The intrinsic resistance, r, may be defined as r = 1/k. The cake resistance Rc is given by

$$R_c = r_c \Delta L \tag{4}$$

where r_c = intrinsic resistance of cake.

The cake resistance and filter medium resistance are independent, so the total resistance, R of cake and filter may be added together to get,

$$R = R_c + R_f \tag{5}$$

where R_f = resistance of the filter medium

The volume of cake formed, V_c is

$$V_c = A\Delta L \tag{6}$$

Let the specific deposit, be the volume of cake formed per unit volume of filtrate, then

$$\sigma V = A\Delta L \tag{7}$$

Equation (3) becomes;

$$\frac{dV}{dt} = \frac{\Delta \Delta P A^2}{\mu(r_c \sigma V + R_f A)} \tag{8}$$

Expressing the intrinsic resistance, r_c, in terms of mass of dry cake solids formed per unit volume of filtrate,w,the specific resistance, r_{wc} is related to r_c by;

$$R_{wc} w = r_c \sigma \tag{9}$$

Substituting in equation(8) we have

$$\frac{dV}{dt} = \frac{\Delta \Delta P A^2}{\mu(r_{wc} w V + R_f A)} \tag{10}$$

$$\int_0^t dt = \mu \int_0^v \left(\frac{w r_{rc} V}{\Delta P A^2} + \frac{R_f}{\Delta P A} \right) dV \tag{11}$$

At constant pressure, on integration over time,

$$t = \frac{\mu w r_{wc} V^2}{2 \Delta P A^2} + \frac{\mu R_f V}{\Delta P A} \tag{12}$$

$$\frac{t}{V} = \frac{\mu w r_{wc} V}{2\Delta PA^2} + \frac{\mu R_f}{\Delta PA} \quad (13)$$

The specific resistance r_{wc} is calculated from the slope m of the line

$$r_{wc} = \frac{2\Delta PA^2}{\mu w} m \quad (14)$$

Procedure for the Determination of Specific Cake Resistance

200 ml of the sludge sample was placed in 500 ml beakers and varying dosages(1000 to 6000mg/l) of *Moringa oleifera* powder was added. The beakers were placed in the jar test apparatus. The paddles were inserted and thoroughly mixed at 100 rpm for 1 minute. The speed was reduced to 40 rpm and continuously stirred to prevent sludge settling. 50 ml of each of the prepared samples was added to the Buchner funnel containing a filter pad and connected to the vacuum pump. Vacuum pressure of 69000 N/m^2 was applied at 15 seconds intervals and the volume of the filtrate measured. Observations were made until the vacuum broke or the filtrate volume remained constant.

RESULTS AND DISCUSSION

Gravity Settling Studies

Table 1 shows the summary of the results of gravity settling of waste activated sludge for varying dosages of *Moringa oleifera*, shelled blended and shelled blended oil extracted from 3750 to 5000 mg/l. It was observed that increasing dosage of *Moringa oleifera* resulted in increasing reduction in sludge volume compared to the control. For the shelled blended category, from a control with sludge reduction of 4.6%, increasing dosage of *Moringa oleifera* resulted in increase in sludge volume reduction reaching a peak at 12% at 4750 mg/l dosage and reducing to 10 % at 5000 mg/l dosage. For the shelled blended oil extracted category, increasing dosage of *Moringa oleifera* also resulted in increased reduction in sludge volume from the control of 4% reduction to 6.7% at 3750 mg/l, to 8.7% at a dosage of 4250 mg/l and decreasing to a minimum of 7.3 % at 5000 mg/l dosage. Similarly, in Table 2 for the dry powder(shelled blended) application, it was observed that sludge volume reduction increased with increasing dosage of Moringa powder from 5 % at control to 13 % at 1200 mg (6000 mg/l). After which continued dosage gave constant sludge volume reduction.

When the results are compared to the control, it was observed that the shelled blended category was able to achieve a maximum of 2.6 times reduction in sludge volume compared to the control at a dosage of 4750 mg/l. The shelled blended oil extracted category was able to achieve a maximum of 1.9 times sludge volume reduction at dosage of 4250 mg/l . Application of the dry powder(shelled blended) was also able to achieve a maximum of 2.6 times sludge volume reduction compared to the control.

In general, application of the dry seed powder (shelled blended) was found to be more effective than using the shelled blended oil extracted solution. Further studies need to be carried out in terms of cost and ease of application, as well as equipment and facilities which will be required for each application method so as to select the most efficient method application. The findings from this study the first of its kind, has a potential for its application to existing sludge holding tanks and drying beds as well as new sludge treatment plants. The capacity of new sludge holding tanks and drying beds

can be reduced considerably whilst existing ones can be retrofitted with *Moringa oleifera* dosing system after pilot scale studies to enhance the filterability and settling characteristics of the sludge. It is pertinent to note that up to 30% vegetable oil was extracted from the shelled *Moringa oleifera* seed. Further studies may be carried to explore possible commercial use of the oil.

TABLE 1
Summary of results of gravity settling studies of waste activated sludge on application of varying dosages of *Moringa oleifera* seed (shelled blended and shelled oil extracted)

Dosage (mg/l)	Sludge volume reduction (%) after gravity settling for 30 mins.		Ratio of sludge volume reduction after gravity settling to control	
	Shelled Blended	Shelled blended oil extracted	Shelled blended	Shelled blended oil extracted
Control	4.6	4.6	1	1
3750	7.3	6.7	1.6	1.5
4000	8	8	1.7	1.9
4250	9.3	8.7	2	1.7
4500	9.3	8	2	1.7
4750	12	8	2.6	1.7
5000	10	7.3	2.2	1.6

TABLE 2
Summary of results of gravity settling studies of waste activated sludge on application varying dosages of dry *Moringa oleifera* seed powder (shelled)

Dosage of shelled blended Dry *Moringa* powder (mg)	Sludge volume reduction(% after gravity settling for 30mins.	Ratio of sludge volume reduction after gravity settling to control
Control	5	1
500(2500 mg/l)	9	1.8
600(3000 mg/l)	10	2
700(3500 mg/l)	11	2.2
800(4000 mg/l)	11	2.2
900(4500 mg/l)	11.5	2.3
1000(5000 mg/l)	12	2.4
1100(5500 mg/l)	12.5	2.5
1200(6000 mg/l)	13	2.6
1300(6500 mg/l)	13	2.6
1400(7000 mg/l)	13	2.6

Determination of Specific Cake Resistance and Optimum Dosage

For each dosage of shelled blended *Moringa oleifera* applied, plot of t/V versus V was plotted which gave straight lines from which the specific resistances were calculated using equation 14. From Fig. 4, it is observed that the optimum dosage of *Moringa oleifera* was 4000 mg/l with specific resistance, rwc of 2.5 x 10 12 m/kg for vacuum filtration. This value compares well with that reported by Droste(1997) for synthetic polymers.

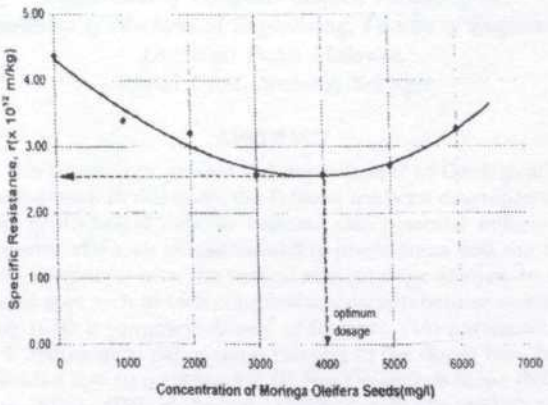

Fig. 1 Specific cake resistance variation with Moringa oleifera dosage

CONCLUSIONS

1. Within the economic dosage range of *Moringa oleifera* of 3750 to 5000 mg/l, sludge volume reduction increased with increasing dosage.
2. The shelled blended category applied in dry powder form performed better than the solution of shelled blended oil extracted categories of *Moringa oleifera.*
3. For vacuum filtration, the specific cake resistance was found to decrease with increasing dosage of *Moringa oleifera* to an optimum of 2.5 x 10^{12} m/kg at a dosage of 4000 mg/l.
4. Up to 30% vegetable oil was extracted from the *Moringa oleifera* seed using the Soxhlet method.

REFERENCES

CLARKE J. W., W. Jr. VIESSMAN and M. J. HAMMER. 1997. *Water Supply and Pollution Control.* Harper & Row Publishers.

DROSTE, R. L. 1997. *Theory and Practice of Water and Wastewater Treatment.* John Wiley & Sons Inc.

INDAH WATER SDN. BHD. 1997. Sludge treatment and disposal strategy. Planning Report.

JAHN, S. A. A.1989 Using *Moringa oleifera* seeds as coagulants in developing countries. *J. Amer. Water Works Association* **8**: 43 – 50.

MUYIBI, S. A. and C. OKUOFU. 1995. Coagulation of low turbidity surface waters with *Moringa oleifera* seeds. *International Journal of Environmental Studies* **48**: 263-273

NDABIGENGESERE, A., K.B. NARASIA and B.G. TALBOT. 1995. Active agents and mechanisms of coagulation of turbid waters using *Moringa oleifera. Water Res.* **(29)**: 703 – 710.

SULEYMAN AREMU MUYIBI. 1998. *Moringa oleifera* seeds in water treatment. *J. Insti. Engi. Malaysia.* **(59)3**: 37 – 50.

ISSN: 0128-7680
Pertanika J. Sci. & Technol. Supplement 9(1): 39 - 49 (2001)

Geological Rating for D-Slope

Husaini Omar[1], Mohamed Daud[2], Norwati Mustapha[3], Zainuddin Md. Yusof[1], M.R. Osman[4] & Ratnasamy M.[1]

[1]Department of Civil Engineering, Faculty of Engineering,
[2]Department of Biology and Agriculture, Faculty of Engineering,
[3]Department of Computer Science, Faculty of IT,
[4]Department of Mechanical Engineering, Faculty of Engineering,
Universiti Putra Malaysia,
43400 UPM, Serdang, Selangor

ABSTRACT

The purpose of this paper is to present the development of Geological Rating (GR) to carry out slope assessment. In this study, the D-Slope has been developed using geological, hydrological and geotechnical data to evaluate the potential failure of slopes. The geological complexity, the scale of the instability phenomena and the high number of interacting factors complicate most the natural and cut slope analysis. In order to be able to have a structured approach to such complexity, a comprehensive method based on the Geological Rating (GR) is proposed. A total of fourteen (14) parameters (12 geological parameters and 2 hydrological parameters) relating to the slopes have been considered. The slopes are divided into four categories: (I) Not Dangerous Slope (NDS), (II) Slightly Dangerous Slope (SDS), (III) Moderately Dangerous Slope (MDS), and (IV) Highly Dangerous Slope (HDS). The definitions of these categories are discussed.

Keywords: Geological rating, slope stability, expert system

INTRODUCTION

Large-scale instability phenomena in natural and/or cut slopes frequently occur in structurally and geologically complex regions, particularly in the mountainous areas. Most mountainous areas, the topography is very steep and slope failures are often caused by the construction of roads. But, very little attention has been given to the assessment of slope stability when planning roads in steep mountainous areas. In fact, techniques of planning roads in mountainous areas have not yet been generalized and, at present, success of such works depends on the individual knowledge and experience of experts.

The purpose of this study is to develop an expert system that can be used to evaluate the potential failure of slopes.

Expert System

An Expert System is a system that employs human knowledge captured in a computer to solve problems that normally require human expertise. It is used to propagate scarce knowledge resources for improvement and results.

Expert Systems were developed by the Artificial Intelligence (AI) community as early as the mid 1960s. During the 1970s expert system was mostly a laboratory curiosity. Researchers are focussed on developing ways of representing and reasoning about knowledge in a computer, and not designing the actual system. Very few applications especially for engineers were developed. Most of the expert systems in 1970s were developed on powerful workstations using languages such as LISP, PROLOG, and OPS (Durkin 1994).

In 1979, a group of individuals who were intimately involved with the development of earlier expert systems met a workshop chaired by Don Waterman and Frederick

Hayes-Roth. This workshop was to exchange ideas or knowledge in the field of expert systems and also to formulate a way of developing such systems (Hayes-Roth *et al.* 1983).

During 1980s, the number of expert systems developed had slightly increased with a report of 50 deployed systems by 1985. Now, the increase is very rapid due to the spreading of the success stories of the technology. At present, with the Personal Computers and the introduction of easy-to-use expert system software development tool which is called "shell" are available the opportunity to develop an expert system is now in the hands of many individuals from all disciplines (Fig. 1). For example, a system called EXOFS was constructed with an expert system shell named Xi Plus from Inference Corporation. The shell includes both frame and rule representation (Turban 1992).

According to Turban (1992), Expert Systems can provide major benefits to users such as increased output and productivity, increased quality, reduced downtime, flexibility, reliability, accessibility to knowledge, and increased capabilities of other computerized systems.

The development of expert system in engineering field is still in the early stage. According to Durkin (1994), 150 expert systems have been developed in the engineering area. Manufacturing, business and medicine showed the highest expert systems application being developed. Fig. 2 shows the number of expert systems that have been developed in each area.

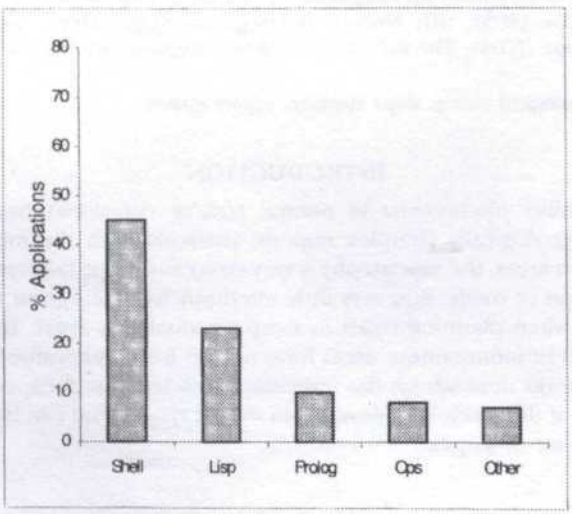

Fig 1. Software used in expert system development (Durkin J. 1994)

THE DEVELOPMENT OF D-SLOPE

The D-Slope is a system that imitates the reasoning processes experts used to solve slope stability problems. It is developed using three main types of data, namely:

1. Geological Data
2. Geotechnical Data
3. Hydrological Data

The aim of the D-Slope is to provide a technique for carrying out slope assessment in a proper manner. A number of steps have to be followed and these include the choice of parameters relevant to the problem and the rating assignment to different classes of

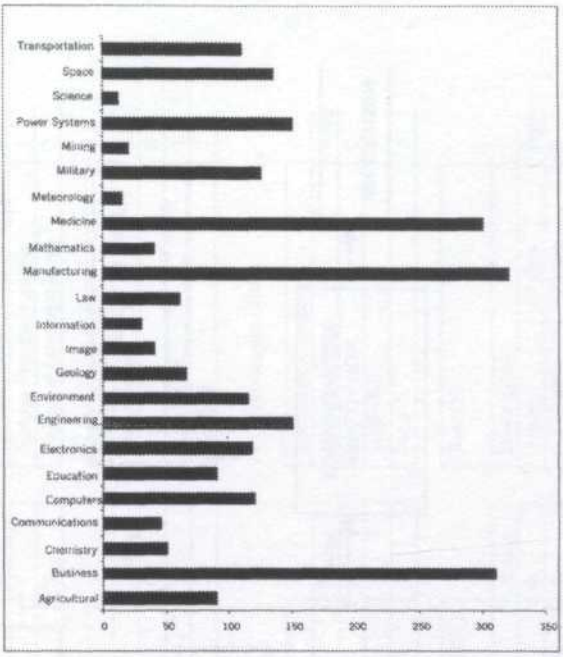

Fig 2. Number of developed expert systems in various application areas (Durkin J. 1994)

parameters. The progress chart for the development of D-Slope is shown in Fig. 3. The Geological Rating (GR) is proposed because of the need to incorporate these data into the analysis of the potential of slope instability. The proposed GR is discussed in detail in the next chapter.

Geological Data

Twelve (12) geological parameters are considered for the D-Slope and they are based on the of slope failures in tropical countries. The parameters are:

1. previous instability
2. faults
3. joints
4. folds
5. aperture
6. persistence
7. spacing
8. number of major sets
9. orientation
10. geology
11. weathering
12. slope dimension

According to Mazzoccola and Hudson (1996), the rating for the parameters is between 0 to 2. This is shown in Fig. 4.

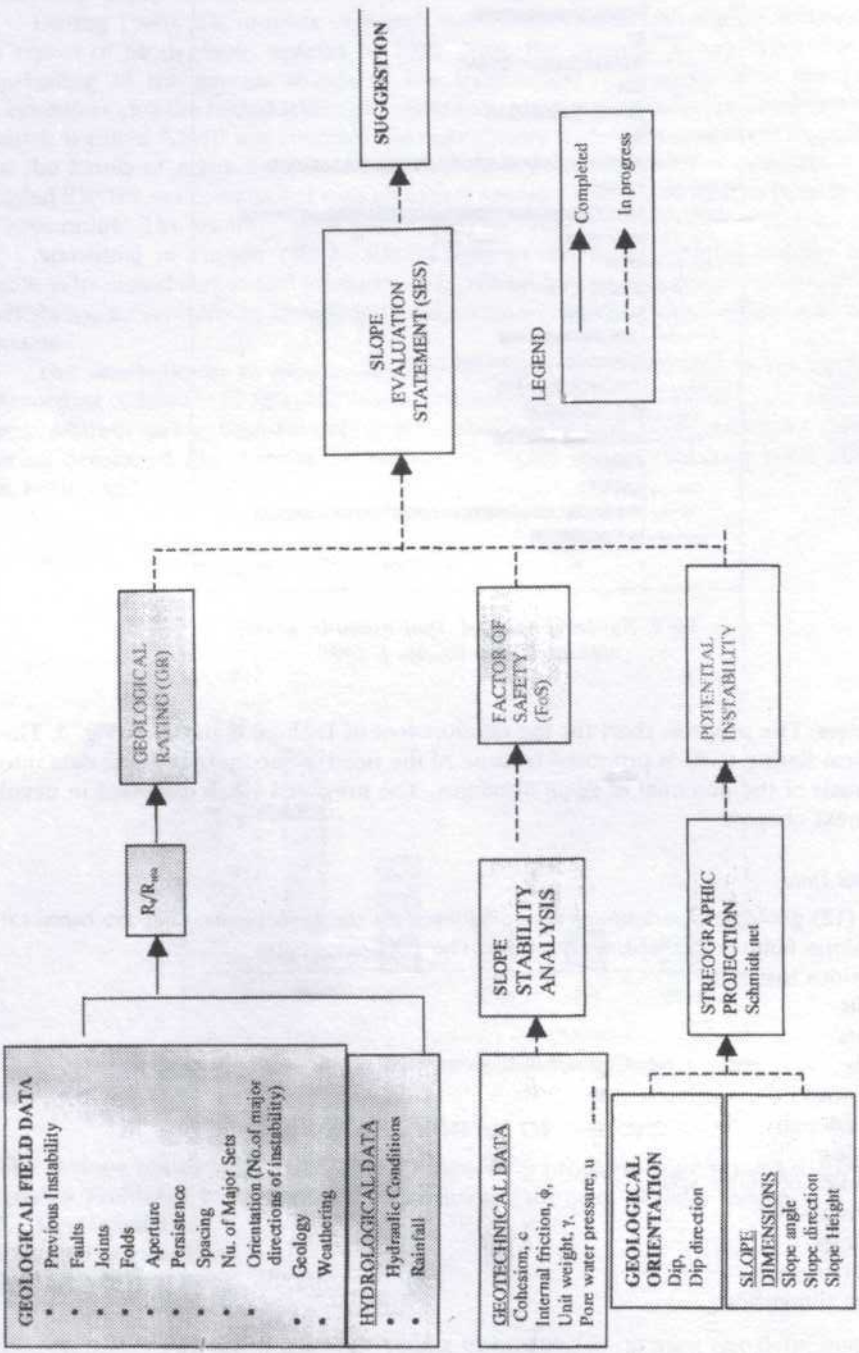

Fig 3. The progress chart for development of D-Slope

Geological Data

Faults	
on	Rating
Not present	0
Minor	1
Major	2

Spacing	
Description	Rating
Not present	0
Minor	1
Major	2

Geology	
Description	Ratir
Granite gneiss	0
Metasedimentary gneiss	1
Complex intercalations	2

Aperture	
Description	Rating
< 10 mm	0
10-50 mm	1
> 50 mm	2

Number Of Major Sets	
Description	Rating
1	0
1-3	1
4	2

Slope Dimensions	
Description	Ratir
4 m	0
4 m-100 m	1
> 100 m	2

b) Hydrological Data

Persistence	
Description	Rating
< 5 m	0
5-10 m	1
> 10 m	2

Weathering	
Description	Rating
Unweathered	0
Discolored	1
Infilling material	2

Hydraulic Conditions	
Description	Ratir
Dry	0
Wet	1
Flow	2

Orientation (no. of major directions of instability)	
Description	Rating
< 2	0
2-5	1
> 5	2

Mechanical properties (JRC)	
Description	Rating
> 14	0
7-14	1
<7	2

Rainfall		
Description		
3 days	10 days	Ratir
< 110 mm	170 mm	0
110-220m m	170-330 mm	1
>220 mm	> 330mm	2

Fig 4. The rating parameters (Mazzoccolla and Hudson 1996)

Geotechnical Data

Four geotechnical parameters are considered which are cohesion, internal friction, unit weight and pore water pressure. These parameters are needed to calculate the Factor of Safety of the slopes. The Factor of Safety of the slope is part of the criteria that determines the slope condition.

Hydrological Data

There are two hydrological parameters they are hydraulic condition and rainfall. The rating of these two parameters are shown in Fig. 4.

THE GEOLOGICAL RATING (GR)

Based on the three main types of data for the D-Slope, a total of 14 parameters (12 geological parameters and 2 hydrology parameters) are selected to develop the Geological Rating (GR). The data for the parameters was collected at Pos Selim Highway. This highway is still under construction by MTD Capital Bhd. The sample of field data is shown in Fig. 5.

DATA SHEET: 1
CHAINAGE : CH 3+370 TO CH 3+430 DATE : 14.4.1999
LOCATION : CH 3+400 TIME : 10.00A.M.
GEOLOGICAL AFFECTED AREA (GA): 402 m^2 ANGLE OF FRICTION (φ): 34.65°
INVESTIGATED AREA (IA): 1110 m^2 DENSITY OF SOIL (γ): kg/m^3
COHESION (C): 11.9 kg/m^2 WATER LEVEL: m

	DESCRIPTIONS	RATING	REMARKS
GEOLOGY	GRANITE	2	COMPLEX
ORIENTATION	3	1	
SLOPE DIMENSIONS	37m	1	
WEATHERING	MODERATELY TO COMPLETELY	2	
HYDRAULIC CONDITIONS	FLOW	2	
PREVIOUS INSTABILITY	ACTIVE	2	
RAINFALL	175mm(3days) 300(10days)	1	

GEOLOGICAL STRUCTURES	MAJOR/ MINOR	APERTURE (mm)	PERSISTENCE (m)	NO. OF SETS	SPACING (m)
JOINTS	MAJOR	1-15	8-30	3	0.34-1.75
RATING	2	0	2	1	0

DIP(°)	DIP DIRECTION(°)
50	120
58	240
30	070

Fig 5. Pos Selim data sheet

The individual parameter rating based on Mazzaccolla and Hudson (1996) is then assigned to the field data. The total rating for each location of the slope, R_t, is calculated. The maximum rating, R_{max}, is 28. The Rt at each location is tabulated in Table 1.

The formula for Geological Rating (GR) is shown below.

$$GR = R_t / R_{max} \quad (1)$$

where,

GR = Geological Rating
R_t = Total individual rating collected at site
R_{max} = Maximum rating

Thus, based on the above formula, the GR then calculated and is shown in Table 2.

TABLE 1
The total individual rating collected at site

Location	Slope Height	R_t
CH 3400	37	16
CH5080	28	14
CH6800	17	11
CH8870	48	16
CH9100	49	15
CH10360	24	15
A	8	10
B	12	15
C	13	17
1UPM	8	11
2UPM	7	14
3UPM	7	11

TABLE 2
The Geological Rating

Location	Slope Height	GR
CH 3400	37	0.667
CH5080	28	0.583
CH6800	17	0.458
CH8870	48	0.667
CH9100	49	0.625
CH10360	24	0.625
A	8	0.417
B	12	0.625
C	13	0.708
1UPM	8	0.458
2UPM	7	0.583
3UPM	7	0.458

The graph GR versus Slope Height is plotted below (Fig. 6). From the graph of correlation between GR and Slope Height, there is an indication showing that the GR increases with the increase of the Slope Height.

The data for Geological Affected Area, GA, is obtained at the site. The Area Ratio,

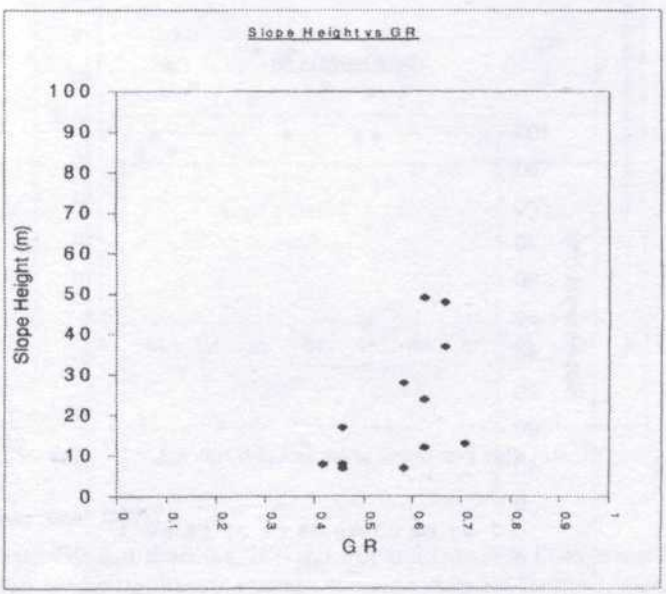

Fig. 6. Slope height vs geological rating

AR is calculated by dividing GA with Investigated Area, IA.

$$AR = GA/IA \quad (2)$$

where,

AR = Area Ratio
GA = Geological Affected Area
IA = Investigated Area

The results of AR are summarized in Table 3 below. Correlation is made between AR and the Slope Height. This is shown in Fig. 7. From the graph, the AR increases with the increase of the Slope Height.

TABLE 3
The results of calculated Area Ratio

Location	Slope Height	AR
CH 3400	37	0.300
CH5080	28	0.429
CH6800	17	0.526
CH8870	48	0.361
CH9100	49	0.347
CH10360	24	0.952
A	8	0.075
B	12	0.129
C	13	0.149
1UPM	8	0.250
2UPM	7	0.178
3UPM	7	0.101

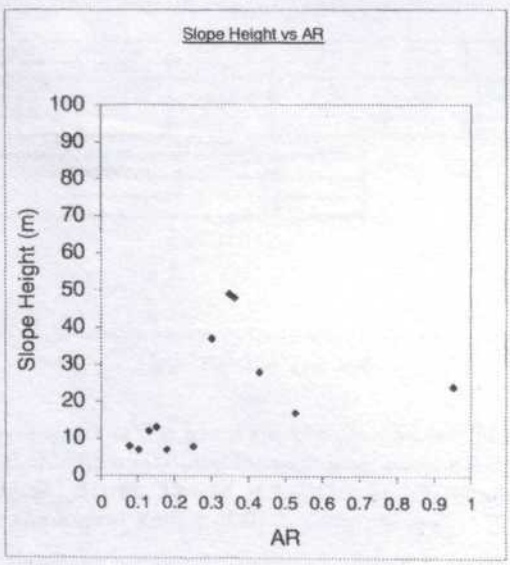

Fig. 7. Slope height vs area ratio

Slope Category

For the D-Slope to perform the assessment, the slope category is required. A correlation between GR and AR is developed. This is shown in Fig. 8. From the graph, a simple slope category is proposed. The proposed slope categories are:

I Not Dangerous Slope (NDS)
II Slightly Dangerous Slope (SDS)
III Moderately Dangerous Slope (MDS)
IV Highly Dangerous Slope (HDS)

Based on Fig. 8, the range of GR for each category is selected. This is summarized in the Table 4 below.

The definition of each slope category is described below.

TABLE 4
The slope category and the range of GR

Slope Category	Geological Rating (GR)
Not Dangerous	$0 < GR \leq 0.4$
Slightly Dangerous	$0.4 < GR \leq 0.5$
Moderately Dangerous	$0.5 < GR \leq 0.6$
Highly Dangerous	$0.6 < GR \leq 1.0$

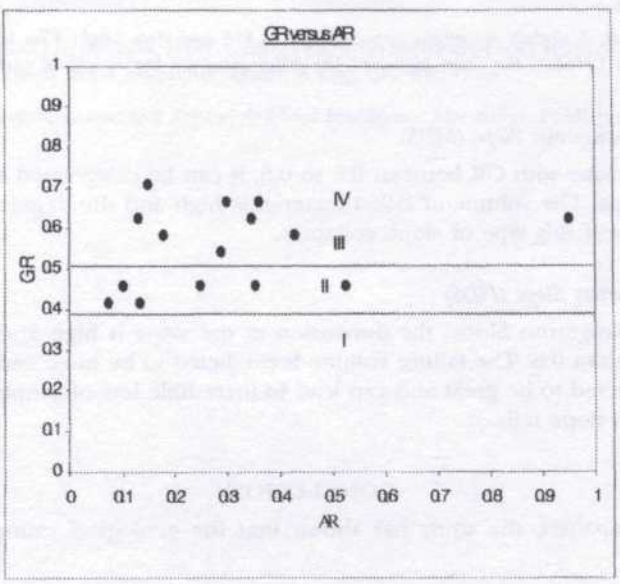

Fig. 8. Geological rating versus area ratio

I Not Dangerous Slope (NDS)

For a slope with GR less than 0.4, it is categorized into Not Dangerous Slope because the destruction is not significant enough to cause damage to the highway even if the slope collapses.

II Slightly Dangerous Slope (SDS)

For a slope to be rated as Slightly Dangerous Slope, its GR is normally between 0.4 to 0.5. It is said to be slightly dangerous because the failure of this kind of slope would only be a temporary nuisance to the highway by partially closing the road and in addition the remedial cost is low. Fig. 9 shows a slope rated as SDS is situated at CH6800 Pos Selim Highway.

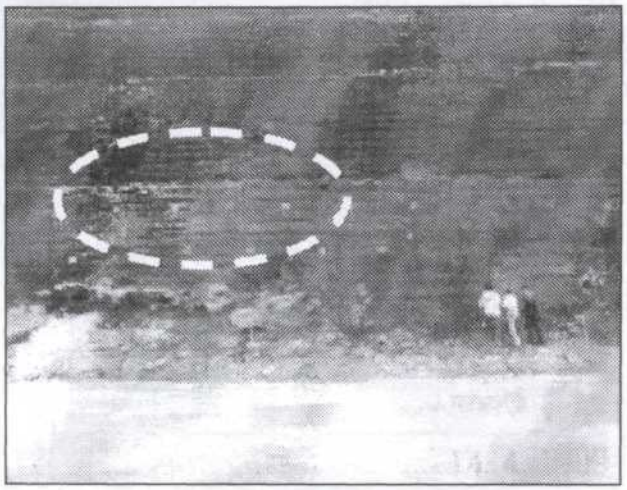

Fig. 9. A slightly dangerous slope with GR 0.458 and slope height 17m located at CH6800 Pos Selim highway. The failed areas are highlighted in circle.

III Moderately Dangerous Slope (MDS)

Basically for a slope with GR between 0.5 to 0.6, it can be categorized as a Moderately Dangerous Slope. The volume of failed material is high and the degree of hazard and risk is moderate if this type of slope collapses.

IV Highly Dangerous Slope (HDS)

For a Highly Dangerous Slope, the dimension of the slope is high and the geological rating is more than 0.6. The failure volume is predicted to be huge and the severity of damage is expected to be great and can lead to incredible loss of properties and heavy casualties if the slope fails.

CONCLUSION

Based on the analysis, the study has shown that the geological rating (GR) can be expressed as:

$$GR = R_t / R_{max}$$

where,

GR = Geological Rating
R_t = Total individual rating collected at site
R_{max} = Maximum rating

The slope categories can be expressed with GR as follows:

I Not Dangerous Slope, $0 < GR \leq 0.4$
II Slightly Dangerous Slope, $0.4 < GR \leq 0.5$
III Moderately Dangerous Slope, $0.5 < GR \leq 0.6$
IV Highly Dangerous Slope, $0.6 < GR \leq 1.0$

NOTATION

GR Geological Rating
Rt field affected geological rating
R_{max} maximum rating for the geological parameters
AR Area Ratio
GA Geological Affected Area
IA Investigated Area

ACKNOWLEDGEMENTS

The authors wish to thank MTD Capital Berhad and its subsidiaries for the assistance accorded in giving the data and support throughout this study.

REFERENCES

DURKIN, J. 1994. *Expert Systems, Design and Development.* Prentice-Hall, Inc.

HAYES-ROTH, F., D.A WATERMAN and D.B LENAT. 1983. *Building Expert Systems.* Reading, Mass: Addison-Wesley.

MAZZOCCOLA D.F. and J.A. HUDSON. 1996. A comprehensive method of rock mass characterization for indicating natural slope instability. *Quart. J. Engi Geo.* **29**: 37-56.

TURBIN, E. 1992. *Expert Systems and Applied Artificial Intelligence.* Macmillan Publishing Company Inc.

ISSN: 0128-7680
Pertanika J. Sci. & Technol. Supplement 9(1): 51 - 57 (2001)

Utilising Malaysian Fibre in Stone Mastic Asphalt as a Replacement of Imported Fibre

Ratnasamy Muniandy, Jeyan Vasudevan,
Megat Johari Megat Mohd Noor & Husaini Omar
Department of Civil Engineering, Faculty of Engineering
Universiti Putra Malaysia
43400 UPM, Serdang, Selangor

ABSTRACT

Stone Mastic Asphalt (SMA) technology is currently used in many countries. This is a gap grade mix with a high percentage of coarse aggregates. As such there is a tendency for the binder in the gap-graded mix to drain down during the hot weather that may cause premature failure of the mix. Various fibre types have been used successfully in SMA. However, the overall cost of the mix tends to be much higher than that in conventional mix. This paper looks into the suitability of the Malaysian fibre for the use in SMA.

The fibre is analysed and compared with traditional European fibre that is commonly used in SMA. Several experiments on the fibre have been done including Fibre Drain Down Test and Morphological analysis using the Scanning Electron Microscope (SEM). Besides this, chemical analysis was also carried out with a variation of cellulose content, particle size and Gas Chromatograph analysis. The result of the preliminary analysis shows that Malaysian fibre has the potential to replace the imported traditional fibre.

Keywords: Stone mastic asphalt, imported fibre and Malaysian fibre

INTRODUCTION

In this current economic situation, the limited resource that is available should be used at an optimum level to reduce the expenditure of the government in the laying of roads. Roads are the lifelines of a country. The sustainability, of this country's economy depends much on the land transportation system. According to roads branch (JKR 1987) for the past ten years, an estimated RM3581 million has been spent to build roads, of which RM1560 million is spent on the maintenance of the existing roads, due to the fatigue cracking, rutting and stripping problem.

The above figure indicates that maintenance cost for road is very high. To cut down maintenance cost and probably the overall cost of road laying and maintenance, an alternative approach using the most advanced and durable pavement material such as Stone Mastic Asphalt (SMA) has to be conducted.

Objective of Project Study

The main objective of this study is to analyse the suitability of the Malaysian fibre used in Stone Mastic Asphalt. Several experiment or fibre analysis was conducted to determine the characteristic of Malaysian fibre and its usage in SMA. This fibre study includes production, screening, pulping, chemical and mechanical analysis.

BACKGROUND ON STONE MASTIC ASPHALT

Stone Mastic Asphalt (SMA) is a gap-graded mix with a high coarse aggregate content of 70-80%, binder content of 6.5-7.0% and filler contents of around 7-9%. The percentage of fibre that is required for SMA 0.3% and air voids of around 4%.

The skeletal formation of the coarse aggregate provides high resistance to deformation. Adding the fibres to the binder will prevent the asphalt from draining off during storage, transport and laying. Very soft binder may drain down easily. Bethune(1993) states that mastic fills the voids and retaining chips in position. It has an additional stabilising effect, as well as providing the design air voids. The result is a highly durable rut resistant asphalt mix.

SMA can be used on all types of road and it is ideal for roads with heavy traffic. Its high binder content gives a longer life than conventional mixes. The second advantage is its coarse and open texture which generally provides high skid resistance at all speeds, as well as good drainage and fewer spray problems (Bethune 1993).

Analysis of Fibre Morphology by Scanning Electron Microscope

The Scanning Electron Microscope (SEM) output is shown in Plates1,2,3 and 4. Plate 2 shows a thick presence of Malaysian fibre whilst Plate 1 shows otherwise. Plates 3 and 4 shows the state of cellulose fibre after recovering from slight damage after mixing.

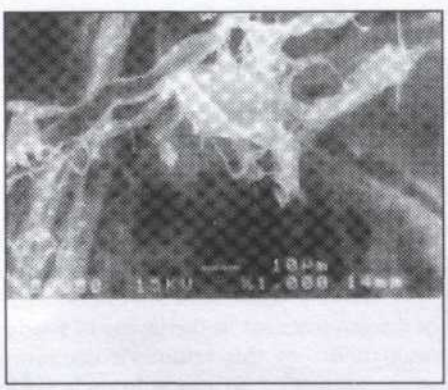

Plate 1: Imported fibre (1000X Magnification)

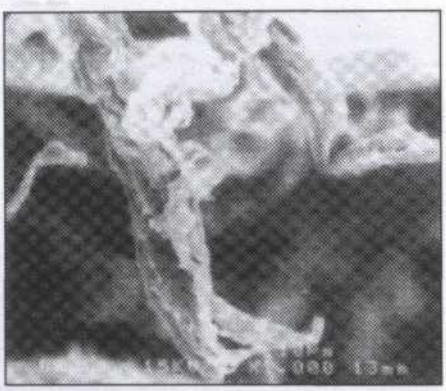

Plate 2: Malaysian fibre (1000X Magnification)

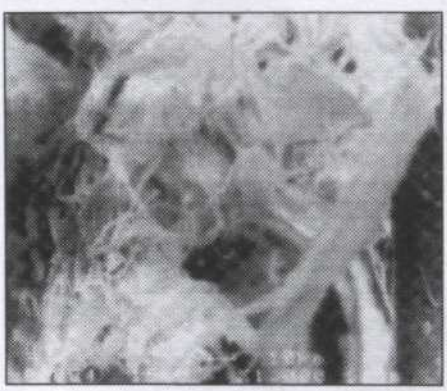

Plate 3: Recovered imported fibre (1000X)

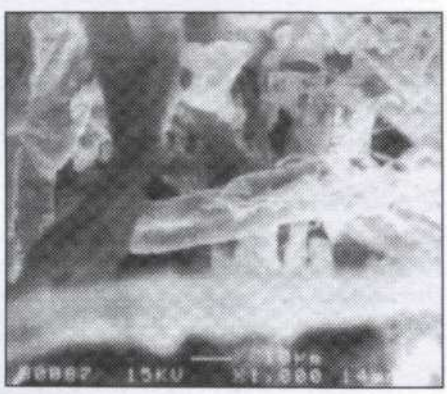

Plate 4: Recovered Malaysian fibre 1000X

Chemical Analysis of Fibre

The imported traditional fibre is cellulose based fibre which is approximately 80% cellulose, whilst the Malaysian fibre is about 65% cellulose fibre. From Fig. 1, it can be seen that the percentage distribution of Holocellulose below 200μm is almost similar. From 200μm to 600μm a linear increment is observed. However, upon approaching a percentage distribution of 77% Holocellulose stage occur to the graph before reaching its ultimate condition from 600μm.

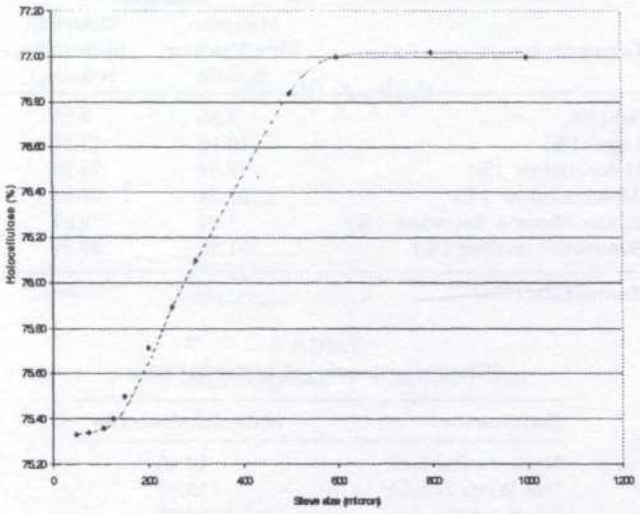

Fig. 1. % Holocellulose vs particle size

From Fig. 2, the percentage of alpha-cellulose below 200mm is constant but a gradual decrement is noticeable. From 200μm to 600μm a linear decrement is observed. However, at 600μm the graph remains constant at 62.5% alpha-cellulose.

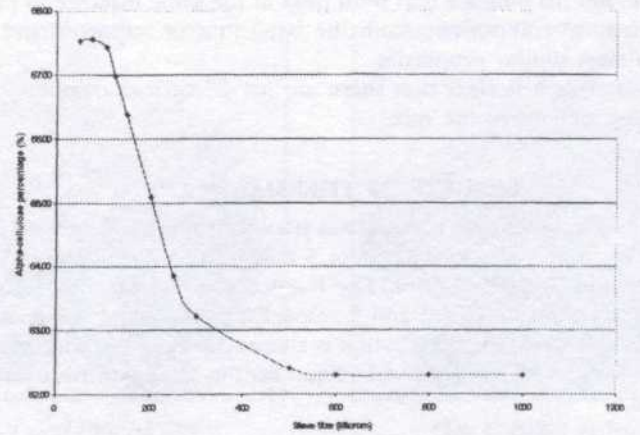

Fig. 2. % Alphacellulose vs particle size

The chemical analysis on Malaysian fibre by Liew and FRIM (1994) have been taken into consideration. This analysis was conducted to monitor the presence of any deleterious substance that would react with asphalt. Table 1 and Table 2 show the chemical composition and chemical properties of Malaysian fibre and imported fibre respectively.

TABLE 1
Chemical composition of Malaysian fibre

Constituents	Sample	
	Malaysian fibre Vascular Bundle	Malaysian fibre (after refining)
Ash(%)	3.36	3.23
Lignin(%)	19.16	17.50
Holocellulose (%)	77.04	75.33
Alpha-cellulose (%)	62.24	67.53
Ethanol-Aceton Extractive (%)	1.94	2.87
Summative analysis (%)	101.50	99.23

Source: Liew(1996)

TABLE 2
Chemical properties of Malaysian fibre

Constituents	Malaysian fibre (%)
Moisture Content	10.40
Hot Water Soluble	13.40
Alkali soluble	29.90
Alcohol benzene soluble	3.20

Source: FRIM(1994)

Pyrolysis Gas Chromatography Analysis

Figure 3 shows the mixture for both asphalt with imported fibre and asphalt with Malaysian fibre. Results indicate that both peak at the same instance as plain asphalt for the asphalt chemical component. Both the behaviour of imported and the Malaysian fibre display almost similar properties.

From this analysis it is clear that there are no deleterious components in the fibre that may cause problems to the mix.

RESULTS OF THERMAL PULPING

After the grinding process, the particle was passed through a sieve size of 500μm prior to the pressurised thermal pulping. Plates 5 and 6 show the outcomes of pulping the Malaysian fibre and iImported fibre. The fractional screening for Malaysian fibre and imported fibre is shown in Figs. 4 and 5 respectively. From the result obtain, it can be seen that the trend of particle distribution is almost the same for both Malaysian and the imported fibre but the sizes differ from 500μm for the Malaysian fibre and 50μm for the imported fibre.

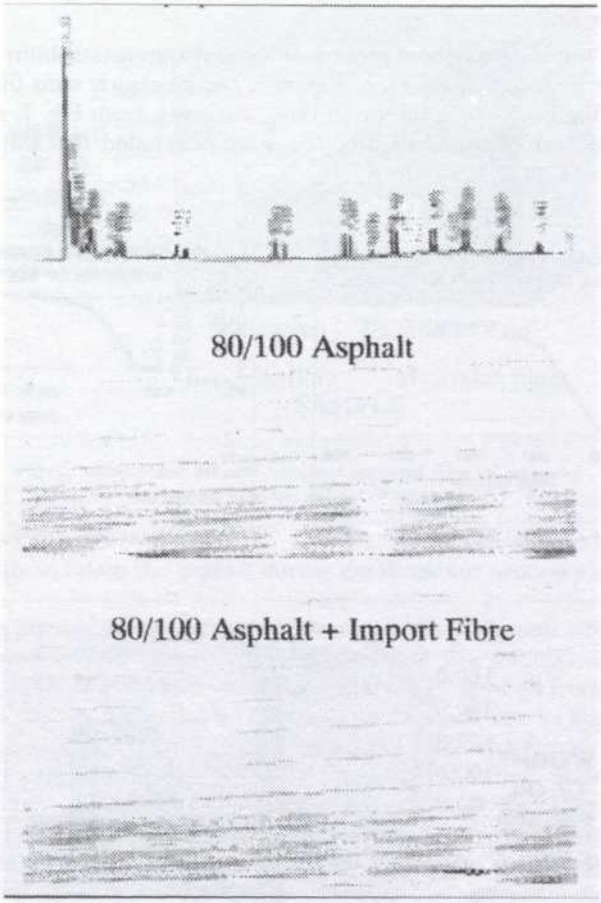

Fig. 3. Pyrolysis gas chromatograph

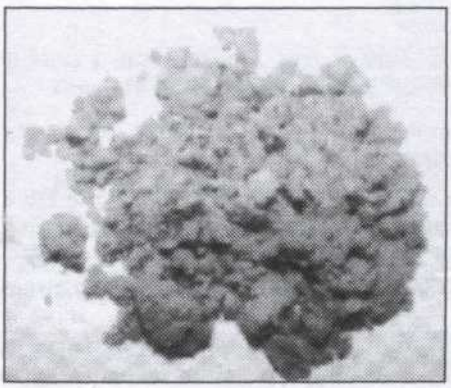

Plate 5. Pulped imported fibre

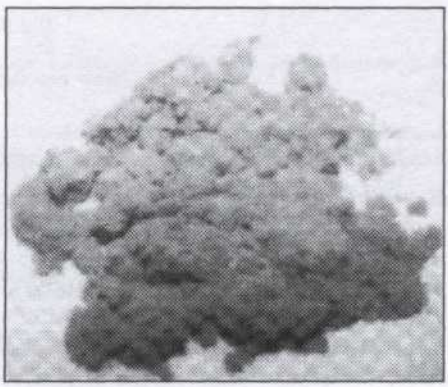

Plate 6. Pulped Malaysian fibre

Fibre Drain Down Test

The drain down test is a traditional procedure to carry out sustainability of the Malaysian fibre against the imported fibre. From Fig. 6, it can be clearly seen that the Malaysian fibre is performing better than imported fibre. However, from Fig. 7, the performance of the recovered fibre dropped slightly. It can be concluded that the performance of Malaysian fibre was quite satisfactory.

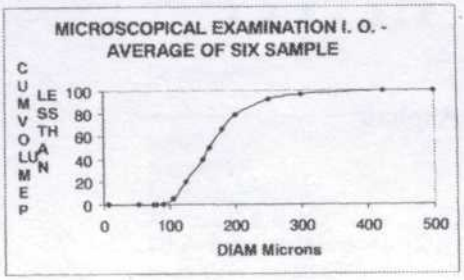

Fig. 4. Fractional screening for Malaysian fibre

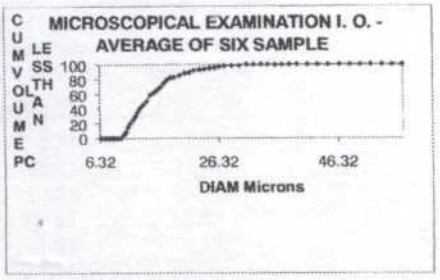

Fig. 5. Fractional screening for imported fibre

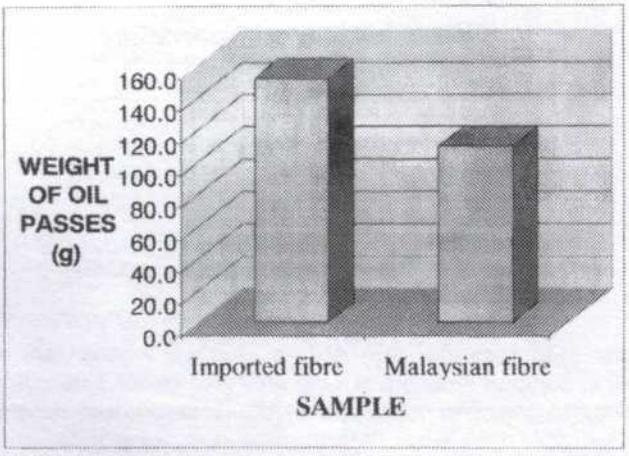

Fig. 6. Comparison between imported & Malaysian fibre vs weight of oil passes

CONCLUSION

Based on the results obtained, the following conclusions were made. Firstly, the Fibre Morphological analysis by Scanning Electron Microscope (SEM) and Fraction Screening Analysis (sieve analysis) show that the pulped Malaysian fibre seemed to be thicker (below 500mm) compared to imported fibre (below 50mm). This condition of Malaysian fibre can be improved by further pulping.

Secondly, according to the results obtained from the chemical analysis, Malaysian fibre contains cellulose content of up to 65%, whilst imported fibre contain higher cellulose of up to 80%. The advantage of the imported fibre is its soft structured nature in texture of alpha-cellulose, allowing easier expansion when heated up. This analysis also shows that the expansion of the cellulose makes the asphalt more viscous and

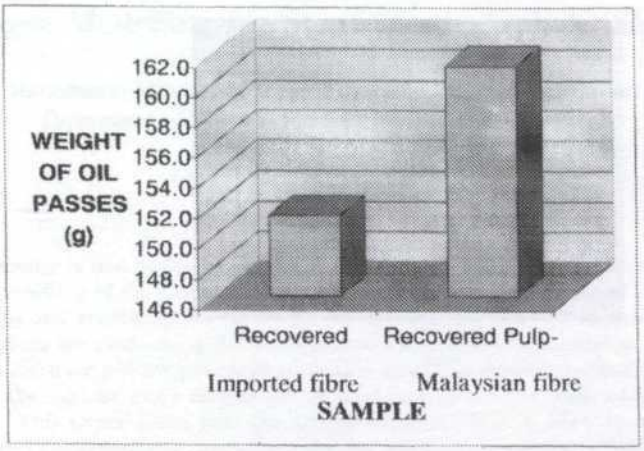

Fig. 7. Comparison between recovered imported fibre & recovered Malaysian Fibre vs weight of oil passes

provides the ability to retain the asphalt during the drain out process when temperature increases.

In the Fibre Drain Down test, by using motor oil, Malaysian fibre shows better performance than imported fibre within the allowable five minutes duration time of draining out period. There is however, a noticeable dripping of oil from Malaysian fibre indicating that it has yet to be stable. This may be assumed due to the thick presence of Malaysian fibre. This assumption can be accepted when the Recovered Fibre Drain Down Test shows a stable drain out within the allowable duration. However, the results are still inferior compared to imported fibre. Even though the drain off rate is not comparable to imported fibre but it is still acceptable because the performance of the Malaysian fibre is still within the given range, set by the European cellulose producer.

The main conclusion is that Malaysian fibre does perform comparably to imported fibre and could be an alternative supplement to replace imported fibre. However, more finding is required to improve its performance.

REFERENCES

Bethune J. and D. Potter. 1993. Asphatic Innovations: Oversees Experience, Australian Asphalt Pavement Association, Hawthorn, April 1993.

Liew, Lionel. 1994. Properties of medium density fibreboard made from oil palm (*Elaesis Quineensis*) trunk. B.Sc. Forestry (Wood Industry) Project Report. Faculty of Forestry, Universiti Pertanian Malaysia, Serdang.

Tappi Testing Procedures. 1985. Atlanta: American National Standards Institute.

FRIM. 1994. Tests Data of Forest Research Institute Malaysia in Fibre From Oil Palm Fruit Bunches. Brochure of Sabutek (M) Sdn. Bhd. Kuala Lumpur, Malaysia.

National Asphalt Pavement Association (NAPA). 1996. Guidelines for Materials, Production, and Placement of Stone Matrix Asphalt (SMA).

Asphalt Overlays for Highway and Street Rehabilitation. AI. Manual Series No. 17 (MS-17), Second Edition, 1983.

ISSN: 0128-7680
Pertanika J. Sci. & Technol. Supplement 9(1): 59 - 63 (2001)

Fatigue Modelling for Stone Mastic Asphalt (SMA)

Ratnasamy Muniandy, Tang Eng Loong & Husaini Omar
Department of Civil Engineering, Faculty of Engineering,
Universiti Putra Malaysia
43400 UPM, Serdang, Selangor

ABSTRACT

Fatigue cracking is one of the major distresses found in many asphalt pavements. The premature cracking of the pavements results in the increased annual cost of resurfacing, maintenance and rehabilitation. Generally, any asphalt mix is tested in the laboratory and predictions are made using the performance curves and local conditions. However, in Malaysia there are not any pavement prediction models developed yet that can be used to predict the asphalt mix's fatigue life performance under the local environmental conditions. This paper looks into the fatigue characteristics of SMA by using local materials and environmental conditions. For the purpose of evaluation SMA14 (SMA with 14mm aggegate as nominal) with 5 different gradations within the JKR's ACW14 gradation envelope were used. The repeated load indirect tensile tests at three different temperatures (30°C, 40°C, 50°C) and five different dynamic loadings (500N, 750N, 1000N, 1250N, 1500N) were carried out under stress controlled mode using the MATTA Machine. The fatigue performance test results plotted on a logarithmic scale of fatigue strain and load repetitions showed a good agreement with the historic trend of the fatigue data. The logarithmic relationship between fatigue loading and strain was evaluated and found to be linear at certain reliability regardless of the testing condition and mix parameter. This indicates that the fatigue model for SMA is a function of asphalt volume, resilient modulus and the fatigue strain values.

Keywords: Fatigue modelling, stone mastic asphalt

INTRODUCTION

The surveys of asphalt pavement performance conducted in the United States and United Kingdom indicated that fatigue cracking was generally the most important type of distress (Rogers *et al.* 1963; Finn *et al.* 1972). The same problem also happened in Malaysia, based on the investigations into the distresses on Malaysian roads. The studies also showed that one of the primary modes of pavement distress was fatigue cracking in bituminous surfacing, especially on heavily trafficked roads (Bullman *et al.* 1977; Ministry of Works 1987). This shows that the conventional mixes around the world including Malaysia, are inadequate in minimizing fatigue cracking in road pavements.

The Pavement Engineering Unit of Universiti Putra Malaysia had been working on the formulation of the Stone Mastic Asphalt (SMA) mix design modified to suit the local environment and traffic loading (Ratnasamy *et al.* 1995; Ratnasamy *et al.* 1996). Since then, the Unit had come to the point where SMA was used in the analysis to predict fatigue cracking. It was because SMA had shown good performance including longer fatigue life in Europe, the United States and Australia (Wonson 1996), it is necessary to predict the fatigue life of SMA in order to be effective in evaluating and controlling the fatigue cracking of SMA Pavements.

SPECIMEN PREPARATION

Materials

The materials for the preparation of the SMA samples were selected based on the standard set by the European countries. However, the Malaysian JKR specifications were widely used in confirming the properties of the binders and aggregates. Since SMA is a

gap graded mix, cellulose fibers were used to ensure its durability in tropical climates. In this study granite stones and Petronas rubberized asphalt were used.

Mixtures

At the beginning of this study, SMA14 (SMA with 14 mm aggregate as nominal) with five different gradations within the JKR's ACW14 gradation envelope were used. Several adjustments were in the gradations to ensure high percentage of coarse aggregates. The five different aggregate gradations (G1, G2, G3, G4 and G5) and a typical SMA gradations are presented in Fig. 1. The SMA formulation was done by using the modified Marshall method and the Asphalt Institutes MS-2 specifications.

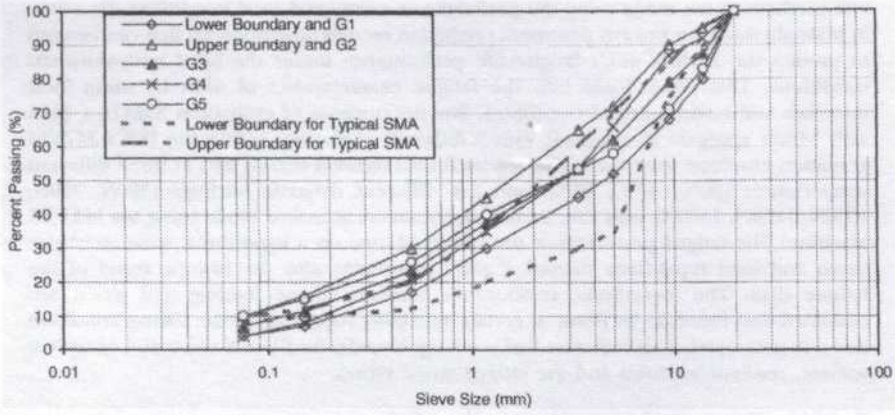

Fig. 1. Five aggregate gradations for SMA14 mix and typical SMA

Test Apparatus

The Repeated Load Indirect tensile Test was used for investigating the fatigue performance of SMA mix. This method has been chosen due to its convenience for routine measurements. The sophisticated and user-friendly universal testing machine called Material Testing Apparatus (MATTA) from Australia has been used to carry out the fatigue tests. The pneumatic and electronic control and data acquisition equipment is conveniently housed in a compact stainless steel trolley, and an environmental chamber that provides accurate control of temperature (2°C – 60°C) for bituminous mixture testing.

Fatigue Performance Test Procedure

The timing of the dynamic loads is selected in such a way as to simulate the actual load pulses on the pavement by the moving vehicles on the roads. Pavement temperatures can reach 60°C during real hot weather. As such a range of temperatures were selected for the fatigue tests. The tests were ran under the following conditions:

- Loading time was set at 0.1s while rest time set to 0.4s.
- Three different temperatures (30°C, 40°C and 50°C) were selected.
- Five different dynamic loads (500 N, 750 N, 1000 N, 1250 N and 1500 N) were selected.

Fig. 2 shows a general outline of fatigue performance test procedure for SMA14. The data from the fatigue tests and voids analysis were used to develop the SMA14's fatigue model.

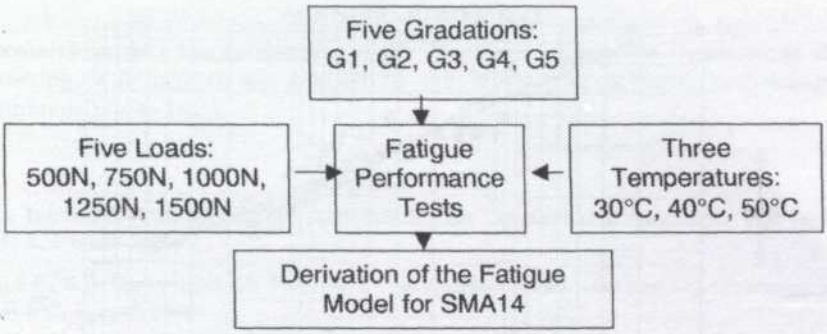

Fig. 2. General outline of fatigue performance test procedure

VARIABLES USED IN THE MODELLING

The fatigue performance of any asphalt mixes are a function several variables. In this study, the following parameter were used extensively.

Percentage of volume of asphalt
Percentage of volume of voids in the mix
Percentage of voids in mineral aggregates
Strain values of the mix

RESULTS AND DISCUSSION

The fatigue life is defined as the total number of load repetitions that cause a fracture of the specimen. The strain levels were measured at 200th load cycles.

When all the fatigue performance data of SMA14 mixes were plotted on an initial strain-fatigue life logarithmic basis, the fatigue life of SMA14 can be represented by only one fatigue life equation. Fig. 3 presents the relationship between initial strain and fatigue life. The relationship between fatigue life and initial strain for SMA14 displayed a definite trend or pattern in material behavior. This is quite similar to studies under taken previously in the 60's and 70's (Saal and Pell 1960; Epps *et al.* 1972; Pell and Cooper 1974; Brown *et al.* 1974).

The linear relationship between fatigue life and initial strain can be improved by adding other variables into the model. This has been done by using three regression methods: forward, stepwise, and backward elimination procedures. The regression methods were conducted to determine which variables made a significant contribution to explain fatigue life. Variables of interest in the development of the fatigue model are: fatigue life (N_f), percentage volume of asphalt (V_A), percentage volume of air voids (V_v), percentage of volume voids in mineral aggregate (VMA), percentage of voids filled with asphalt (VFA), resilient modulus (MR), and initial strain (STRN).

Two different fatigue model equations were developed. The equations are as follows:

The fatigue model (with the Mallows $C_p = 83.6$, $R^2 = 0.847$, and adjusted $R^2 = 0.845$) is:

$$\mathbf{LN = - 0.337 + 3.568\ LA + 0.828\ LR - 1.129\ LSN}$$

While the fatigue model (with the Mallows $C_p = 5.55$, $R^2 = 0.932$ and adjusted $R^2 = 0.927$) derived from backward elimination procedure is:

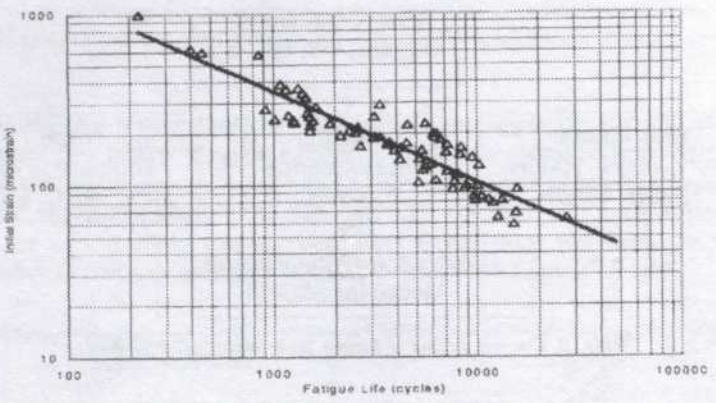

Fig. 3. The relationship between fatigue life and initial strain

$$\mathbf{LN = - 655.459 - 334.736\ LA - 12.454\ LV + 358.946\ LVM + 319.614\ LVF - 1.39\ LSN}$$

where:

LN = log(Fatigue life, N_f in unit of cycle)
LA = log(Percentage volume of asphalt, V_A)
LV = log(Percentage volume of voids, V_V)
LVM = log (Percentage of volume voids in mineral aggregate, VMA)
LVF = log(Percentage of voids filled with asphalt VFA),
LR = log(Resilient modulus, MR in unit of MPa)
LSN = log(Strain, STRN in unit of 10^{-6})

Theoretically, the second model seems to be the best fatigue model in the regression analysis because of the bigger R^2 and adjusted R^2 compared to the first model. Whereas, the Mallows CP in the second model is smaller than first model.

However, the pairwise correlation r of –0.84 between LA and LV, 0.90 between LA and LVF, 0.97 between LA and LVM, –0.99 between LV and LVF, and –0.94 between LVM and LVF. The pairwise correlation of the pair of predictors (LR, LSN) is –0.92. It is more effective to include only one of four volume variables LA, LV, LVF and LVM in the fatigue model. The first fatigue model only contains the LA predictor among LA, LV, LVM, LVF predictors. For this reason, the first fatigue model has been selected.

CONCLUSIONS

There is a linear relationship between initial strain and fatigue life when data plotted on a logarithmic scale. The linear relationship shows good agreement with the historic trend of the fatigue data.

The fatigue life can be related to the asphalt volume, the resilient modulus, and the initial strain by the equation:

$$\mathbf{LN = - 0.337 + 3.568\ LA + 0.828\ LR - 1.129\ LSN}$$

Where the LN is the log of fatigue life in the number of load applications, LA is the log of asphalt volume in percentage, LR is the log of resilient modulus in MPa, and LSN is the log of initial strain in unit of 10^{-6}.

ACKNOWLEDGEMENT

The research project was carried out at the Pavement Laboratory, Department of Civil Engineering. The project was funded by the Ministry of Science, Technology and Environment under IRPA.

REFERENCES

ASPHALT INSTITUTE. 1984. Mix Design Methods for Asphalt Concrete and Other Hot Mix types MS-2, United States.

BROWN, S.F., K.E. COOPER and P.S. PELL. 1974. Transportation and road research laboratory, Report LR 633, Crowthorne.

BULLMAN, J.N. and H.R. SMITH. 1977. Pavement Performance and Deflection Studies on Malaysian Roads, Department of the Environment, TRRL Report LR 795, Crowthorne.

EPPS, J. and C. L. MONISMITH. 1972. Fatigue of Asphalt Concrete Mixtures -A Summary of Existing Information, Fatigue of Compacted Bituminous Aggregate Mixtures, Report STP 508, American Society for Testing and Materials.

FINN, F.N., K. NAIR and C.L. MONISMITH. 1972. Applications of Theory in the Design of Asphalt Pavements. In *Proceedings of Third International Conference on the Structural Design of Asphalt Pavements*, p. 392-409.

IVONSON, K. and M. RATNASAMY. 1996. The use of ground tire rubber in Stone Mastic Asphalt. Final Year Project Thesis, Faculty of Engineering, UPM.

MINISTRY OF WORKS. 1987. National AxlLoad Study, *Technical Notes* No. 3 and 17, Kuala Lumpur.

PELL, P.S and K.E. COOPER. 1974. The Effect of Testing and Mix Variables on the Fatigue Performance of Bituminous Materials. In *Proceedings of the Association of Asphalt Paving Technology* **43**: 1-37.

ROGERS, C.F., H.D. CASHELL and P.E. IRICK. 1963. Nationwide Survey of Pavement Terminal Serviceability Highway Research Board, Record No. **42**: 26-40.

SAAL, R.N.J. and P.S. PELL. 1960. *Kolloid-Zeitschrift MI*, **Heft 1**: 61-71, London.

TAN, G.H. and M. RATNASAMY. 1995. Stone Mastic Asphalt for heavy traffic. Final Year Project Thesis, Faculty of Engineering, UPM.

WONSON, K. 1996. SMA – The European Experience, AAPA Pavement Industry Conference, p. 11-14.

Pertanika J. Sci. & Technol. Supplement 9(1): 65 - 72 (2001)
ISSN: 0128-7680

Spatial Information Technology for Disaster Management

Rohaya Mamat, Shattri Mansor & Tee Tuan Poy
Department of Civil Engineering, Faculty of Engineering
Universiti Putra Malaysia
43400 UPM, Serdang, Selangor

ABSTRACT

Most major geohazards such as floods, forest fire and oil spills occur suddenly, and require an immediate response. This paper describes the development and establishment a spatial information technology and engineering system that uses GIS and Remote Sensing technologies to detect, monitor and assess geohazards, including floods, forest fire and oil spills. The potential application of Remote sensing and GIS techniques for floods and oil spills is discussed. The oil spill risk management system study was developed for coastal zone of Peninsular Malaysia. The development of GIS database used remotely sensed data from Landsat TM, SPOT Panchromatic and MSS, AVHRR and air-borne images.

For the flood studies, Digital Elevation Model (DEM) was created for Klang River Basin from the input data of contour lines. DEMs stored the data for the slope analysis, terrain analysis and also visualizing for the flood simulation. SCS TR-55 Model was used to predict the extent of inundation and depth of flooding. Parameters of rainfall, land-use and hydrological relief were adopted as the main input data. These two case studies will provide the technical guidelines for in-depth study in GIS and remote sensing for disaster management.

Keywords: Spatial information technology, disaster management

INTRODUCTION

The world is confronted by the ever-increasing threat of the loss of life, property, and natural resources due to natural disasters. In the past three decades, the frequency of natural disasters has increased (Kriemer and Munasinghe 1991; Anderson 1991). A natural disaster is considered to be an event, triggered by a geophysical, or climatological phenomena resulting in, or having the potential to result in widespread loss of life and property, and destruction of the community's infrastructure of such significance that the community has to seek outside assistance to recover from the effects of the phenomena.

Advances in sciences and information technology (which include GIS and Remote Sensing) has given a way of solution to save the community. Spatial information technologies are extremely useful in the management of disasters because of these resources, activities, and natural conditions can be represented digitally as describe by McKee *et al.* (1998). This means that information about them can be:

- Collected by means of remote sensing using wireless communication to devices with sensors. The devices may be fix firmly, or may be mobile with wireless communication devices reporting their GPS-determined locations and sensed values.
- Displayed on computer displays on desktops, in vehicles, or handheld devices.
- Merged and analysed by GIS, which overlays and co-locates digital maps so that queries can produce new maps.
- Communicated over the same communication networks that carry voice and other kinds of data communications.

The integration of this remote sensing data and GIS as the operational tools will built up a proper system for disaster management. It is also expandable to include additional

disaster-related data and models with their associated remote sensing data requirements and distributed data sources.

An important of environmental remote sensing to land resources management is its potential to map resources and to monitor changes that occur in boundary surface conditions over extended period of time. From the viewpoint of land management, the results of scientific research need to be interpreted and integrated in a practical way for "real time" application. The theories derived from scientific research need to be incorporated into a practical model; environmental and land management data need to be integrated; and a "real-time" methodology needs to be developed to evaluate, monitor and manage land resources.

The paper reviews the literature from a disaster management perspective followed by a discussion of the GIS literature based four phases of disaster management. Finally, the requirements for research on the application of GIS and remote sensing in disaster management are discussed. Examples of two types of the disaster, flood and oil spill study, are describe below by using the integrated scheme of remote sensing and GIS.

DISASTER MANAGEMENT

Disaster management in actual action constitutes a complex process. To understand their constituent, the process can be simplified into 3 major phase of action that is before, during and after the event.

Before Event (pre-event)

Phase one is before the event. It's constitute of two stages; the preparation and the prediction. During the preparation stage, the acquisition of data or more specifically, creating the database are the major focus task. The planning should start long before the disaster strikes and ready to access whenever the event occur. The database will recognize the area of interest with related features of disaster. Preparation for disasters can be done such as emergency plans, monitoring and also training of volunteers. Understanding the cause and needs of the disaster will conduct an action undertaken. Mitigation of disaster is also one of the preparation stage in order to prevent the disaster.

The second stage is the prediction and warning system. Real-time data or predicted data from other sources such as meteorological department or any detector used to observe the hazard by analyzing and modelling.

During Event

During the disaster is the time when everybody have to make vital decision. The need for accurate information at this phase is very urgent. Normally, this phase occur short time after the predicted date. Various measures may include the information of area influence, transportation access, alert system, mobilization of resources, evacuation of victims to recognized safety places, suppression of the hazard and even the assessment of the immediate emergency needs. This is an important phase when a disaster manager, along with the community, has to make many vital decisions involving many agencies.

After the Event

The system may continue to move on restoration of damages into normalcy such as land use control, building regulations, or other non-structural measures. Damage assessment has to be done in written hardcopy or archive. Efforts to rebuild a better and more disaster-resistant community based on the experience of the disaster. Information and

experiences in the disaster are documented for a better understanding and mitigation of disasters in the future. It is very important to equip the community with measures to cope with the disaster and reduce the vulnerability of the community to the damaging impacts of the disaster.

The action of each step is overlapped on each other and appears in cyclical pattern. The monitoring of the natural phenomena is continued for further study of the phenomena.

The System

The GIS and remote sensing technologies are evolve with the evolution in hardware and software. In development of an operational system, it is important to provide a real-time early warning system.

Data

One of the most important requirement for GIS system to work is the data. There are two types of data required for disaster response: static data and dynamic data (Boone 1995). Static data are the data that does not change very frequently, use to show the spatial area and features of interest. The database created by applying this static data are examples of information; are needs for creating the database could be population, demographic, location, topographical relief and etc.

Whereas the dynamic data refers to the event-specific and the available in real-time. Stage of event, spatial location, influenced area and types of event are some of the examples of the dynamic data.

The integration of these static and dynamic data is the main criteria in disaster management and the system of GIS is the best solution for this requirement. The process includes the incorporation and interpretation of data from various sources of agencies.

As the system will interfere with the various agencies and individuals, GIS should accommodate for the public access of data.

Software and Hardware

GIS is a technology in evolution with rapid advances in hardware and software. Selection of a suitable operating system is very important, as it is necessary to train people. For the final decision, to interact with the community, the software should support the multimedia function.

A survey of bidding vendors conducted by the State of Florida's Emergency Management Agency revealed that none of the GIS software products had the desired level of spatial statistical analysis capability (Bales and Loomis 1995). To make the investment in GIS more cost-effective, the multi tasking of the GIS with multiple agencies is suggested by Bales and Loomis (1995). However, it is the state of believing that between the requirement of the appropriate system and the impact of system management still fair enough.

Personnel

The person who takes charge of the whole process is someone that is well trained in these disciplines. Most of them are normally the scientist and engineers who are experienced in coping with the data handling and data manipulation. It is rather important for the disaster manager to be familiar with the capabilities of GIS so that he/she can put the technology to good use.

The Limitations of Disaster Management

Even though our information technology era has improved, we still confront some of the limitations such as the data, software, officer and even agencies.

The main limitation of the system will be the ability to get the real-time data from satellite receiving stations. The repeat coverage of some satellite are very long for example for Landsat TM, 16 days and SPOT will take about 26 days to orbit for the second image for each scene.

Though there have been rapid advances in the hardware in terms of speed, storage, and manipulation capability, the existing commercial software presents difficulties in serving all the needs of a disaster manager for example lacking of built-in spatial statistical capability. In some purpose of study, we need to interchange the data processing between the software in according to avoid the insufficient task of the certain software. In this case, the problem occur when data support system are. Furthermore more changing the data format in some case will eliminate some properties of data and which might be useful information.

The well-trained officer is another problem. Disaster management is still a profession in evolution and lacks of well-trained officials competent at using computers and other advanced technology (Drabek 1991). The problem of person in charge is very critical problem because without them, there is no action can implement.

Such institutional support may not be possible in many developing countries, providing a major obstacle to the use of this technology in areas most prone to disasters.

GIS APPLICATION IN OIL POLLUTION

The Marine Spill Response Corporation, USA carried out a research and development (R&D) of an operationally optimised aerial remote sensing system for oil spill response to enhance oil spill containment and cleanup capabilities. Also, the Emergencies Science Division of Environment Canada had a mandate to develop operational oil spill remote sensing to respond to oil spill emergencies. The particular requirements for oil spill remote sensing include; short response time to minimise environmental impact, good discrimination between oiled and unoiled surface, and information on the location, distribution, and quantity of oil in the environment (Giammona *et al.* 1993; Fruhwirth *et al.* 1993)

THE GIS BASED OIL SPILL RISK MANAGEMENT SYSTEM

For the past two decade, coastal and marine application have benefited from the information derived from commercial satellite imagery and used GIS as a powerful tool to manage the oil pollution at the coastal area. Inm which, GIS applications are heavily dependent on both the timeliness and currency of the data they contain and the geographic coverage of the database. However, the remote sensing can provide timely data at appropriate scales to GIS context.

The Peninsular Malaysian water is fragile ecological and economic area with heavy ship traffic. The result is high risk of oil pollution, both intention and accidental. Oil spill detection by means of remote sensing and spatial management in GIS became possible with the advent of the integration data.

GIS-based risk management systems was developed and used the latest information technology to store data required for oil spill risks assess, response, planning, and risk management. GIS is the most efficient system for analysing and visualising a comprehensive range of variables, held in large databases, which relate to an oil spill. The effects of alternatives coastal zone development strategies can be tested and presented in an easily

understandable format. Response co-ordinator may utilise this system to better understand and manage the incident under their responsibility.

This study discusses the work done utilising GIS and remote sensing technologies to develop an Oil Spill Risk Management System (OSRMS). This is a GIS-based prototype system, developed for Peninsular Malaysia focused on the construction of an integrated database for coastal management especially for oil spillage issues. The OSRMS is designed into three parts; there are development of GIS database, remotely sensed data processing, and the oil slick movement prediction.

It is crucial to identify the sources and risk in a spillage incident in order to formulate counter responses for the emergency situation alertly. However, there is a problem in incorporating critical stages of data and information needs for emergency management prior to impact, the immediate post-impact response period, the recovery period, and opportunity for mitigation are defined. In addition, oil pollution problem covers a large extent of spatial area, it is essential to have a response management system, which can manage the large collection of spatial geographic information and simplify all manipulation of data for analysis, and faster access for emergency co-ordinator to the best information possible.

THE SIGNIFICANCE OF STUDY

The OSRMS is designed to assist rapid and effective decision making in oil spill containment and clean up operation in Peninsular Malaysia coastal areas. Oil spill data, access and protection information will be placed in GIS database and interfacing it with a GIS database for rapid access, retrieval and query. While, the remotely sensed data as spatial data input were used to monitor and derive valuable information about marine water pollution, especially on oil spillage. These remotely sensed data including LANDSAT TM, SPOT Panchromatic and Multispectral Scanner (MSS), AVHRR and air-borne images were integrated in the GIS based oil spill risk management system for Malaysia coast in order to detect, assess the risk and handle the oil spills problem in an alert situation.

The information can be required from this system such as location of oil spills, quantity of oil spills, distribution of this in the affected area; for example location of the areas of heaviest contamination, the length of shoreline affected by the oil slick. An oil slick movement model was incorporated into this system in favour of predicting the oil slick movement direction and duration to reach the shoreline. Wind, wave and current are the main parameters for this model.

The GIS-based system can be used to establish the appropriate response and locate the dense areas in a slick and local surveillance, to permit clean up vessels to detect the oil to be cleared in rapid circumstances. This risk management system will allow new opportunities for assessment, multiple resource planning, permit viewing of the state's natural resources in ways out, therefore realised, improve the decision-making process, and provide a baseline for future assessments.

Thus, the information system described in this project will emphasize in the mapping, visualising, analysing and modelling capabilities of GIS software with a properly designed database management system for oil spill containment in Peninsular Malaysia coastal area.

Analysis of the image of the SPOT MSS in Terengganu oil spill clearing demonstrated the utility of satellite data as a means of detecting oil on the marine surface and of assessing the distribution of the oil that issued from the incident. Despite, it had prevented by cloudy weather, this satellite image was effectively in monitoring at 16 days intervals of oil spill cases along Peninsular Malaysia coastline.

Full integration of OSRMS and its modelling output will be undertaken by portable computer or response sites. In addition, OSRMS is also readily adaptable to other marine environmental management applications.

OSRMS is intended to be a tool for detection and management of environmental emergency situation. GIS database and its functionality are powerful tool in visualising the results of modelling, and analysing and visualising potential impacts. As more data are collected, new layer can be produced, stored, updated and analyse to improve the sensitive and risk asses map or management system. In outline, benefits of OSRMS includes improved pre-spill assessment of sensitive shorelines that would require protection or clean up, improved capabilities to decide equipment deployment and clean up logistics, improved resource damage assessment and ability to conduct litigation for damage compensation.

Lastly, OSRMS is not only intended to be a detection system, it will also be a system for management and support when the emergency situation happens, and provide a baseline for future assessment.

FLOOD STUDIES

A system was developed to monitor and forecast flood event by using the advantage of remote sensing and GIS technology. The database was developed from infrastructure such as road network, hydrological data, topographical relief provided by JUPEM, land use aspect provided by DOE and also the real-time image provided by MACRES. The SPANS software is use as the platform for the study activity. This software have the reliable built-in spatial statistical capability required for the study.

Information from contour line, subject to DEM analysis to determine areas subject to flood inundation. Input data used are digital topographic maps with contours at 20m intervals scaled 1:10,000 project to Malayan Grid System. Flood prone areas defined from the structured model DEM. Interpolation algorithms, Triangulated Interpolation Network (TIN) are use as the scaffolding in the process of creating DEM. Information may be extracted in two ways, by visual analysis of graphic representation or by quantitative analysis of digital elevation data. For a 3-D viewing of the landscape, layers of information such as land cover and hydrographic can be overlaid onto DEM. The DEM will provide automatic layers for slope analysis, terrain analysis, hydrographic analysis and flood simulation.

Based on the historical data of flood (records), the subjected area are zoned to severity code of flooding and this area is known to be the aimed area when the big storm is predicted to strike.

The second phase of the study is the statistical flood forecasting modeling. SCS TR55 Model was used by adopting assumptions/limitations in use by the model. Rainfall data are accessed from DID branch, Ampang from raingauge site. Input data of various flood levels for the certain interested location will allow the early prediction of the extent of inundation and depth of flooding. Public are warned from time to time before the disaster strikes to reduce damages and more important are the lives.

For further research, this database can be used for in-depth study and updated for specific needs individually or agencies.

Using the data base and GIS spatial modelling operations, theories and principles derived from more traditional geographical research can be technologically applied to the real-world' land modelling operations, the system also provides the potential for "real-time" assistance for decision-making activities in flood mitigation.

CONCLUSIONS

There is a large literature relating to the use of GIS in understanding the physical and natural phenomena leading to disasters. There is less evidence of transformation of technical studies on particularm phenomena into information usable by the disaster planner and manager. Information on the people, socio-economic characteristics, vulnerability, behavior and perception, and institutional supports available are as important for responding to disasters as the phenomena itself. A lot of study is geographically referenced and GIS can be used not only as a management tool, but also as a tool assisting disaster research. The potential for the use of GIS for all aspects of disasters, including management and research, is very promising as more and more data becomes available in the real-time through advancements in remote sensing techniques and quick transfer of data. Networking capabilities in recent GIS products also holds promise for a distributed decision support system, particularly in circumstances which do not allow large investment in a large monolithic emergency information system. The limitations due to data, software and hardware, training of end users and the institutional capabilities of the disaster management agencies have to be addressed for the widespread use of this technology.

The integration of remote sensing with GIS techniques offers an effective tool for analysis of the risk management. The success of utilisation the remote system and GIS technology is the user can predict the risk of disasters in an efficiency and alert situation.

In short explanation, the advantages of the technologies are;

1. Allows long-term time series studies and storage of information for future situation.
2. GIS & remote sensing improves information accessibility. RS data covers larger area inspection saving in cost and time spend. GIS bring together vast amount of information from a wide variety of sources and applicable.

Improving the management of disasters remains a societal objective. Advances in science and technology have to be applied to mitigate disasters in order to meet this objective. Geographic information systems provide an invaluable tool which can largely assist in streamlining the response to disasters and help in informed decision-making by individual as well as public official.

REFERENCES

La Barbera, P.L., Lanza and F. Siccardi. 1993a. Flash Flood Forecasting Based On Multisensor Information. In *Extreme Hydrological Events: Precipitation, Floods and Droughts*, eds. Z.W. Kundzewicz, D. Rosbierg, S.P. Simonovic and K. Takeuchi, p. 21-23. UK, Wallingford. IAHS Publication No. 213, IAHS Press.

Lanza, L. M. Conti and P. La Barbera and F. Siccardi. 1993b. Early Warnings and Quantitative Precipitation Forecasting. In *Coping with Floods*, ed. G. Rossi, N. Harmancioglu and V. Yevjevich (in press).

Barrett, E.C., M.J. Beaumont and R.W. Herschy. 1990. Satellite remote sensing for operational hydrology: present needs and future opportunities. *Remote Sensing Review* **4(2)**: 351-466

Barrett, E.C. and J.M. Mifsud. 1991. The use of satellite imagery in meteorological hazard monitoring and forecasting in the Mediterranean region. In *Current Topics in Remote Sensing.* Vol. 2: *Remote Sensing for Hazard Monitoring and Disaster Assessment* eds. E.C. by Barrett, K.A. Brown and A. Michallef, p. 157-180. Gordon and Breach.

Nawang, W.M. 1988. Remote Sensing and Information Systems Support for Hydrological Modelling. Paper presented at the *Seminar on Earth Resources: Data, Systems & Applications*, Kuala Lumpur.

Brussieux, M., & G. Massart. 1984. Oil on the sea: application of pattern recognition techniques to thermal infrared and SPOT images. In *Remote Sensing For The Control Of Marine Pollution*, ed. J.M. Massin, p 193 - 199. New York, USA: Plenum Press.

Bruzewicz, A.J. and H.L. McKim. 1995. Remote sensing and GIS for emergency management: effective implementation. http://ltpwww.gsfc.nasa.gov/ISSSR-95/ remotese.htm#bruzewicz-reference DOE report, (1995). http://www.jas.sains.my/doe/eqr95/html/4g.html#9.

El-Raey, M., A. F. A-Kader, S. M. Nasr and H. I. El-Gamily. 1996. Remote sensing and GIS for oil spill contingency plan, Ras-Mohammed. *Egypt. Int. J. Remote Sensing* **7(11)**: 2013-2026.

Estes, J. E. and L.W. Senger. 1972. The multispectral concept as applied to marine oil spills. *Remote Sensing of Environment* **2**: 141 - 163.

Fedra, K. and E. Feoli. 1998. *GIS Technology and Spatial Analysis in Coastal Zone Management.* EEZ Technology. 3rd ed. USA: ICG Publishing.

Garner, B.J. 1995. Environmental application of geographical information systems. In *Proceedings of the Regional Workshop on Remote Sensing and GIS For Land And Marine Resources and Environment in The Pacific Subregion.* 13 -17 February 1995.

Giammona, C.P., F.R. Engelhardt and K.S. Binkley. 1993. Development of an operationally optimized aerial remote sensing system for oil spill response. In *International Symposium Operationalization of Remote Sensing,* 19– 23 April 1993, The Nertherland, ITC Enschede.

Guinasso Jr., N.L., I.R. Macdonald, S.G. Ackleson, J.F. Amos, R. Duckworth, R. Sassen, J.M. Brooks, C.P. Giammona and F.R. Engelhardt. 1993. Remote sensing estimates for rates of natural oil seepage in the Gulf of Mexico. In *International Symposium Operationalization of Remote Sensing,* 19 – 23 April 1993, The Nertherland, ITC Enschede.

Gundlach, E. R., M.O. Hayes and C.D. Getter. 1981. Sensitivity of coastal environments to oil spills. In *Proceeding of the Petroleum Industry and the Nigerian Environment,* ed. A.A. Thomopoulos, p. 82-88.

Jensen, J. R. and E. W. Ramsey. 1990. Environmental sensitivity index (ESI) mapping for oil spills using remote sensing and GIS technology. *Int. J. Geographical Information Systems* **4(2)** : 181-201.

King, B.A. 1996. Oil Map for Risk Assessment: HYPERLINK http://ibm590.aims.gov.au/oilmap/papers/stochmodel/sto http://ibm590.aims.gov.au/oilmap/papers/stochmodel/sto ch.html

King, B.A., A. L. Kilborn and R. A. Bell. 1994. A computerizes oil spill management system for BHP Petroleum's Otway basin. http://ibm590.aims.gov.au/oilmap/papers/otway/otway.h\tml

McKee, L., C. Kottman and F. Corle. 1998. *The Future of Geospatial Technologies in EEZ Management.* EEZ Tecnology, 3rd ed. USA: ICG Publishing.

Fruhwirth, M., M.F. Fingas and C.E. Brown. 1993. The development of operational oil spill remote sensing in Canada. In *International Symposium of Operationalization of Remote Sensing,* 19 – 23 April 1993, The Nertherland, ITC Enschede.

Alexander, David. 1991. Information Technology in real-time for monitoring and managing natural disasters. *Progress in Physical Geography* **15**: 238-60.

Bales, Emory Scott and Loomis, James E. A. 1995. Case Study on the State of Florida's Emergency Management Information System. Atlanta, Georgia. Boone, Bill. (1995) FEMA-GIS Standard Operating Procedures. Unpublished Manuscript for Federal Emergency Management Agency.

Kriemer, Alcira, Munasinghe, Mohan. 1991. *Managing Environmental Degradation and Natural Disasters: An Overview.* Washington D.C.: The World Bank.

SNDR. 1992. Reducing the Impacts of Natural Hazards: A Strategy for the Nation: Subcommittee on Natural Disaster Reduction, Committee on Earth and Environmental Sciences.

Pertanika J. Sci. & Technol. Supplement 9(1):73 - 79 (2001)
ISSN: 0128-7680

The Determination of Pile Capacity Using Artificial Neural-net: An Optimization Approach

Rosely Ab.Malik & Mohamed Jamil S.
Department of Civil Engineering, Universiti Putra Malaysia
43400 UPM, Serdang, Selangor

ABSTRACT

From standard static formula for bearing capacity of a single pile foundation, an algorithm using a reliability approach for the determination of service load was developed. Using the developed algorithm, the safety measures involved are such as reliability index and the probability of failure; instead of only factor of safety if conventional deterministic approach is used. In this study, the developed algorithm is further expanded to include computation of the weight-matrix of a sequential associative feedback-type neural net model for the determination of service load of a single pile is introduced. The proposed technique concludes improved efficiency over the conventional method of commissioning the functional formula of the weights by exploiting the structural properties of the matrices appeared in the codification of the service load to a single pile problem as a quadratic zero-one optimization program. Those structural attributes are distinguished and described in terms of template-matrix contributions of the constraint functions of the quadratic optimization, to the weight-matrix asynchronous auto-associative neural net. It is stated by using those templates, the weight matrix can be taken in intuitively. Performance results of this research study reveal that neural net deterministic approach could be a better choice for implementation in identifying the required weight-matrix.

Keywords: Design chart, reliability design approach, auto-associative feedback neural-net, pile foundation, static formula, learning, potential function, fuzzy-information processing

INTRODUCTION

We can consider that neural net is a mathematical modeling of information process. It provides a method of representation of relationship, which is quite dissimilar from the sequential, conventional logic based digital computer. It represents a quantum range of artificial neural processing model. These are relatively simple mathematical constructs that are often thought to loosely model biological metaphor systems. It's representation involves densely inter-linked networks. The inherent computational speed and parallelism of neural net is the basic characteristics. Researchers approach neural nets from divergent perspectives. Summarizing all the approach is a fairly complex task, since neural net is rapidly changing. However, from architectural viewpoint, current neural net theory has three main branches: perceptron, associative memory, and biological models. These are suggestive labels, not a classic terminology, which shows the branches and researchers associated with each branch. The perceptron branch associated with Rosenblat in the 1950s is a good example. Currently, most neural nets are perceptron of one form or another. The associative memory branch is the source of current research to which Hopfield in 1982 published an influential paper which gave attention to the associative properties of a class of neural nets. Neural nets model are being accepted in the civil engineering problems (Goh 1995). Neural net can address the tasks of interpretation, classification, prediction, estimation and optimization. In civil engineering problem, most of the neural net applications have focused in feed-forward neural nets, while a few significant work has contributed in using recurrent feedback type neural net. Usually, the feed-forward neural net is more applicable in civil engineering application as compared to other class of problems to which the purpose-state is priorly

known to a given initial state (such as a sequence of n × 1 input column load vectors). On the other hand, recurrent feedback neural net (auto-associative neural net) is used where the conclusion is not known in advance. The determination of service load of a single pile by reliability approach can be an optimization problem. Among feedback neural nets, the associative neural net indicates a better fit to solving a combinatorial optimization issue. An auto-associative neural net is a single layer feedback neural net in a dynamic system, evolving in time, in either a sequential discrete or continuous output space. The transition in neural net towards an asymptotically stable solution (i.e., a minimum, local or global), is a dissipated potential function, E. A combinatorial optimization problem can be mapped on to an auto-associative feedback configuration of neural net by building pertinent potential function to which the global minimum is a solution of the optimization process. One of the difficult tasks facing designers is the translation of optimization problem into the minimization of this function. Moreover, the derivation of the weight matrix, associated with this function of the associative feedback neural net, involves complex symbolic computations. The purpose of this paper is to present a simplistic way to derive the weight-matrix of a neural net for the determination of the service loading (capacity divided by the assumed factor of safety) of a single pile foundation. The service load of a single pile have been developed earlier (Ab. Malik 1996); this study is to develop a neural net model for it. The implementation of neural net is described after a brief introduction of neural net.

NEURAL-NET

From an application perspective, one can explore neural net suits in nonlinear, parallel processing and adaptive. The term neural net is defined by a combined adaptive network and parallel processing technology. So, it requires a coherent study including application need, neural net model, and parallel processing. A neural net is an abstract sophisticated information process simulation system imitates the biological nature that pertains to the class of machine learning. It is a process of acquiring and retrieving knowledge. Neural net is characterized not only by its architecture but also by the type of neurons used by the learning procedure and by the principle of operation. It processes as deterministic or stochastic systems. In deterministic neural nets, all parameters and signals are deterministic nature. In stochastic neural nets, signals and parameters (linked-weights) are changed randomly (some probability) by some random amount.

Our sequel in-search and analysis will aim to address the following questions during the undertake of this development and research project:

1. How does the auto-associative feedback memory-based neural net algorithm behave with a current prototype Single pile loading test system?
2. Given a fixed set of training data set pattern, is it better to adjust the linear weight-matrix after each pattern or (In which case the method becomes a version of neural net for linear or quadratic programming) all the patterns?
3. How far do the answer of the first two questions apply to the related method such as mapping on recurrent neural net multi-layer perceptron (MLP) based architecture?

OPTIMIZATION PROCEDURE FOR DETERMINATION OF CAPACITY: DETERMINISTIC VS. RELIABILITY APPROACHES

The determination of predicted capacity, Q_p (and consequently the allowable capacity, Q_a) can be computed by a depth integration process preferably set up on a spreadsheet for calculations for every foot of the embedded length of pile. The recommended procedures can summarized as:

Select the recommended factor of safety, SF, or reliability index, β, to the respective method of determination. Determine the perimeter surface area of pile shaft, A_s and the toe bearing area, A_t. The reliable method to determine the pile capacity is to perform a loading test. The pile could be loaded by using a hydraulic jack and jacking against reaction piles, or a weighted platform. Piles are often tested after driving when load test equipment has been made. A detailed comparison of the various methods or testing systems is beyond the scope of this paper. The density function ¶(q) can be determined from the previously developed algorithm (Ab.Malik 1996) :

$$f(q) = Q_p = \left(\sum_{i=1}^{n} \left[(p'_{ov} K_s \tan\delta)_i \right] (A_s)_i + (p'_t N^*_q A_t) \right)$$

$$= \sqrt{\left(\sum_{i=1}^{n} [Q_s] + Q_t \right)^2} \qquad (1)$$

Where, Q_p, Q_s, Q_t are the predicted capacity, shaft capacity, and toe capacity respectively from the recommended equations. Also, note that this density function is selected to be quadratic for mathematical reasons only because and the total predicted capacity from the algorithm may be found from the different criteria. The variability of the predicted capacity of a particular site, s.

QUADRATIC ZERO-ONE PROGRAMMING TO SOLVING PILE CAPACITY

It was originally developed for the equality constrained optimization problem, which we repeat here for convenience. Minimize

$$f(x) = c^T x + \tfrac{1}{2} x^T Q x, \ldots \qquad (2)$$

$x \in \{0, 1\}^n$, where $c \in \Re^n$, $Q \in \Re^{n \times n}$ is a symmetric n×n matrix. The components of the design vector x can take only discrete (binary) values 0 or 1. In other words, the design vector x is represented by an n-dimensional cube called a unit hypercube with vertices at the points $x = [x_1, x_2, \ldots, x_n]^T$, $x_i \in \{0, 1\}$ (i = 1, 2, ..., n). In ordinary, such a unit hypercube has 2^n distinct vertices which corresponds to 2^n possible states of the neural net employed to solve the problem. The problem is written equivalently as min

$$f(x) = x^T Q^* x, \; x \in \{0, 1\}^n$$

where,

$q'_{ii} = c_j + q_{ij}/2$

subject to $h_i(q) = 0$ (i=1,2, ..., n), $q \in \Omega \subset \Re^n$.

For this , we will put the construct of the Lagrange function below as

$$L(Q,\lambda) = f(Q) + \sum_{i=1}^{n} \lambda_i h_i(q), \qquad (3)$$

where the components of the vector $\lambda = [\lambda_1, \lambda_2, \ldots, \lambda_n]^T$ are the Lagrange multiplier.

1st type of constraint of the pile loading optimization refers to the Pile settlement movement s_i of each activity si and this could be expressed as

$$h_i^{(1)}(Q) = \sum_{k_1(i)}^{K_2} q_i^{(k)} - s_i \qquad (4)$$

I = 1,2,& , I with I denoting the total number of noncritical tests, while $k_1(i)$ and $k_2(i)$ are expressed as

$$k_1(i) \cong EST_i + 1 \qquad (5)$$
$$k_2(i) \cong EST_i + s_i + TF_i \qquad (6)$$

in eqns. (5) and (6), ESTi and TFi denote, the earliest start time and the total float of activity i.

Having a defined constrains associated with the single Pile loading test patterns and a procedure of augmented Lagrangian multiplier optimization, the equality- constrained quadratic optimization has been replaced by the unconstrained minimization of the augmented Lagrangian

$$L(Q) = f(Q) + \sum_{i=1}^{I} \lambda_i h_i^{(1)}(Q) + \frac{1}{2}\sum_{i=1}^{I} \beta_i \left[h_i(Q)\right]^2 + \qquad (7)$$

Where λ_i, β_i denote the Lagrange multiplier and associated penalty parameters. The augmented Lagrangian has been interpreted as the signal Potential function of an auto-associative feedback (Hopfield) neural net. Consequently, a solution to the single pile loading problem can be obtained by minimizing the augmented Lagrangian function,

$$E = L + \text{factors of safety functions.} \qquad (8)$$

The augmented optimization of this phase onto the proposed neural net architecture, is frame-work modelled to next section.

MAPPING MULTIPLIER OPTIMIZATION ONTO THE FEEDBACK ASSOCIATIVE NEURAL NET

In order to design neural net for a specified optimization problem, we attempt to construct a suitable computational function whose minimization leads to a system of differential equations. There are a number of approaches in the use neural net to optimization problem; such as follows:

i) Searching type neural net (Parallel Feedback associative - memory or BAM neural net)
ii) Self- organization map (SOM)
iii) MLP recurrent neural net
iv) Hybrid method combining the above approaches.

In a search type neural net, the neural net is set up in such a way that the dynamic of the network is constrained toward a local minimum which represent a possible solution.

$$\frac{du_m}{dt} = \frac{1}{c}\left(\sum_{n=1}^{N} T_{mn} V_n - \frac{u_m}{s_m} + x_m\right) \tag{9}$$

$$v_m = g_m(u_m) = \frac{1}{2}\left(1 + \tanh \lambda_{u_m}\right) \tag{10}$$

The output of each neuron (PN) is represented by v_m, which is related to u_m called the net input, by the output function, g_m. λ_{u_m} scale constant which control the speed of the convergence of neural net. The augmented Lagrangian E of Eqn. (3) can be written in a matrix form as

$$f(x) = E(Q) := c^T x + \tfrac{1}{2} x^T Q x + \vartheta \tag{11}$$

where, ϑ is a constant, and the unconstrained optimization problem that consists of minimizing the augmented Lagrangian E of Eqn. (11) can be solved on line by employing the neural network architecture proposed by Savin *et al.* The basic building block of this architecture is a feedback associative neural net, whose dynamics result in minimizing an potential function $E_H(v)$, which in a quadratic form of the output vector x i.e.

$$E_H(v) = -t^T v - \tfrac{1}{2} v^T W v \tag{12}$$

In Eqn. (12), t is a column vector denoting the threshold inputs to the neurons, and W is symmetric matrix whose entries are given by the weights of the neural net. To consider of Feedback associative neural net to minimize the Lagrangian E of Eqn. (11), the output v of a feedback associative net (Hopfield) is interpreted as the design vector x associated with a given project, and the weight matrices of the neural net are replaced as

$$t = -c \text{ and } -Q = W \tag{13}$$

The key problem facing the mapping of the Pile loading issue on to a Hofield neural net is auto-associated with deriving an efficient technique for determining the matrices Q and c of Eqn. (11). Potential function,

$$E = -\frac{1}{2}\sum_{m=1}^{M}\sum_{n=1}^{N} T_{mn} u_m V_n + \frac{1}{\lambda}\sum_{m=1}^{M}\frac{1}{s_m}\int_0^{v_m} g_m^{-1}(v)dv - \sum_{m=1}^{M} x_m v_m \tag{14}$$

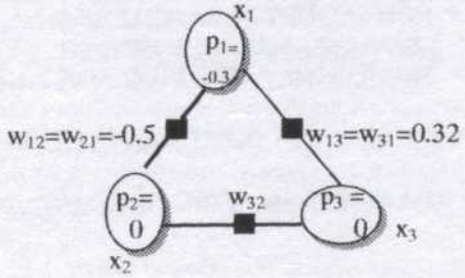

(a)

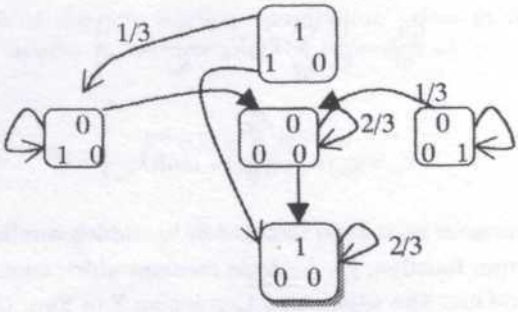

(b)

Fig. 1. A simplified auto-associative feedback neural net and its partial-state transitions

DEVELOPING NEURAL-NET: CAPACITY OF SINGLE PILE

Developing on neural net prototype is depicted by the requisite phase-cycle of a Neural net. Prototype from the conceptual to implementation steps. The phase cycle of developing an neural net prototype as described in appendix Fig. 2 and Fig. 3 includes the following issues (Al-Sugair 1997): Neural net feasibility-study, Initialization and Algorithm analysis, data-set preparation for train/or learning, neural-net architecture selection, net test and reliability factors, net-training, neural-net self-organization & adaptation and Implementation.

CONCLUSIONS

These findings are feasible and theoretically feasible, given the relatively small sample of a single pile calculation and suggest the possibility of developing a model method to

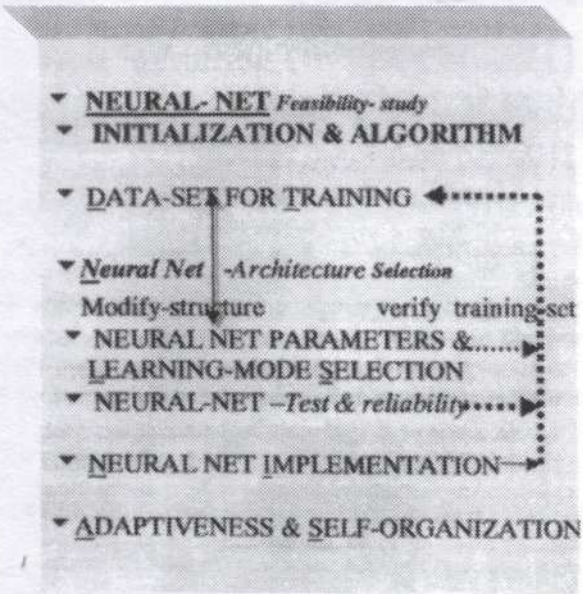

Fig. 2. Neural net Prototype for pile capacity test system

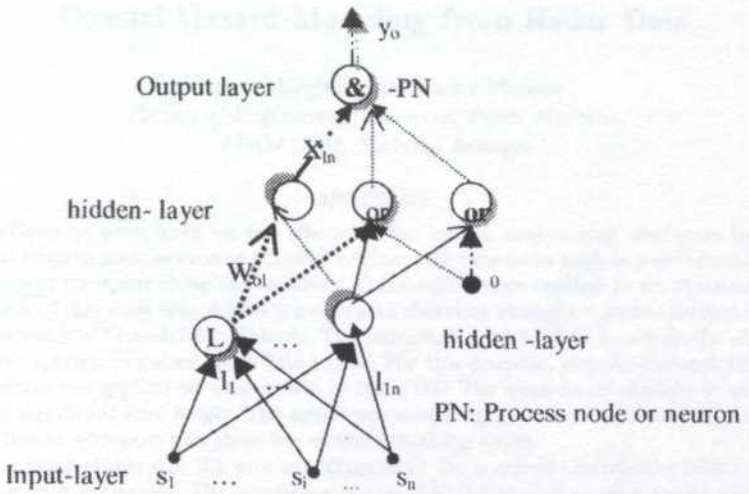

Fig. 3. A fuzzy neural-net model

allow optimization of resulting nonlinear weight-matrix concentrations on the basis of the configuration of the neural net. If these results are reproduced in large-scale research studies, that could provide a cheap and effective model method to asses different single pile loading spreadsheet design test plans.

We believe these are two important factors coming from the present research. Apart from that, this paper will also provide some attention to some aspect of program development. We hope that these results may provide the necessary impetus to applying feedback neural net (reduce-flaws) to non-linear and adaptive system identification.

ACKNOWLEDGEMENT

This research wouldn't have been such a success without the support and comfort, as well as assistance from the Ministry of Science, Technology and Environment, Universiti Putra Malaysia and GeoEnTech Sdn. Bhd. We wish to express sincere thanks to those for a number of superb discussion of the neural-net.

REFERENCES

Al-Sugair Abdullah, M. and A. A. Al-Quadrah. 1997, Artificial Neural Network Approach for Pavement Maintenance. In *Proc. of 1st Congress on Computing in Civil Engineering*, ASCE.

Ab. Malik, R. 1996. Design of pile foundation: correlation of safety measures from deterministic and reliability-based approaches. *J. of IEM.* **57(1)**.

Embree, P. and B. Kimble. 1991. *C-Language Algorithm for Digital Signal Processing.* Prentice hall.

F. Fazio, S. P. Alkass and Savin. 1998. To calculate weight – matrix of neural net for resource-leveling. *J. of Computing in Civil Engineering*: 241-247.

Harvey, R. L. 1991. Recent Advances in Neural Networks for Machine Vision. In *Proceedings of the Third Biennial Acoustics, Speech, & Signal Processing Mini Conference* (p. IV.1-IV). Weston, MA: IEEE Central England Council.

Niez J. and L. Herault. 1991. Neural networks and combinatorial optimization: A study of NP-complete graph problems. In *Neural Networks: Advances and Applications.*

Pertanika J. Sci. & Technol. Supplement 9(1):81 - 86 (2001)
ISSN: 0128-7680

Coastal Hazard Modeling from Radar Data

Maged Marghany & Shattri Mansor
Faculty of Engineering, Universiti Putra Malaysia
43400 UPM, Serdang, Selangor

ABSTRACT

The effects of wave force or the effects of the coastal engineering structures induce coastal hazards such as erosion. Coastal engineering structures such as jetties could trap a sediment transport along the coastline. This could induce erosion in the downstream. The aim of this study is to model the effects of shoreline changes to jetties located along coastal water of Chendering, Malaysia. The numerical model will be based on the change of wave spectra extracted from ERS-1 data. For this purpose, two-dimensional Fourier Transform was applied on window size of 200 × 200. The quasi-linear model was used to model significant wave height. The significant wave height was used to model the volume of sediment transport and shoreline evaluation along jetties.

The result shows that the erosion occurred in the south of Chendering with rate of change of 4 m/month. The prediction shows that the rate of erosion would increase within 10 years. This study shows the location of jetty decreases the rate of sediment transport along the south of Chendering. It can be said that ERS-1 data are able to predict shoreline evaluation along the coastal structures. The jetty induced an equilibrium beach profile along jetty. This is due to that jetties-trap sediment in the north of Chendering, which lead to erosion in the south of Chendering.

Keywords: erosion, sediment transports

INTRODUCTION

Coastal erosion occurs due to the effects of the coastal construction such as jetties, which is an interesting topic between scientists. Kraus *et al.* (1984) and Hanson *et al.* (1990) used a numerical model of waves in order to predict shoreline change due to the present of breakwater. Kraus *et al.* (1984) found that the accumulation of the sand was began to take place as the breakwater progressed and by the time the latter were completed, nearly 370,000 cu. yds. of sand were found deposited in the harbor. Up to now, there are few studies on wave effects on coastal structures, which were conducted on the East Coast of Malaysia. Stanely *et al.* (1985) reported that erosion along the shoreline of Chendering port due to the jetty traps the sediment and causes erosion at the down of littoral drift and accretion to the upper littoral drift. However, this study could not model the shoreline rate changes between seasons. Moreover, this study could not answer question such as what the breakwater effects in terms of short time and long time. Recently, Maged and Shattri (1997) used radar data (ERS-1) to predict the shoreline changes along port of Chendering. They found that the rate of erosion was 4 m/yr. Maged and Shattri (1997) could not identify the location of erosion and sedimentation. Some other studies such as Salleh *et al.* (1991) used numerical model to investigate the effect of tidal current on nearshore sediment transport. However, the nearshore sediment transport does not induce by tidal current but induces by the wave effects. The aim of this study is to model the effects of shoreline changes to the jetties located along coastal water of Chendering, Malaysia.

METHODOLOGY

Study Area

The study area is located in the South China Sea between 5° 14' N to 5° 18' N and 103° 10' E to 103° 12' E. This area lies in an equatorial region dominated by two monsoon

seasons (Rosnan 1987 and Maged 1994). The southwest monsoon lasts from May to September while the northeast monsoon lasts from October to March. The monsoon winds affect the direction and magnitude of the waves. Strong waves are prevalent during the northeast monsoon when the prevailing wave direction is from the north from December to February, while during the southwest monsoon (May to September), the wave direction from the south (Wong 1981). The rate of longshore drift based on wave effects is about 40,000 to 50,000 cubic meters per year (Stanely *et al.* 1985).

Wave Spectra Model

Wave spectra are derived from the C-band ERS-1 by applying two-dimensional Fourier Transform from PCI's EASI/PACE image-processing system this. The wave spectra derived from C-band ERS-1 were mapped into the real wave spectra by using quasi-linear model. This model was simplified by Vachon *et al.* (1994) as follows

$$S(Q) = H(Kx; Kc)\, S(L)\, S(k) \quad (1)$$

where S (Q) is a quasi- linear transform function, Kx is wave number azimuth direction; Kc is the cut-off wave number, which function of wind speed. S (k) is an ERS-1 wave spectrum while S (L) is real wave spectra measured in situ.

Equation 1 used to model significant wave height (Hs) along the jetty as

$$Hs(Kc) = F(Kc, U) \quad (2)$$

where U is wind speed m/s.

The modulation spectra were used to model the wave diffraction feature along the jetty located on Chendering port. The method of Huygen was used to plot wave ray diffraction.

Shoreline Change Model

The governing equation for shoreline position y is given by

$$\partial Y/\partial t + 1/D(\partial Q/\partial x \pm q) = 0 \quad (3)$$

where x is the longshore coordinate, t is the time, D is the depth of closure (beyond which the profile is assumed not to be move), and Q is the longshore sand transport rate. The predictive expression for the longshore transport rate is taken as

$$Q = H_b^2 C_{gb}/16(\rho_s/\rho - 1)(1-p) * (K_1 \sin 2\theta_{bs} - 2k_2 \partial H_b/\partial x \cot\beta \cos\theta_{bs}) \quad (4)$$

where C_{gb} is the wave group velocity at the jetty line, (ρ_s(ρ) is the sand water density, p is the sand porosity, θ_{bs} is the angle of the breaking wave crests to the shoreline and tan β is the beach slope. The coefficient K_1 and K_2 are treated as the parameters in the calibration of the model (Kraus *et al.* 1984).

RESULTS AND DISCUSSION

Fig. 1a shows that the wave peaks propagated from southeast direction. When the wave spectra approached the jetties, the wave spectra turn to propagate toward the southwest

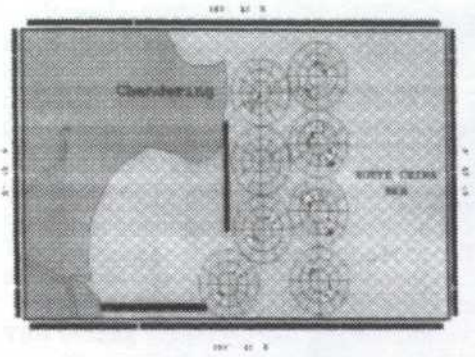

Fig. 1. (a) Wave spectra model from Ers-1 data

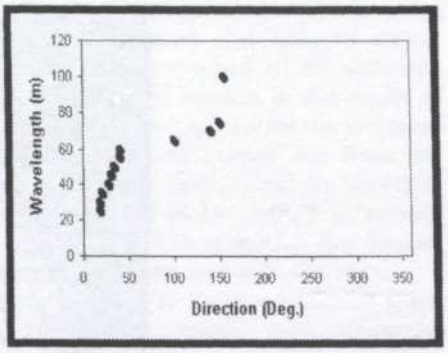

Fig. 1. (b) Wave spectra direction and length

direction and tend to curve along the jetties (Fig. 1a). The wavelength along the jetties ranged from 25 m to 100 m (Figure 1b). It obvious that the wavelength decreased when the wave spectra changed their directions (Figure 1b). Figure 2 shows that the wave orthogonal tended to curve along the jetties. The wavelength decreased near the jetties and inside the port. This indicates that the wave diffraction patterns. A similar finding is in Fig. 1. Figure 3 shows that the longshore current vectors moved with velocity ranged from 0.3 m/s to 1.3 m/s towards the northwest direction. The maximum velocity was observed in the south jetty while the minimum velocity was observed in the north jetty. This means that the jetty could reduce the longshore current velocity. The longshore current curved inside the port and moved out the port with minimum velocity towards the north of Chendering. Figure 4 shows that the erosion occurred in the south of Chendering and north of Chendering with approximately 4 m/month. The sedimentation occurred near to the south jetty with -2.3 m/ month.

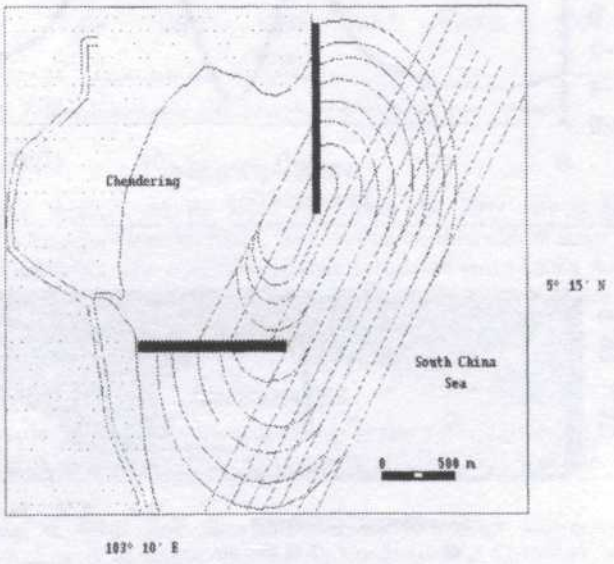

Fig. 2. Wave diffraction pattern along Port Chendering

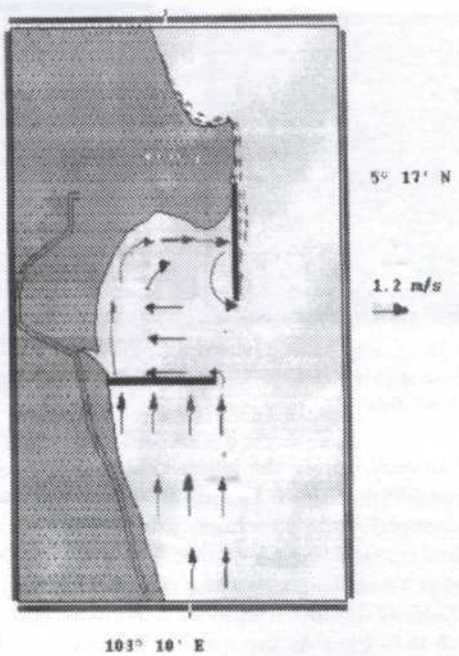

Fig. 3. Longshore current modeled from wave spectra

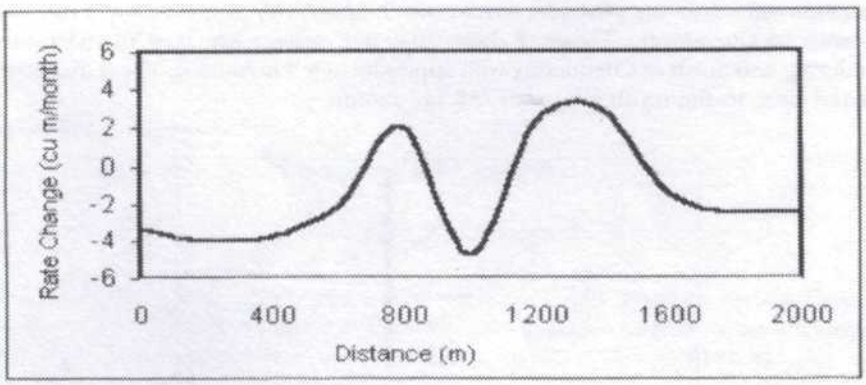

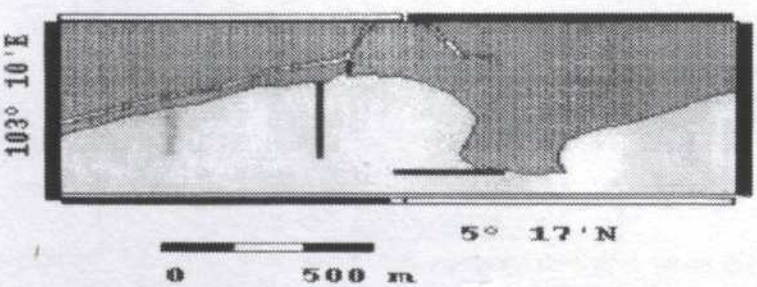

Fig. 4. Shoreline change modeled by quasi-linear transform

It can be explained that the mechanism of the shoreline change along the Chendering as: the southerly wave when approached the jetty diffracted and induced strong longshore current at the southerly jetty. This southerly jetty trapped all the sediment transport and deposited beside the jetty. This action caused erosion in the south of Chendering. Inside the Chendering port the current meander and carried the sediment out the port causing erosion inside the port. The sediment carried out from the Chendering deposited along the north jetty. Due to the weak littoral drift the shoreline extends along the north of Chendering exposed to erosion by less than 3 m/month. These results are not similar to study of Stenely *et al.* (1985). This is because that Stenely et al., 1985 did not use the diffraction as an index of erosion and sedimentation.

Fig. 5 shows that the rate of erosion could be exceeded to 5 m/year with 10 years. This finding suggested that the location of the jetty cause continuos erosion along the year. The ground data coincided with the quasi-linear model. This can be suggested that high accuracy involve with the model.

In spite of that, August represents a southwest monsoon season in which characterized by less wave energy in coastal water of Kuala Terengganu, erosion occurred along the Chendering shoreline. This suggests a future study, which includes the modeling of the shoreline change along the Chendering by using the integration of Kapas Island and jetty in shoreline configuration.

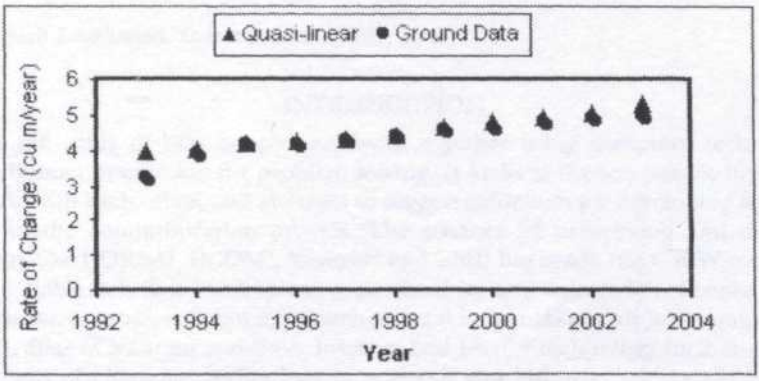

Fig. 5. Shoreline erosion rate in south of Chendering over 10 years

CONCLUSION

In conclusion, ERs-1 data could be used to derive the jetty effects in shoreline configuration. This is because that the ERS-1 data can be used to model wave information compare to classical methods. The shoreline change simulated from ERS-1 data suggested that jetty caused erosion along the coastal water of Chendering. With above study it was found that the rate of erosion could be increased with time.

REFERENCES

KRAUS, N.C., H. HANSON, H. SOICHI. 1984. Shoreline change at Oarai Beach: Past, Present and Future Proceeding of 19th Coastal Engineering Conference. p: 2107-2123. September 3-7, (1984), Houston, Texas.

HANSON, H. M.C. KRAUS, M. ASCE. 1990. Shoreline Response to a Single Transmissive Detached Breakwater. Proceeding of 22 coastal Engineering Conference. p. 2034-2046. July 2-6, 1990, Delft, Netherlands.

MAGED, M.M. 1994. Coastal water circulation off Kuala Terengganu. M.Sc. Thesis, Universiti Pertanian Malaysia.

MAGED, M.M. and S.B MANSOR. 1997. Offshore and Onshore wave Spectra along Chendering Coastline. Paper presented in *18th Asian Conference on Remote Sensing.* October 23-27 Kuala Lumpur, Nikko Hotel.

ROSNAN, Y. 1987. Geophysical studies in Setiu Lagoon Estuary System. M. Sc. Thesis, Universiti Pertanian Malaysia.

SALLEH, M.N., A.Z. IBRAHIM and A.K. WAHAB. 1990. Application of Mathematical Model in Port Planning and Maintenance. *Proceeding of Coastal Engineering in National Development,* 4-6 March 1991, Hotel Shangrila, Kuala Lumpur, Malaysia: E18-E37. Stanley Consultants Inc. 1985. Malaysian National Coastal Erosion Study. Vol. II. Kuala Lumpur: UPEN.

VACHON P.W., K.E. HAROLD and J. SCOTT. 1994. Airborne and spaceborne synthetic aperture radar observations of ocean waves. *J. Atmo.-Ocean* **32(10)**: 83-112.

WONG, P.P. 1981. Beach changes on a monsoon coast Peninsular Malaysia. *Geol. Soc. Malaysia. Bull.* **14**: 59-47.

ISSN: 0128-7680
Pertanika J. Sci. & Technol. Supplement 9(1): 87 - 95 (2001)

A Java Based Multimedia Distributed Computer Supported Collaborated World (CSCW) Environment Over the Internet

Chee Boon Kok, Malay R. Mukerjee, Borhanuddin Mohd Ali & Abdul Rahman Ramli

Department of Computer & Communication System Engg
Universiti Putra Malaysia, 43400 UPM Serdang, Selangor, Malaysia
Email: cbkok@cae.upm.edu.my

ABSTRAK

Computer Supported Collaborative Work (CSCW) and distributed computing have been termed as the next paradigm of computing which allows users to interact and collaborate with each other seamlessly over the network. As a result, many collaborative distributed CSCW system have been proposed and developed. However, most of the system fall short in providing platform independent system that address many real-world needs of users working together in a CSCW system. In this paper, efforts have been focused on creating a Distributed Computer Supported Collaborative Work environment for efficient collaborative editing and interaction among the participating users over the internet that support asynchronous and synchronous collaboration. Java has been used developed language.

Keyword: Distributed, Collaboration, CSCW, Java

INTRODUCTION

CSCW is the study of how people may work together using computer technology to facilitate human interaction for problem solving. It looks at the way people interact and collaborate with each other, and attempts to suggest guidelines for developing technology to assist in the communication process. The advance of networking and distributed technology like CORBA[1], DCOM[2], Voyager[3] and RMI[4] has made the CSCW concepts an ideal and viable solution for improving productivity and innovation. People can now communicate, interact, collaborate, search or send information with just a simple mouse click regardless of location and time. Internet and Java™[5] technology further accelerate the adoption of computer technology in research and industry.

This trend might be extended to a flexible-working trend in the future. In contrast to the traditional working style (with employees actually clocking in and off of shifts controlled by factory klaxons), future employees might come and go within certain hours, and would be free to organize their time as long as they meet the deadlines. In another scenario, employees might just work from their home, eliminating the need to commute to the office and meet their colleagues face to face.

CSCW system plays an important role on the success of teamwork and flexible-working concepts. CSCW system will assist groups in communicating, collaborating and coordinating their activities. While the idea of supporting these activities is not new, the realization of any form of computer support has been more difficult than most would

1. OMG Home page CORBA http://www.omg.org/
2. Microsoft Distributed Component Object Model (DCOM). http://www.microsoft. com/com/dcom.asp
3. Object Space Voyager. H=http://www.objectspace.com/products/voyager/index.html
4. JavaTM Remote Method Invocation. http//java.sun.com/products/jdk/rmi/index.html
5. JavaTM Technology Home. Http://java.sun.com/
6. Flexible JAMM (Java Applet Made Multiuser). http://simon.cs.vt.edu/jamm
7. Tango2. TANGO 2 Documentation." http://trurl/krzysztof/tangodoc/

have anticipated. This is because of the diverse nature of task undertaken by groups, diffrerent styles of group working, and a host of behavioral factors which are difficult to overcome. The challenge to the CSCW designer will be to come out with a solution to solve different problem domains of a workgroup environment. Recent (Shirmohammadi & Georgamas 1997), projects like JAMM[6], Tango[7] and JETS by MCRLab of University of Ottawa[8], show various approaches utilizing different techniques and models to create CSCW system. Java Distributed Collaborative Environment (JDCE) is an attempt to offer different solution for solving problem in a general system.

COLLABORATION MODEL

Asynchronous Collaboration

In asynchronous collaboration, the interaction between users happens regardless of the time factor. Users are not required to be online simultaneously for collaboration. Users can log on to the system at different times but still can collaborate on the shared data as long as the collaboration system is running. There is also no strict timing requiremet for data delivery. Users can log in into the system and modify the shared data at any time while the system will maintain the consistency of the data. The system updates the modified data to other users at later times when they log in into the system again. It is the main responsibility of the asynchronous system to make sure that all the users get the updated shared data. In this case, the reliability of the data delivered becomes the key factor of asynchronous system. Example of asynchronous collaboration system is email, Network News Transfer Protocol (NNTP) (Kantor & Lapsley 1986).

Synchronous Collaboration

In synchronous collaboration, users must be online simultaneously for collabration. A message sent from one users is immediately sent to all others in the same collaboration session. There are two general approaches to provide awareness for synchronous collaboration. One is the sharing of legacy single-users applications. This is referred to as collaboration transparency because the sharing is provided by a mechanism that is unknown, or transparent to the advantage of allowing the users to utilize legacy application that they are familiar with and, thus increases the productivity of the users. Several collaboration transparency systems that have been implemented include Old Dominion University's XTV(Abdel - Wahab and Feit 1991), Sun Microsystem' ShowMe SharedApp(1994) and Microsoft's Netmeeting (1998).

The second approach, known as collaboration awareness, is where the application are specifically developed to support cooperative work. These applications may be developed ad hoc or with a groupware toolkit such as the University of Calgary's GroupKit (Roseman & Greenberg 1996) and Old Dominion University's Java Collaborator Toolset (JCT) (Abdel - Wahab *et al.* 1996). This approach offers the freedom of building more visual awareness to the applications targeting special collaborative activities. This type of synchronous collaboration model has been adopted in JDCE.

Hybrid Collaboration Model

JDCE is a CSCW system that implements the hybrid model were both the asynchronous and synchronous model are supported. This provides the maximum flexibility for users working in this environment.

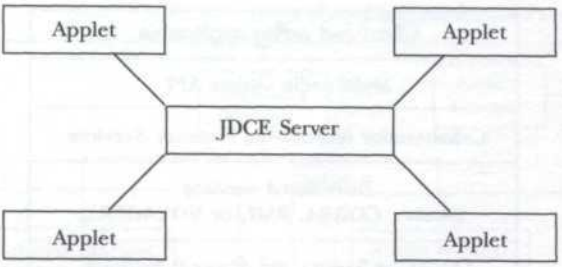

Fig 1. JDCE client-server architecture

NETWORK ARCHITECTURE

In a collaborative environment, the resources and users are normally distributed over a vast network. The system needs to provide the communication channels for efficient interaction between users and the system. Various architectures requirements of a particular system and application. Generally, collaboration architecture can be divided into three main models:

- Client-server architecture - centralized model
- Server network architecture - partially distributed model
- Peer-to-peer architecture - fully distributed model

JDCE has been implemented using the client-server architecture since the client of JDCE is built as Java applet where it can only connect to the originating server. Fig. 1 shows the diagram of client-server architecture implemented in JDCE.

A central points of communication makes it easy for message routing and state management. Access to the system can be controlled easily and different floor control can be applied for effective collaboration. This architecture also allows the implementation of shared object that are accessible by all the users. Shared object helps in keeping the consistency of the application shared-data state. The server control access to the shared object through an object looking mechanism. A user who wants to change the share object state must look at the shared object first, perform the modification and release the lock. Other users are only allowed to modify the shared object when the lock on the object is released. This approach is also good for latecomers who can get the latest shared object states which are synchronized with other users in the same collaboration session.

SYSTEM ARCHITECTURE

This environment has been built using an object-oriented layering architecture API. The system layering architecture is presented as illustrated in Fig. 2. The purpose of using the layering architecture is to partition the system into layers responsible for different tasks. A clear interface is defined between layers, which provide a public protocol for communication between them. Thus, changes in one layer will not have any effect on other layer.

At the top layer, there exist various multimedia application like video conference, electronic notebook, shared whiteboard and distance learning applications. These applications use the services of Multimedia Object API.

The second layer is a Multimedia Object API. This layer has been constructed using object-oriented approach and consists of object classes that can be used to generate,

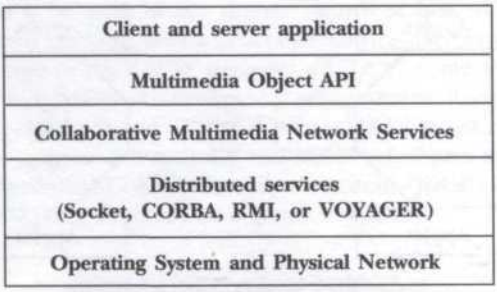

Fig 2. Object-oriented layering architecture API

display and modify the content of multimedia data. Example of the multimedia object classes are text, graphics, audio and video object classes. Most of the new Java Media APIs have been incorporated into this layer. An open approach is used to accommodate future media that are not supported now.

The third layer consists of distributed multimedia services that are needed to support the operation and management of distributed multimedia applications. This layer is further divided into different subsystem that provide different services to the multimedia applications. The subsystem are Communication Service, Session Service, Naming Service and Management Service.

The fourth layer offers distributed network services. Currently, Java socket has been used as the vehicle of the distributed services. However, these services can be easily extended to include the support for CORBA, Java RMI or voyager distributed system.

SYSTEM INDEPENDENT COLLABORATION PROTOCOL (SICAP)

The performance of this environment has been improved by the introduction of a system-independent Collaboration Access Protocol (SICAP). SICAP is a high level protocol. Fig. 3 illustrates the communication between SICAP and other distributed services like CORBA, RMI, Voyager and network protocols.

The key design objective of SICAP is to increase the efficiency, utilization and performance of client-server communication by reducing the bandwidth usage and yet offer a wide range of functions and facilities that are needed for distributed collaborative

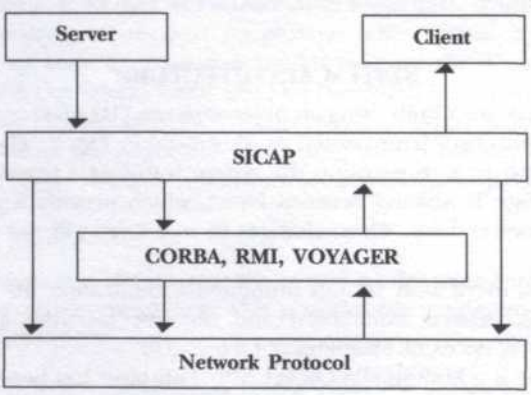

Fig 3. Communication between SICAP, client and server

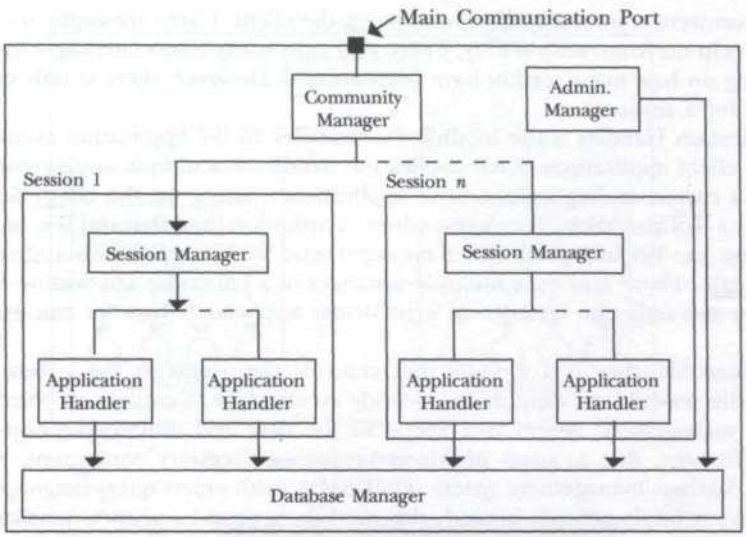

Fig 4. Communication between SICAP, client and server

environments. More detail description about SICAP are available in (Boon Kok *et al.* 1998).

IMPLEMENTATION

JDCE Server

The JDCE server is the main component of the JDCE system. The JDCE server consists of several modules. Fig. 4 illustrates the general structure of the server and relationship between them.

Community Manager is a module that controls the operation of the whole server. It accepts messages from a client and responds to the client's request through a well known port number. This module has direct control of the session manager modules. It keeps a lists of all active sessions currently in the system. Actions such as joining or leaving a session and session creation are handled by the community manager module. Any changes in the system state are broadcast to all members in the community. The module is also responsible for terminating the session when there is no users left in the session. It communicates with the administration manager to receive configuration setting and system data. Only one instance of such a module exists in running server.

Administration Manager is a module that provides the functionality for system administrator to change and set up the configuration of the server. In the current implementation, only the system administrator has direct acces to this module. This is to protect any changes to the system level state by unauthorized users. As with the community manager, each running server has only one instance of the administration manager module.

Session manager is a module responsible for controlling and providing services for all activities in a session. Each session created is associated with one instance of this module. Each module keeps a list of application handler that can be referred by the client applications. This module accepts control messages from the community manager directly and its controls all the application handler running under the same session. It

accepts connection from a session window on the client. Client messages are broadcast to all users in the same session only. There may exist many session manager in the server depending on how many session have been created. However, there is only one session manager for a session.

Application Handler is the module that handles all the application event messages from the client applications. Each application handler is a unique implementation that matches a corresponding collaborative application running on the client side. For an example, a collaborative document editor application handler on the server. This application handler interprets all the messages send by this application and responds to the messages. There may exist multiple instances of a particular application handler in the server but only one instance of a particular application handler can exist in one session.

Database Manager is a module that controls the access to the system database. Initially, this module was supposed to provide an interface to control an object-oriented database management system that keeps all the data and multimedia objects in the system. However, due to some problems in getting necessary equipment, the object-oriented database management system (OODBMS) (with object query language support) has not been implemented. Instead, this module is used to provide persistent object services to store and retrieve the multimedia object and data. A simple object-oriented database management system (without support for object query language) is implemented partially and is controlled by this module. All application handler send request to the database manager directly for getting any multimedia object. The administration manager accesses the database manager directly when updating the system database.

The server functions are discussed in (Boon Kok *et al.* 1998a) and (Boon Kok *et al.* 1998b). A snapshot of the running server are shown in Fig. 5.

JDCE Client

The JDCE client consists of three important components for the proper operation of the client; Mainapplet, Session Window and Collaborative Application. Fig. 6 shows the three components of the client and relationship between them.

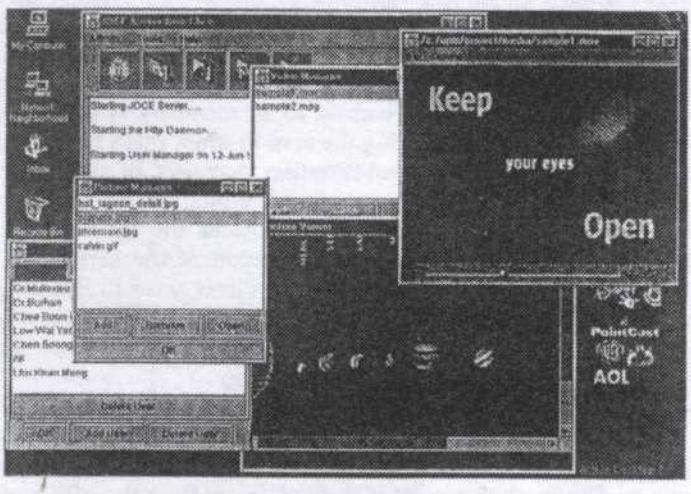

Fig 5. JDCE server in action

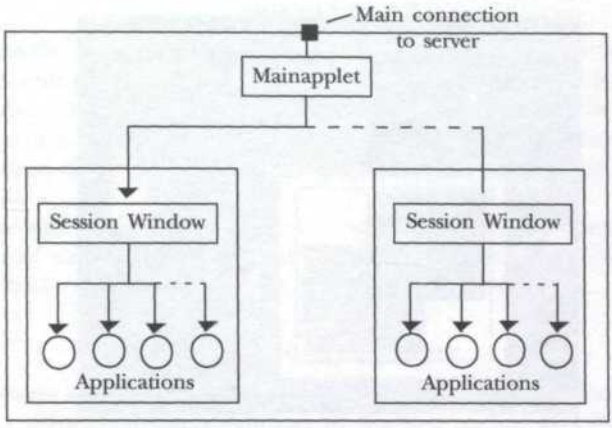

Fig 6. General structure of JDCE client

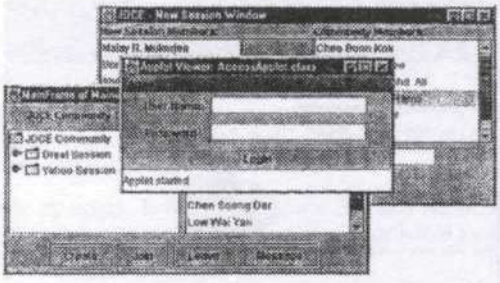

Fig 7. Mainapplet in action

Fig 8. Session Window of JDCE client

The Mainapplet is the main component of the JDCE client. Mainapplet is the central control for the JDCE client. This component provides the necessary user interface for a user to log in remotely to the server. This component communicates with the server directly to establish a connection for control message distribution. It is also displays all running session in the server and all the active users in the system. Any changes to the system state are send to Mainapplet by the server. This component controls the creation of Session Window and passing the necessary data to the Session Window like port number of the corresponding session manager on the server. There is only one instance of Mainapplet in every running client. Mainapplet screen shot is shown in Fig. 7.

The Session Window is a component that groups a set of collaborative application that are available for a particular session. When a user join a particular session, this

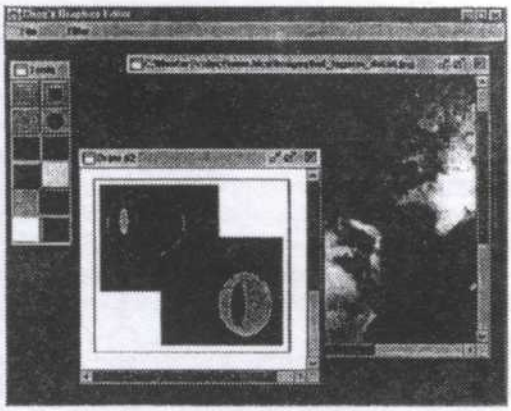

Fig 9. Graphics editor in action

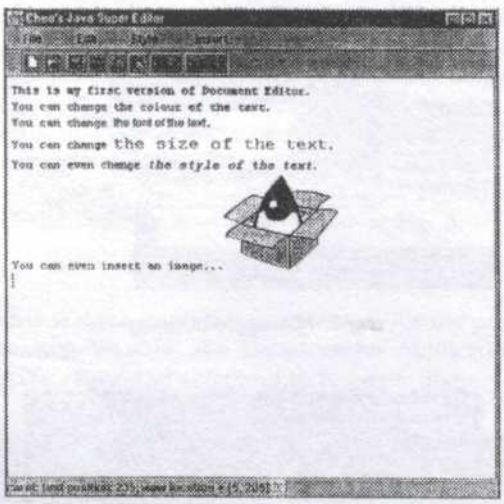

Fig 10. Word editor in action

window is created dynamically by the Mainapplet. When created, this component opens a connection to the corresponding session manager and passes it to the right application ID that comes with the message. The Session Window is shown in Fig. 8.

The Collaborative Application is a tool that provides facility for collaborative work. A set applications which provides different functionalities has been included in each session to help the users to finish their tasks. These application can be activated through the Session Window. Any application event message received from the Session Window. JDCE provides various collaborative applications such as chat client, graphics editor and word editor. Figs. 9 and 10 show snapshot of the graphics editor and word editor respectively.

CONCLUSION

A new multimedia distributed CSCW enviroment has been presented which permits workers in different physical location to work together on a multimedia document using internet resources. The set-up of user interface is an improvement in earlier proposals in that a reduction in bandwidth has been achieved, more collaborative- aware user interface has been designed and text and graphics editing is possible as a collaborated activity.

Though the system has been developed using Java, it is flexible enough to incorporated different kind of existing user environment. The effectiveness of the operation with CORBA and similar ORB environments is still under investigation.

ACKNOWLEDGEMENT

The authors would like to acknowledge the research support provided by the University Putra Malaysia through financial support to the first author and the use of existing facilities.

REFERENCES

ABDEL-WAHAB H. and M. FEIT. 1991. XTV: A Framework for X Window Clients in Remote Synchronous Collaboration. In *Proc. of IEEE TriComm:* 159-167.

ABDEL-WAHAB H., B. KVANDE S. NANJANGUD, O. KIM and J. P. FAVREAU. 1996. Using Java for Multimedia Collaborative Applications. In *Proc. of the 3rd Int. Workshop on Protocols for Multimedia Systems (PROMS'96),* October 1996, Madrid.

CHEE BOON KOK, MALAY R. MUKERJEE, BORHANUDDIN MOHD. ALI and ABDUL RAHMAN RAMLI,"SICAP: A system- independent Collaborative Access Protocol For Distributed Collaborative Environment," Proc ICIMU 98, UNITEN September 1998.

CHEE BOON KOK, MALAY R. MUKERJEE, BORHANUDDIN MOHD. ALI and ABDUL RAHMAN RAMLI. A Java Based Object-Oriented Multimedia Distributed Collaborative Environment Over the Internet. In *Proc. NCTT'98,* UPM, December 1998.

KANTOR B. and PHIL LAPSLEY. 1986. Network News Transfer Protocol: A Proposed Standard for the Stream- Based Transmission of News. RFC 977, U.C. San Diego and U.C Berkeley.

Microsoft Net Meeting. 1998. Microsoft. http://www.microsoft.com/netmeeting/

ROSEMAN M. and S. GREENBERG. 1996. Building real time groupware with groupKit, a groupware toolkit. Transaction on computer interaction. *Computer Human Interaction.* **3(1)**: 66-106.

SHIRMOHAMMADI, SHERVIN and NICOLAS D. GEORGANAS. 1997. JETS: a Java-Enable Telecollaboration System. 541-547. *Proc. IEEE Conference of Multimedia Computer and System* (ICMCS'97), Ottawa.

The Complete Guide to ShowMe 2.0.1. Sun Microsystem Inc., Mountain View, CA. 1994. http://www.sun.com/product-n-solution/sw/ShowMe/product/ShowMe_SharedApp.html.

Preparation of Manuscript

General
The manuscript, including footnotes, tables, and captions for illustrations, should be typewritten double spaced on paper 210 x 297 mm in size, with margins of 40 mm on all sides. Three clear copies are required. Typing should be on one side of the paper only. Each page of the manuscript should be numbered, beginning with the title page.

Title page
The title of the paper, name of author and full address of the institution where the work was carried out should appear on this page. A short title not exceeding 60 characters should be provided for the running headline.

Abstract
Abstracts in Bahasa Melayu and English of not more than 200 words each are required for full articles and communications. No abbreviation should appear in the abstract. Manuscripts from outside of Malaysian may be submitted with an English abstract only.

Keywords
Up to a maximum of ten keywords are required and they should be placed directly below the abstract.

Footnotes
Footnotes to material in the text should not be used unless they are unavoidable. Where used in the text, footnotes should be designated by superscript Arabic numerals in serial order throughout the manuscript. Each footnote should be placed at the bottom of the manuscript page where reference to it is made.

Equations
These must be clearly typed, triple-spaced and should be identified by numbers in square brackets placed flush with the right margin. In numbering, no distinction is made between mathematical and chemical equations. routine structural formulae can be typeset and need not be submitted as figures for direct reproduction but they must be clearly depicted.

Tables
Tables should be numbered with Arabic numerals, have a brief title, and be referred to in the text. Columns headings and descriptive matter in tables should be brief. Vertical rules should not be used. Footnotes in tables should be designated by symbols or superscripts small italic letters. Descriptive materials not designated by a footnote may be placed under a table as a *note.*

Illustrations & Photographs
Illustration including diagrams and graphs are to be referred to in the text as 'figures' and photographs as 'plates' and numbered consecutively in Arabic numerals. All photographs (gloosy black and white prints) should be supplied with appropriate scales.

Illustrations should be of print quality; outputs from dotmatrix printers are not acceptable, Illustrations should be on separate sheets, about twice the size of the finished size in print. All letters, numbers and legends must be included on the illustration with the author's name, short title of the paper, and figure number written on the vereso. A list of captions should be provided on a separate sheet.

Unit of Measure
Metric units must be used for all measurements.

Citations and References
Items in the reference list should be referred to in the text by inserting, within parentheses, the year of publication after the author's name. If there are more than two authors, the first author should be cited followed by '*et al*'. The names of all authors, however, will appear in the reference list.

In the case of citing an author who has published more than one paper in the same year, the papers should be distinguished by addition of a small letter, e.g. Choa (1979a); Choa (1979b); Choa (1979c).

In the reference list, the names should be arranged alphabetically according to the name of the first author. Serials are to be abbreviated as in the *World List of Scientific Periodicals.*

The abbreviation for Pertanika Journal of Science and Technology is *Pertanika J. Sci. Technol.*

The following reference style is to be observed:

Monograph
Alefed, G. and J. Herzberger. 1983. *Introduction to Interval Computations.* New York: Academic Press.

Chapter in Edited Book
Muzzarell, R.A.A. 1980. Chitin. In *Polymers in Nature,* ed. E.A. MacGregor and C.T. Greenwood, p. 417-449. New York: John Wiley.

Serials
Kamaruzaman Ampon. 1991. The effect of attachment of hydrophobic imidoesters on the catalytic activity of trypsin. *Pertanika* **14(2)**: 18-185.

Proceedings
Mokhtaruddin, A.M. and L.M. Maene. 1981. Soil erosion under different crops and management practices. In *Agricultural Engineering in National Development,* ed. S.L. Choa, Mohd Zohdie Bardaie, N.C. Saxena and Van Vi Tran, p. 245-249. Serdang, Malaysia: Universiti Pertanian Malaysia Press.

Unpublished Materials (e.g. theses, reports & documents)

Sakri, I. 1990. Proper construction set-up of Malaysian Fish Aggregating Devices (Unjam). Ph.D. Thesis, Universiti Pertanian Malaysia, Serdang, Selangor.